UNIVERSITY OF SOUTHAMPTON

FACULTY OF MEDICINE, HEALTH AND LIFE SCIENCES

School of Medicine

MECHANICAL AND BIOLOGICAL AUGMENTATION OF ALLOGRAFT AND SYNTHETIC GRAFT IN IMPACTION BONE GRAFTING.

Benjamin JRF Bolland

Thesis for the degree of Doctor of Medicine

February 2008

UNIVERSITY OF SOUTHAMPTON

ABSTRACT

FACULTY OF MEDICINE, HEALTH AND LIFE SCIENCES
SCHOOL OF MEDICINE

Doctor of Medicine

MECHANICAL AND BIOLOGICAL AUGMENTATION OF ALLOGRAFT AND SYNTHETIC GRAFT IN IMPACTION BONE GRAFTING.

By Benjamin JRF Bolland

Aims:

This thesis has three main aims:

- To investigate the potential role of human bone marrow stromal cells (HBMSC) in Impaction Bone Grafting (IBG).
- To investigate the potential role of a synthetic graft, Poly (DL-lactic acid), ($P_{DL}LA$) as a tissue engineering scaffold and a graft extender in IBG.
- To investigate methods to improve graft compaction and reduce fracture risk in IBG.

Methods:

Part I: The biocompatibility and mechanical properties of HBMSC seeded onto allograft or $P_{DL}LA$ were compared to allograft or $P_{DL}LA$ alone *in vitro*.

Part II: Evidence of biocompatibility, neovascularisation and new bone formation in impacted allograft and $P_{DL}LA$ scaffolds seeded with HBMSC, *in vivo* was assessed and compared to allograft and $P_{DL}LA$ alone.

Part III: The laboratory work was translated into the clinical setting with implantation of impacted allograft seeded with HBMSC for the treatment of bone defects in two case studies.

Part IV: The role of vibration in IBG technique to reduce fracture risk and improve graft compaction and prosthetic stability was assessed in an *in vitro* femoral IBG model.

Results:

Part I: HBMSC seeded onto morsellised allograft or $P_{DL}LA$, and cultured under osteogenic conditions *in vitro* were able to withstand the forces equivalent to a standard femoral impaction and were able to differentiate and proliferate along the osteogenic lineage. The living composite formed provided a biomechanical advantage, with increased interparticulate cohesion and shear strength when compared to allograft alone.

Part II: HBMSC seeded onto morsellised allograft or $P_{DL}LA$, impacted and implanted subcutaneously in nude mice demonstrated cell viability and histological evidence of new bone formation and neovascularisation after 28 days.

Part III: In two case studies impacted allograft augmented with marrow-derived autogenous cells was used to treat bone voids in the proximal femur. Both patients made an uncomplicated clinical recovery**.** Imaging confirmed filling of the defects with very encouraging initial graft incorporation. Histochemical staining of graft samples demonstrated that a live composite graft with osteogenic activity had been introduced into the defects. Alkaline phosphatase and immunohistochemical staining techniques confirmed the bone phenotype of the autotransplanted cells.

Part IV: Vibration assisted compaction of morsellised allograft reduced the peak loads and hoop strains transmitted to the femoral cortex during graft compaction, improved graft compaction in the proximal and middle femoral regions, which in turn conferred improved mechanical stability of the prosthesis under cyclical loading, demonstrated by a reduction in stem subsidence.

Conclusions:

- HBMSC when combined with either allograft or synthetic graft ($P_{DL}LA$) can survive the forces of a standard IBG and under osteogenic conditions, differentiate and proliferate along the osteogenic lineage. HBMSC and allograft / $P_{DL}LA$ composites confer an additional biomechanical advantage over allograft / $P_{DL}LA$ alone.

- Increased new bone formation and neovascularisation has been demonstrated *in vivo* in allograft and $P_{DL}LA$ / HBMSC composites compared to allograft or $P_{DL}LA$ alone.
- Tissue engineering principles combining morsellised allograft and HBMSC composites have been utilised to fill bony voids in two clinical cases, with good clinical outcome.
- By reducing peak loads, hoop strains and femoral fracture risk, and improving graft compaction and prosthetic stability the use of vibration and a perforated tamp is a potential new safer more flexible IBG technique.
- Utilising tissue engineering techniques and improved graft impaction methods provides avenues to augment the biological and mechanical properties of morsellised allograft, and potentially increase the longevity of revision hip arthroplasty performed using the IBG technique.

TABLE OF CONTENTS

CHAPTER 5

Part III - Clinical translation: Implantation of impacted Allograft seeded with HBMSC for the treatment of bone defects in two case studies

CHAPTER 6

Part IV - A vibration assisted IBG technique to reduce fracture risk and improve graft compaction and prosthetic stability

TABLE OF FIGURES

CHAPTER 4

CHAPTER 5

CHAPTER 6

DECLARATION OF AUTHORSHIP

I, Benjamin JRF Bolland, declare that the thesis entitled:

MECHANICAL AND BIOLOGICAL AUGMENTATION OF ALLOGRAFT AND SYNTHETIC GRAFT IN IMPACTION BONE GRAFTING

and the works presented in it are my own. I confirm that:

- this work was done wholly or mainly while in candidature for a research degree at this University;
- where any part of this thesis has previously been submitted for a degree or any other qualification at this University or any other institution, this has been clearly stated;
- where I have consulted the published work of others, this is always clearly attributed;
- where I have quoted from the work of others, the source is always given. With the exception of such quotations, this thesis is entirely my own work;
- I have acknowledged all main sources of help;
- where the thesis is based on work done by myself jointly with others, I have made clear exactly what was done by others and what I have contributed myself;
- parts of this work have been published as:

- **BJRF Bolland**, K Partridge, S Tilley, AMR New, DG Dunlop, ROC Oreffo. Biological and mechanical enhancement of impacted allograft seeded with human bone marrow stromal cells: Potential clinical role in impaction bone grafting**.** ***Regenerative Med*** (2006).1(4), 457-467.

- S Tilley, **BJRF Bolland**, K Partridge, AMR New, DG Dunlop, ROC Oreffo. Taking tissue engineering principles into theatre: augmentation of impacted allograft with human bone marrow stromal cells. ***Regenerative Med.*** (2006) 1(5), 685-692.

- **BJRF Bolland**, AMR New, SPG Madabhushi, ROC Oreffo, DG Dunlop. Vibration-assisted bone graft compaction in Impaction Bone Grafting of the femur. ***J Bone Joint Surg (Br)*** 2007;89-B:686-692.

- **BJRF Bolland**, S Tilley, AMR New, DG Dunlop, ROC Oreffo.
  Adult mesenchymal stem cells and impaction grafting – A new clinical paradigm shift. ***Expert Rev Med Devices,*** 4(3), (2007);393-404.

- **BJRF Bolland**, AMR New, SPG Madabhushi, DG Dunlop, ROC Oreffo
  The role of Vibration and drainage in femoral Impaction Bone Grafting.
  J Arthroplasty 2008 (In Press).

- **BJRF Bolland,** JM Kanczler, PJ Ginty, SM Howdle, KM Shakesheff, DG Dunlop, ROC Oreffo.
  In Vivo Micro-CT Evaluation Of Neovascularisation In Tissue Engineered Constructs. ***Bone*** 2008 (In Press).

……

Benjamin JRF Bolland MBBS, BSc(Hons), MRCS.

February 2008

ACKNOWLEDGEMENTS

I wish to thank my supervisors, Prof Richard Oreffo and Mr Douglas Dunlop for their incredible support, enthusiasm and encouragement. I would also like to thank Dr Andrew New from the Bioengineering research group, University of Southampton, who helped an enormous amount with many of the projects and became an invaluable colleague and good friend. Mr Simon Tilley deserves much of the credit for initiating the pilot studies in this field and providing me with a wonderful platform from which to start my thesis. Special thanks to all in the Bone & Joint Research Group at the University of Southampton, including Dr Janos Kanczler, Miss Kate Murawski, Dr Trudy Roach, Dr Stuart Dr Kris Partridge, Dr Hadi Mirmalek-Sani, Dr David Green, Dr Suzanne Morgan, Dr Jodie Pound, Dr Jon Dawson, Dr Rahul Tare, Dr Yunhe Xu, Dr Ben MacArthur, Dr Bram Sengers, Ms Stefanie Inglis and Mrs Carol Roberts.

I would like to acknowledge and thank support from the following:

- Dr Gopal Madabhushi, Department of Geotechnical engineering, University of Cambridge, whose ideas, knowledge and advice fuelled much of the work on modernising the surgical technique.
- Orthopaedic surgeons at Southampton General Hospitals NHS Trust for providing human bone marrow samples.
- Prof Kevin Shakesheff, Dr Patrick Ginty, Prof Steven Howdle from the University of Nottingham for the endless supply of synthetic graft material.
- Eric Bonner and Bob Barnes for manufacturing much of the apparatus.
- John Lester for lending us his workshop along with general help and advice.
- Medical Illustration Department, University of Southampton.
- Orthopaedic theatre staff, Southampton General Hospital
- Funding support from the Biotechnology and Biological Sciences Research Council (BBSRC) and Engineering and Physical Science Research Council (EPSRC).
- Stryker (UK) for their generous funding and in particular Donovan Roberts and Carlos Santos for all their additional support.

Special acknowledgement must go to my wife, Prasanti and our two boys George and Charles who have always supported and encouraged me throughout this thesis, and given me the drive to complete this work.

PUBLICATIONS, AWARDS, PRESENTATIONS AND POSTERS

PUBLICATIONS

1. **BJRF Bolland**, K Partridge, S Tilley, AMR New, DG Dunlop, ROC Oreffo. Biological and mechanical enhancement of impacted allograft seeded with human bone marrow stromal cells: Potential clinical role in impaction bone grafting**.** ***Regenerative Med*** (2006).1(4), 457-467.

2. S Tilley, **BJRF Bolland**, K Partridge, AMR New, DG Dunlop, ROC Oreffo. Taking tissue engineering principles into theatre: augmentation of impacted allograft with human bone marrow stromal cells. ***Regenerative Med.*** (2006) 1(5), 685-692**.**

3. **BJRF Bolland**, AMR New, SPG Madabhushi, ROC Oreffo, DG Dunlop. Vibration-assisted bone graft compaction in Impaction Bone Grafting of the femur. ***J Bone Joint Surg (Br)*** 2007;89-B:686-692.

4. **BJRF Bolland**, S Tilley, AMR New, DG Dunlop, ROC Oreffo. Adult mesenchymal stem cells and impaction grafting – A new clinical paradigm shift. ***Expert Rev Med Devices,*** 4(3), (2007);393-404.

5. **BJRF Bolland**, AMR New, SPG Madabhushi, DG Dunlop, ROC Oreffo The role of Vibration and drainage in femoral Impaction Bone Grafting. ***J Arthroplasty*** 2008 (In Press).

6. **BJRF Bolland,** JM Kanczler, PJ Ginty, SM Howdle, KM Shakesheff, DG Dunlop, ROC Oreffo. *In Vivo* Micro-CT Evaluation Of Neovascularisation In Tissue Engineered Constructs. ***Bone*** 2008 (In Press).

ABSTRACTS

1. **BJRF Bolland,** AMR New, ROC Oreffo, DG Dunlop. The role of Vibration in Impaction Bone Grafting. *(Supps JBJS Br), (BOA 07)*

2. **BJRF Bolland,** JM Kanczler, DG Dunlop, ROC Oreffo. Quantification Of Neovascularisation In Tissue Engineered Constructs using Micro-CT. *Tissue Engineering 2007, 13(7): 1749-1750.*

3. **BJRF Bolland,** JM Kanczler, PJ Ginty, KM Shakesheff, DG Dunlop, ROC Oreffo. Poly Lactic Acid Scaffold Augmented With Human Bone Marrow Stromal Cells As A Bone Graft Extender In Impaction Bone Grafting. *Tissue Engineering 2007, 13(7): 1742-1743.*

4. **BJRF Bolland,** JM Kanczler, DG Dunlop, ROC Oreffo.
   In Vivo Micro-CT Evaluation Of Neovascularisation In Tissue Engineered Constructs. *(Supps JBJS Br),* (*BORS, Dundee, July 2007)*

5. **BJRF Bolland,** JM Kanczler, PJ Ginty, KM Shakesheff, DG Dunlop, ROC Oreffo.
   The Potential Role Of Poly Lactic Acid scaffold Augmented With Human Bone Marrow Stromal Cells As A Bone Graft Extender In Impaction Bone Grafting. *(Supps JBJS Br),* (*BORS, Dundee, July 2007)*

6. **BJRF Bolland,** JM Kanczler, DG Dunlop, ROC Oreffo.
   Evaluation of *In Vivo* Neovascularisation in Allograft and Poly D,L-Lactic Acid Tissue Engineered Scaffolds using Micro-Computer Tomography *(Supps JBJS Br),* (*BRS, Glasgow, July 2007)*

7. **BJRF Bolland,** K Partridge, AMR New, DG Dunlop, ROC Oreffo.
   Augmentation of allograft with Human Bone Marrow Stromal cells.
   Validation of cell survival, proliferation, osteogenic phenotype and mechanical strength**.** *(Supps JBJS Br), (BORS 06)*

8. **BJRF Bolland,** S Tilley, K Partridge, AMR New, DG Dunlop, ROC Oreffo.
   Translation from laboratory to theatre: augmentation of impacted allograft with human bone marrow stromal cells *(Supps JBJS Br), (BORS 06)*

9. **BJRF Bolland,** AMR New, ROC Oreffo, DG Dunlop.
   Vibration-assisted graft compaction in impaction bone grafting. Improving bone graft compaction whilst reducing the risk of fracture. *(Supps JBJS Br), (BORS 06)*

10. **BJRF Bolland,** AMR New, ROC Oreffo, DG Dunlop.
    Vibration assisted femoral Impaction Bone grafting: Reducing the risk of fracture whilst Improving bone graft strength *(Supps JBJS Br) , (BHS 07)*

11. **BJRF Bolland**, K Partridge, S Tilley, AMR New, DG Dunlop, ROC Oreffo.
    Improving both the biological and mechanical properties of allograft in impaction bone grafting. The potential role of human bone marrow stromal cells. *(Supps JBJS Br), (EFORT 07)*

PRIZES

1. BORS/BOTA/APOS Prize, Sept 2007
2. L'Oreal Prize, TERMIS-EU Sept 2007
3. TCES Travel Bursary Sept 2007
4. BORS Travelling Fellowship July 2007
5. BORS Podium presentation winner July 2007
6. Medical Futures Innovation awards winner June 2007

7. Gauvain Scientific Meeting (1st Prize) June 2007
8. RSM President's Prize May 2007
9. McKee Prize (British Hip Society) March 2007
10. BORS Travelling Bursary July 2006
11. Gauvain Scientific Meeting (2nd prize) June 2006

PRESENTATIONS

1. **BJRF Bolland,** AMR New, ROC Oreffo, DG Dunlop.
   The role of Vibration in Impaction Bone Grafting. *(BOA, Manchester 2007)*

2. **BJRF Bolland,** JM Kanczler, DG Dunlop, ROC Oreffo.
   In Vivo Micro-CT Evaluation Of Neovascularisation In Tissue Engineered Constructs. (*BORS, Dundee, July 2007)*

3. **BJRF Bolland,** JM Kanczler, PJ Ginty, KM Shakesheff, DG Dunlop, ROC Oreffo.
   The Potential Role Of Poly Lactic Acid scaffold Augmented With Human Bone Marrow Stromal Cells As A Bone Graft Extender In Impaction Bone Grafting. (*BORS, Dundee, July 2007)*

4. **BJRF Bolland,** JM Kanczler, DG Dunlop, ROC Oreffo.
   Evaluation of *In Vivo* Neovascularisation in Allograft and Poly D,L-Lactic Acid Tissue Engineered Scaffolds using Micro-Computer Tomography (*BRS, Glasgow, July 2007)*

5. **BJRF Bolland,** JM Kanczler, DG Dunlop, ROC Oreffo.
   Quantification Of Neovascularisation In Tissue Engineered Constructs Using Micro-CT. (TERMIS-EU*, London, Sept 2007)*

6. **BJRF Bolland,** JM Kanczler, PJ Ginty, KM Shakesheff, DG Dunlop, ROC Oreffo.
   Poly Lactic Acid Scaffold Augmented With Human Bone Marrow Stromal Cells as a Bone Graft Extender in Impaction Bone Grafting (TERMIS-EU, *London, Sept 2007)*

7. **BJRF Bolland**, AMR New, SPG Madabhushi, DG Dunlop.
   VIBONE : Vibration impaction bone grafting system *(Medical Futures Innovations Awards Judging Day, London, May & June 2007)*

8. **BJRF Bolland**, AMR New, ROC Oreffo, DG Dunlop.
   The role of Vibration in Impaction Bone grafting: Reducing the risk of fracture whilst improving bone graft strength *(Gauvain Society Scientific Meeting, June 2007)*

9. **BJRF Bolland**, AMR New, ROC Oreffo, DG Dunlop.
   The role of Vibration in Impaction Bone grafting: Reducing the risk of fracture and improving bone graft strength *(President's Prize Papers, Orthopaedic Section, RSM London, May 2007)*

10. **BJRF Bolland**
    New Developments in Impaction Bone Grafting *(Exeter Hip Symposium, Exeter, May 2007)*

11. **BJRF Bolland**, K Partridge, S Tilley, AMR New, DG Dunlop, ROC Oreffo.
    Improving both the biological and mechanical properties of allograft in impaction bone grafting. The potential role of human bone marrow stromal cells.*(EFORT, Florence, Italy, May 2007)*

12. **BJRF Bolland**, AMR New, ROC Oreffo, DG Dunlop.
    The role of Vibration in Impaction Bone grafting: Reducing the risk of fracture whilst improving bone graft strength *(Engineers & Surgeons: Joined at the Hip. IMeche conference, London, April 2007)*

13. **BJRF Bolland**, K Partridge, S Tilley, AMR New, DG Dunlop, ROC Oreffo.
    Augmentation of biological and mechanical properties of allograft in impaction bone grafting. The potential role of human bone marrow stromal cells**.** *(Engineers & Surgeons: Joined at the Hip. IMeche conference, London, April 2007)*

14. **BJRF Bolland**, DG Dunlop.
    Vibration Impaction Bone Grafting *(ABC Visiting Fellows, Scientific Conference, April 2007)*

15. **BJRF Bolland,** AMR New, ROC Oreffo, DG Dunlop.
    Vibration assisted femoral Impaction Bone grafting: Reducing the risk of fracture whilst Improving bone graft strength *(British Hip Society, March 2007)*

16. **BJRF Bolland**, K Partridge, AMR New, DG Dunlop, ROC Oreffo.
    Augmentation of allograft with Human Bone Marrow Stromal cells.
    Validation of cell survival, proliferation, osteogenic phenotype and mechanical strength. *(BORS July 2006)*

17. **BJRF Bolland,** K Partridge, S Tilley, AMR New, DG Dunlop, ROC Oreffo.
    Biological and mechanical enhancement of impacted allograft seeded with human bone marrow stromal cells: Potential clinical role in impaction bone grafting. *(Gauvain Society Scientific Meeting, June 2006)*

POSTERS

1. **BJRF Bolland,** AMR New, ROC Oreffo, DG Dunlop.
   Vibration-assisted femoral impaction bone grafting**.** *(London Hip Meeting, London, June 2007, Research & Development Conference, April 2007)*

2. **BJRF Bolland**, S Tilley, K Partridge, AMR New, DG Dunlop, ROC Oreffo. Translation from laboratory to theatre: augmentation of impacted allograft with human bone marrow stromal cells *(BORS, Southampton July 2006, Research & Development Conference, Southampton University, April 2007)*

3. **BJRF Bolland**, AMR New, ROC Oreffo, DG Dunlop.
   Vibration-assisted graft compaction in impaction bone grafting. Improving bone graft compaction whilst reducing the risk of fracture. *(BORS, Southampton July 2006)*

4. **BJRF Bolland**, AMR New, ROC Oreffo, DG Dunlop.
   The use of Vibration-assisted graft compaction in Impaction Bone grafting: Reducing the risk of fracture whilst improving bone graft strength *(EFORT, Florence May 2007)*

ABBREVIATIONS

AAOS	American Academy of Orthopaedic Surgeons
α-MEM	Alpha-Minimum essential medium, Eagle's modification
A/S	Alcian blue/Sirius red
AEC	3-amino-9-ethyl-carbazole
Allo	Allograft
ALP	Alkaline phosphatase
AVN	Avascular necrosis
ANOVA	Analysis of variance
BMP	Bone morphogenic protein
BMSC	Bone marrow stromal cells
BSA	Bovine serum albumin
BSP	Bone Sialoprotein
CFU-F	Colony forming unit-fibroblastic
CMFDA	5-chloromethyl-fluorescein diacetate
CTG	Cell Tracker Green
DNA	Deoxyribonucleic acid
DOPC	Determined osteoprogenitor cell
DHS	Dynamic hip screw
DPX	Dibutyl phthalate xylene
EDTA	Ethylenediamine tetra-acetic acid
EH-1	Ethidium Homodimer-1
ES	Embryonic stem cell
FCS	Foetal calf serum
FDA	Food and Drug Administration (USA)
H_2O_2	Hydrogen peroxide
HA	Hydroxyapatite
HBMSC	Human bone marrow stromal cell
HIF α	Hypoxia inducible factor α
IBG	Impaction Bone Grafting
Pa	Pascals

μ-CT	Micro computer tomography
MSC	Mesenchymal stem cell
N	Newton
NaCl	Sodium Chloride
NaOH	Sodium hydroxide
PBS	Phosphate buffer solution
PGA	Polyglycolic acid
PLGA	Poly (DL-lactic-co-glycolic) acid.
$P_{DL}LA$	Poly (DL-lactic acid)
pNPP	Para-nitrophenolphosphate
PTFE	Poly(tetrafluoroethylene)
QALY	Quality assisted life years
SCID	Severely compromised immunodeficient
SD	Standard deviation
SDS	Sodium dodecyl sulphate
SSC	Saline sodium citrate buffer
TCP	Tri-calcium phosphate
TE	Tris-EDTA
THR	Total Hip replacement
TRAP	Tartrate resistant acid phosphatase
vWF	Von Willebrand factor

CHAPTER 1

Introduction

1.1 Burden of Problem

Total hip replacement (THR) remains one of the most successful procedures performed by any surgeon, as measured by Quality Adjusted Life Years (QALY's) with greater than 90% clinical success rate at 10 years (Segal, Bellamy, 1988). Each year in the UK there are over 50,000 total hip replacements (1 million worldwide) performed at a cost of approximately £250 million per annum. With the demographics of an ageing population, this figure is set to rise by as much as 50% by 2026 (Birrell et al., 1999). At the opposite end of the age spectrum, the combination of younger and more active patients with higher expectations and surgeons prepared to perform surgery on this cohort has further exacerbated the growing demand for THR surgery. This cohort will place higher demands on the prosthesis for a longer period of time, further increasing the likelihood of revision surgery. As a consequence revision hip surgery has increased by 100% due to implant failure since 1991 (Dixon et al., 2004) and figures from the American Academy of Orthopaedic Surgeons (AAOS) estimate that this rise will continue at a rate of 20-30% over the next three decades (Kurtz et al., 2007).

There are a number of issues surrounding revision hip arthroplasty namely; i) revision operations are expensive, ii) have a higher complication rate, iii) longer operative time, iv) such procedures typically have significant blood loss in comparison to primary procedures and, v) outcomes are often inferior to the primary operation (Bozic et al., 2005; Crowe et al., 2003).

The cause of many of these difficulties is a result of the extensive bone loss associated with loose implants requiring revision surgery. When an implant fails bone is lost through a combination of stress shielding, osteolysis, instability and / or infection. The surgical treatment of extensive bone loss and voids fall into the categories of replacement, with cement or custom made prostheses, or reconstruction using the technique of Impaction Bone Grafting (IBG). With primary THR's and subsequently revision THR's being performed on younger patients, restoring rather than replacing bone stock needs to be a reliable and successful option.

1.2 Impaction bone grafting – origins to the present day

The technique of Impaction Bone Grafting (IBG) in the acetabulum was first introduced by Slooff and co-workers in Nijmegen (Slooff et al., 1984) in the late 1970's, and in the femur by Ling, Gie and colleagues in Exeter in 1987 (Gie et al., 1993). The procedure involves the progressive compaction of morsellised allograft into contained femoral and / or acetabular cavities into which the prosthesis is cemented. This generates a four layer composite of host bone, allograft bone, cement and prosthesis.

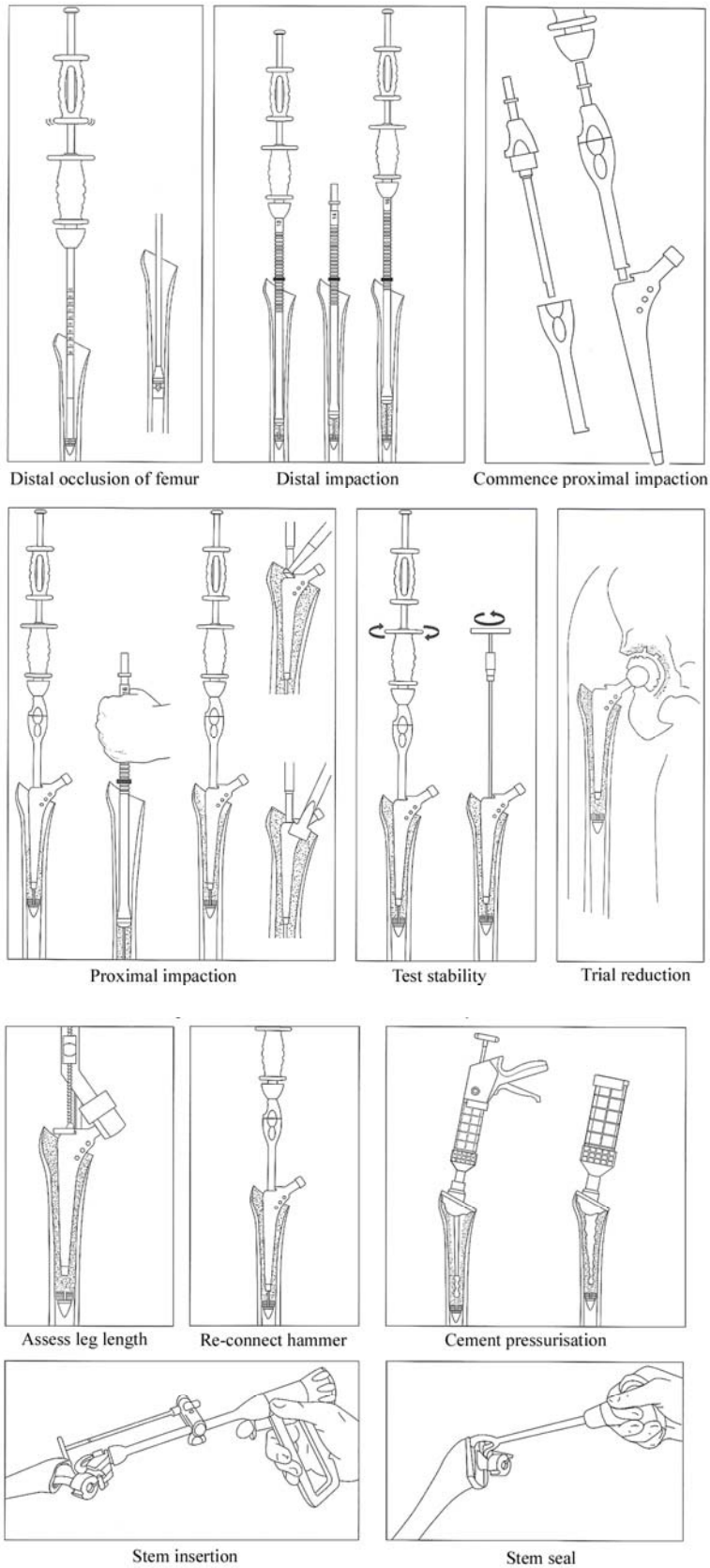

Figure 1-1 Femoral Impaction bone graft grafting: Surgical technique. Adapted from Stryker manual "X-change® Revision Surgical Protocol".

The objective of IBG is to initially provide bone support and stable fixation for the implant, essential for successful clinical outcome as well as subsequent bone ingrowth and remodelling of the impacted allograft with resultant restoration of living bone stock. Thus, the short and long term success of IBG is dependent on both biological and mechanical factors.

Although results from the centres of origin have shown excellent mid-term outcome, with 99% and 100% survival at average 10 year follow up (in 226 and 33 patients respectively with a femoral reoperation due to symptomatic aseptic loosening as the endpoint) (Halliday et al., 2003; Schreurs et al., 2005), this has not been the experience of other centres. In Bristol, a group of 79 hip replacements followed up for just over one year, in whom impaction grafting of the femur had been performed, 9 (11%) showed evidence of significant subsidence (Eldridge et al., 1997). This was defined as subsidence of over 10mm and in all cases occurred in the first 3 months post-operatively. Six hips required subsequent re-revision. A series in Australia found similar subsidence values of 9mm (range 2-37mm) compared to cemented revisions at 24 months (Sharpe P, 1998). The Nijmegen group (van Haaren et al., 2007) recently reviewed 71 acetabulum impaction bone grafting revisions at a mean follow up of 7.2 years. 20 of these cases required re-revision for aseptic loosening giving an overall survival of 72%. 70% of the re-revisions had an AAOS type III or IV defect. Potential factors responsible for the variation include aetiology of failure of the primary THR and subsequent extent of bony defect, implant choice, surgical technique and bone graft preparation and composition.

In terms of graft material of choice, morsellised allograft remains the current gold standard in IBG. Although allograft acts as an adequate mechanical scaffold it is primarily a non viable necrotic tissue with limited osteoinductive potential. Other concerns surrounding use of allograft include the potential for immunogeneic response (Eldridge et al., 1997) or disease transmission (Simonds et al., 1992; Lord et al., 1988; Buck et al., 1989). Since the evolution of allograft for IBG many studies have investigated techniques to improve predominantly, the mechanical and to a lesser extent biological properties of allograft. These have included:-

1.2.1 Preservation of the graft

Bone graft is normally obtained from femoral heads from live donors at THR surgery. The femoral heads are either fresh frozen at -80^{o}C or freeze dried and stored at room temperature. Freeze dried bone reduces the immunogeneic load but the effects on the mechanical properties of the graft remains unresolved. *In vitro* impaction studies comparing freeze dried and fresh frozen morsellised allograft have shown that both reach similar maximum stiffness levels (55MPa) but the freeze dried graft required fewer impactions (Cornu et al., 2003) which is contrast to other studies (Anderson et al., 1992; Pelker et al., 1984) which demonstrated inferior mechanical properties in freeze dried bone. To date, the evidence favouring one form of preservation over the other remains unclear, however the majority of surgeons, and in particular at the centres where the technique originated, continue to use fresh frozen allograft (Halliday et al., 2003).

1.2.2 Graft Preparation (grading, washing)

The techniques employed to prepare bone graft have been shown to affect both the biological and mechanical properties of the graft and play a key role in successful outcome. Studies have utilised soil mechanics theory of aggregates (Smith, 1990; Lambe, 1979) to measure the shear strength of morsellised allograft. In IBG, allograft will fail in shear and therefore the measurement of shear strength and its individual components have been recognized as important properties of the graft. The shear strength of a granular aggregate, like bone graft, depends on the internal friction (Φ), expressed as the angle at which the aggregate will slide, and interlocking of the particles (c), expressed as a stress. The frictional resistance varies in proportion with the normal (compressive) stress (σ) produced by the load supported by the aggregate. The relationship between the parameters can be expressed by the Mohr Coulomb failure law which allows us to calculate shear strength of an aggregate.

$$\tau = c + \sigma \tan\Phi$$

Mohr Coulomb Failure Law

Studies by Dunlop et al (Dunlop et al., 2003) measured these parameters in bone graft to determine the effect particle size and washing had on the shear strength of the graft. Production of a 'well-graded' sample theoretically produces the aggregate most resistant to shear. This grading has been determined for spherical particles by Fuller (Smith, 1990; Craig, 1993) and is best understood by considering the problem of making a pyramid of marbles. A graphical curve of particle distribution was mathematically determined that represented the sequence of marble sizes to fit the 'gaps' (Figure 1-2) which if carried to infinitely small sizes of marbles will allow an infinitely steep pyramid to be constructed (aggregate approaches properties of a solid, cf. fractals).

When considering irregularly shaped particles, it is normal practice to use a linear log of the range of available sizes, to determine an ideal mixture (Figure 1-3). Using morsellised bone graft obtained from a range of bone mills with varying particle size distribution Dunlop et al (Dunlop et al., 2003) found that the closer the graft aggregate mix was to the ideal "well graded" sample i.e. was made up of a broad range of particle sizes rather than a narrow range, the greater the resistance to shear and increased shear strength it conferred.

Dunlop and colleagues also showed that washing improved the shear strength of the graft (Dunlop et al., 2003). Removing the fat and marrow with washing would theoretically provide additional benefit of reducing the immunogeneic load to the patient. On the contrary however, washing could also remove key osteoinductive agents and therefore be seen as detrimental to the important biological properties of the allograft.

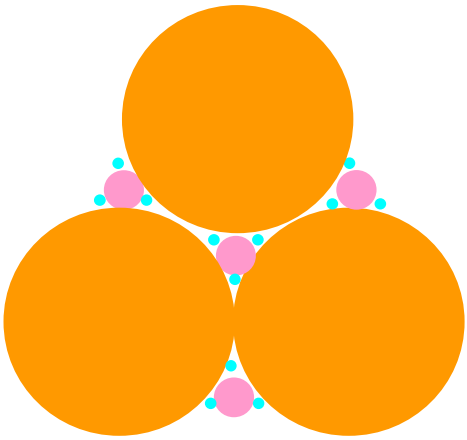

Figure 1-2 Relative particle sizes that allow ideal compaction.

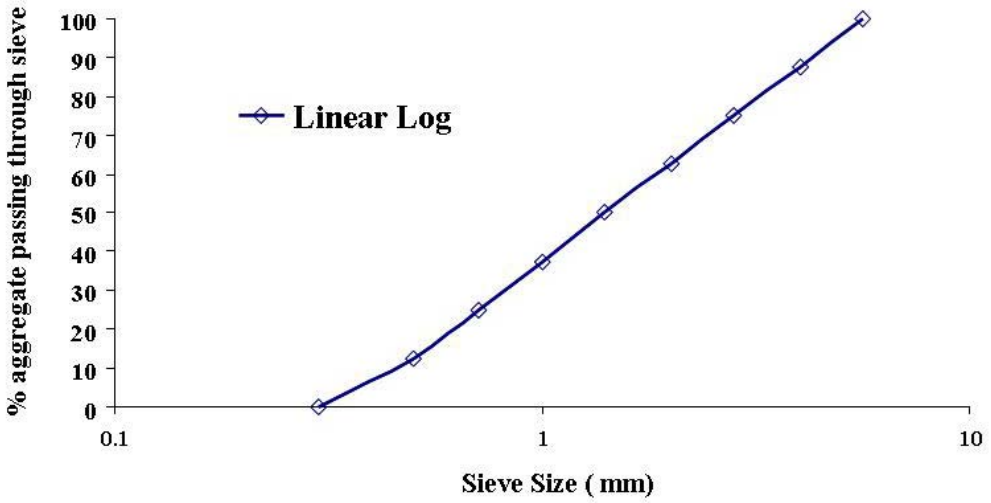

Figure 1-3 Particle size distribution graph. Particle size distribution lines for mixtures exhibiting Linear Log grading characteristics. (Acknowledgement to Mr D Dunlop).

1.2.3 Bone graft extenders

Bone graft alone, either morsellised or whole, has had some success in replacing lost bone stock (Slooff et al., 1984; Friedlaender, 1987). However, with demand outweighing limited supply and the increasing concerns regarding transmission of pathogens, interest in synthetic materials has increased significantly. Early studies concentrated on the mechanical effect of these synthetic materials, which were primarily osteoconductive. Brewster et al (Brewster et al., 1999) showed

the addition of small bioglass particles increased the shear strength of the impacted graft mix. Again, this can be explained with soil mechanics theory whereby the smaller particles fill the gaps left between the allograft particles increasing interparticulate cohesion and shear strength (see Mohr Coulomb failure Law).

Tricalcium phosphate / hydroxyapatite extenders have been shown in *in vitro / vivo* studies to have enhanced mechanical stability over allograft alone (Blom et al., 2005; van Haaren et al., 2005; Arts et al., 2005). Graft incorporation of tricalcium phosphate / HA particles has been observed in a goat model of contained acetabular deficiencies reconstructed with a 50:50 mix of graft and extender (Arts et al., 2005). In addition to the composition of synthetic grafts, morphology could play an important role in improving the mechanical properties of allograft / synthetic graft construct. Important properties affecting the rate of graft resorption include particle size, porosity surface area and crystallinity (LeGeros et al., 2003; Oonishi et al., 1999). Furthermore, the extent of the porosity and interconnectivity of the pores are crucial factors affecting diffusion of nutrients, cell attachment, migration and expression, and tissue ingrowth necessary for bone formation, bone repair and bone regeneration (LeGeros et al., 2003; Klawitter et al., 1976). A macroscopic open structure that interdigitates within the composite, analogous to reinforced concrete, crosses multiple potential shear planes thus providing further resistance to shear and composite failure. Klawitter advised pore sizes larger than 50μm to allow for blood vessel ingrowth and 200μm for osseous ingrowth to occur (Klawitter et al., 1976). In general, however, the optimum morphological characteristics to promote incorporation and remodelling are yet to be fully established.

Polymeric scaffolds including synthetic materials such as poly(DL-lactic acid) or poly(L-lactic acid) ($P_{DL}LA$), poly(DL-lactic-*co*-glycolic acid) (PLGA) and polyglycolic acid (PGA), have attracted significant interest in the tissue engineering community as a consequence of their biocompatibility, ease of processing into three-dimensional structures, their established safety as suture materials and the versatility that they offer for producing chemically defined substrates for bone graft matrices (Uhrich et al., 1999)**.** These scaffolds are manufactured using high pressure carbon dioxide mixing (Davies et al., 2008). This is a highly versatile technique allowing the modulation of porosity and composition, including the incorporation of growth factors

with control release mechanisms (Uhrich et al., 1999). To date $P_{DL}LA$ scaffolds have not been used as extenders in the field of impaction bone grafting.

Figure 1-4 Examples of morsellised synthetic grafts. (a) Tricalcium Phosphate and (b) $P_{DL}LA$ synthetic grafts

1.2.4 Bone graft additives

Although impaction is mechanically beneficial it has been shown to be detrimental to bone ingrowth and remodelling (Tagil, Aspenberg, 1998). This has led to widespread interest in graft additive and in particular the application of bone morphogenic proteins such as BMP-7 or OP-1. In a bone chamber animal model, Tagil et al (Tagil et al., 2000) demonstrated improved initial graft resorption and hastened graft incorporation and remodelling after the addition of OP-1. OP-1 however, not only stimulates new bone ingrowth but simultaneously activates osteoclastic activity. McGee et al (McGee et al., 2004) reported increased resorption associated with stem subsidence, in allograft containing OP-1 compared to allograft alone at 6 weeks in a sheep femoral impaction model. This is likely to be attributable to stimulation of osteoclasts by OP-1. The temporal relationship between bone resorption and regeneration is clearly critical in the clinical scenario of IBG when the graft is to be loaded from the outset. Gaining control of this fine balance has led to studies utilising the role of bisphosphonates in inhibiting bone resorption. Jeppsson and colleagues (Jeppsson et al., 2003) showed that the addition of a bisphosphonate improved bone graft density but also reduced the bony ingrowth when compared to OP-1 alone. Furthermore a clinical study evaluating the effect of mixing OP-1 with morsellised allograft in hip revisions did not demonstrate any trend in improved

fixation and graft incorporation and early re-revisions required in the study group resulted in the study being abandoned (Karrholm et al., 2006).

It is clear that despite all of these studies little progress has been made on the biological augmentation of allograft. Critically, the allograft used in IBG is non - vascularised and it is therefore unclear how successful incorporation is achieved. Histology from biopsy samples has shown viable tissue ingrowth into the graft (Ling et al., 1993), but confirmation of new bone formation within the defects remains limited and, at best, inconsistent (Mikhail et al., 1999; Nelissen et al., 1995; Ullmark, Obrant, 2002).

The expanding emerging discipline of tissue engineering has opened an exciting avenue to improve both the biological and mechanical aspects of allograft in IBG for revision hip surgery.

1.3 Tissue engineering & impaction bone grafting

1.3.1 Definition

The general principle of tissue engineering involves the combination of living cells within a natural or synthetic scaffold, to produce a three dimensional living tissue construct which is functionally, structurally and mechanically equal to, if not superior to that which it has been designed to replace (Stock, Vacanti, 2001).

There are a number of different sources of cells which can be used for tissue repair and regeneration. These include mature cells from the patient, “adult” stem cells such as bone marrow stromal (BMSC) or mesenchymal stem cell (MSC) as well as fetal and embryonic stem cells (ES). This thesis will concentrate on the role of adult stem cells only in IBG.

1.3.2 Classification of marrow stromal cells

The regenerative capacity of bone has long been recognised although existence of a multipotent mesenchymal stem cell has proved elusive due to the low incidence, indeterminate morphology and undefined biochemical phenotype of these cells. Evidence for a population of cells with multilineage mesodermal differentiation capacity was first demonstrated by Friedenstein and colleagues in studies that showed the capacity of clonogenic fibroblastic precursor cells (CFU-F) to generate cartilage, bone, myelosupportive stroma, adipocytes and fibrous connective tissue (Bianco, Robey, 2001).

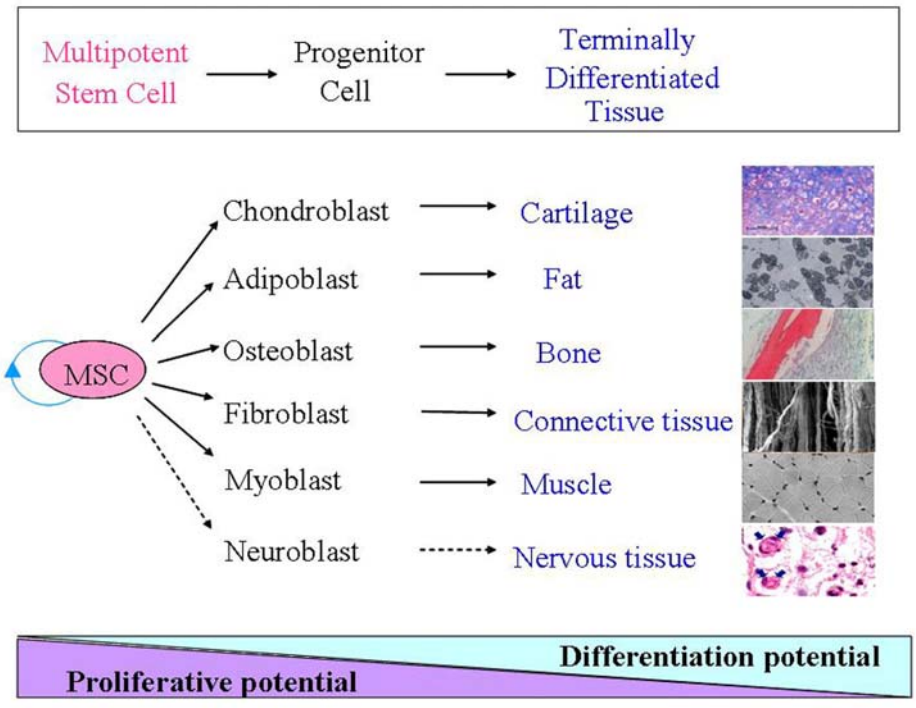

Figure 1-5 Differentiation potential of MSCs along the stromal lineages.

A variety of names including osteogenic stem cells, marrow stromal fibroblastic cells (Triffitt, 2002), bone marrow stromal stem cells (Owen, Friedenstein, 1988), mesenchymal stem cells (Goshima et al., 1991), stromal precursor cells and, more recently, skeletal stem cells (Bianco, Robey, 2001) have

been ascribed to this population of cells although, currently, mesenchymal stem cells (undifferentiated multipotent cells of the mesenchyme) appears to be the popularised term. For this thesis the term mesenchymal stem cell will be used. Mesenchymal stem cells give rise to a hierarchy of cell populations within the bone to produce in essence a developmental continuum, which can be artificially divided into a number of developmental stages including: mesenchymal stem cell, determined osteoprogenitor cell (DOPC), preosteoblast, osteoblast and ultimately, osteocyte. A number of criteria need to be fulfilled before a cell can be termed a stem cell, namely, self-renewal, the ability to differentiate into more than one cell type and the capacity for cell division to be maintained throughout life. It is important to note therefore that osteogenic progenitors are an intermediate between a stem cell and differentiated progeny (i.e. osteoblast) and, significantly, to date, a homogenous human mesenchymal or skeletal stem cell population has yet to be isolated.

In this thesis the cell population derived from human bone marrow samples were not enriched or sorted by any technique. The samples therefore contained a heterogenous population of stromal cells and therefore will be referred to as human bone marrow stromal cells (HBMSC).

1.3.3 Characterisation of marrow stromal cells

Stem cells can be characterised by their ability to self renew and multipotency as well as their cell surface proteins. Although there are defined markers for the haemopoietic stem cell lineages, an equivalent system for the mesenchymal stem cells does not yet exist. There are, however, putative surface markers which can be utilised for the enrichment of MSCs from stromal cell populations.

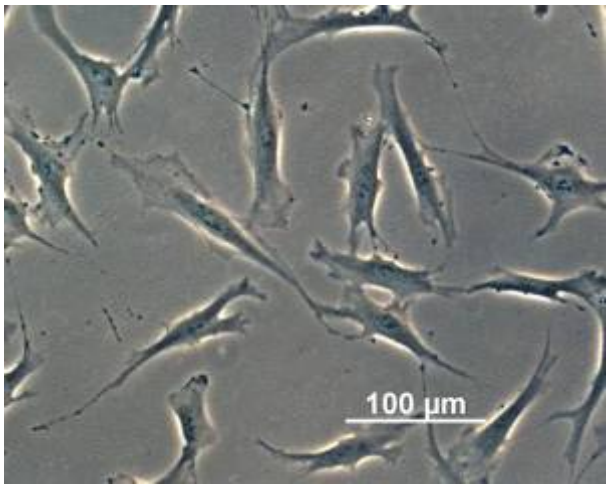

Figure 1-6 Human bone marrow stromal cells in monolayer culture. Cells are adherent and typically fibroblastic in morphology. (Courtesy of Bone & Joint Research Group, Southampton).

It has been recorded that MSC populations are negative for the haematopoietic markers of CD14 and CD34. However negative selection for those epitopes may not preclude other non-haematopoietic cell types possibly being extracted as opposed to just MSCs (Pittenger et al., 2002). Therefore cells can be sorted for surface markers that are positive for MSCs, such as CD49a, CD63 and CD166 (recognised by the HOP-26 and SB-10 antibodies respectively) and the commonly utilised monoclonal antibody STRO-1 (Simmons, Torok-Storb, 1991; Pittenger et al., 2002) (Deschaseaux et al., 2003; Stewart et al., 2003). The STRO-1 antibody is used to isolate cells from the bone marrow based on a trypsin-resistant surface marker that is found on virtually all of the CFU-F cells.

1.3.4 Multilineage differentiation and plasticity

In vitro conditions have been developed to drive MSCs down the stromal lineages. Typically for osteogenesis, the cells remain in Alpha-Minimum essential medium (α-MEM) with the addition of ascorbic acid 2-phosphate, β-glycerol

phosphate and dexamethasone. Culture expanded cells can then be assayed for the release of alkaline phosphatase, a marker of osteogenic differentiation (Jaiswal et al., 1997; Pittenger et al., 1999; Janderova et al., 2003; Pittenger et al., 2002). The cells will also deposit collagenous and non-collagenous proteins, however, as they remain in monolayer growth they are unable to develop mineralised bone matrix. As such they are differentiating osteoblasts and are termed 'osteogenic' or 'bone-like' cells, not osteocytes (when they reach a terminal state) found in native bone. Once cells have reached their differentiated states their morphology and phenotype can be observed by appropriate histological and molecular analysis.

The ability of cell types to move between lineages is referred to as 'plasticity'. A change across expected lineages can be referred to as interconversion (Park et al., 1999; Nuttall, Gimble, 2004). In a study by Park and co-workers, adult human MSCs were cultured and differentiated into adipocytes *in vitro* to research the relationship between adipocytes and osteocytes, as an increased percentage of marrow fat and decreased percentage of bone is observed as a consequence of ageing. Single adipocytes were subjected to osteogenic growth conditions and were found to dedifferentiate to an earlier fibroblast-like state, then redifferentiate to the osteoblast phenotype (Park et al., 1999). This was confirmed by positive alkaline phosphatase activity, staining of the developed osteocalcin and the appearance of visible mineralised aggregates. The study demonstrated the interconversion potential of these cells and supports the model of a common progenitor cell for both fat and bone tissue.

Plasticity within expected cell types can be termed as a 'lineage switch'. However, a number of studies have reported the differentiation of MSCs to non-mesenchymal cell lineages, a process called transdifferentiation (Huttmann et al., 2003).

1.3.5 Mechanisms of plasticity

With the research undertaken there is an emerging picture of the possible routes taken by cells to cross between lineages. It would appear that reversion by the cell to an earlier state does occur as demonstrated by the interconversion between the

progeny of adipocytes to osteoblasts (Park et al., 1999). The adipocytes were observed to dedifferentiate to a more proliferative state before induction to an osteogenic lineage. The cell reversion model may also apply to the process of transdifferentiation, whereby the MSC would dedifferentiate to an earlier stage before then redifferentiating to a new cell line. A study by Seshi et al.(Seshi et al., 2003) into the gene expression of bone marrow stromal cells draws a possible explanation for this plasticity of these cells. Utilising single-cell microarrays it was observed that cells display many different surface proteins at the same time, leading to the observation of a pluripotent cell (Seshi et al., 2003). Initially the MSCs are displaying the many different surface antigens simultaneously, but by 'switching off' those unwanted antigens or pathways this would lead to the differentiation of the cell. Seshi and co-workers therefore proposed that the cells are 'pluridifferentiated', ready to differentiate to the phenotype of the different cell lines as they already possessed the characteristics rather than needing to develop them. If certain characteristics could be 'switched off' it may also be possible that those pathways could be reactivated. This may be a possible explanation for the apparent dedifferentiation or cell reversion.

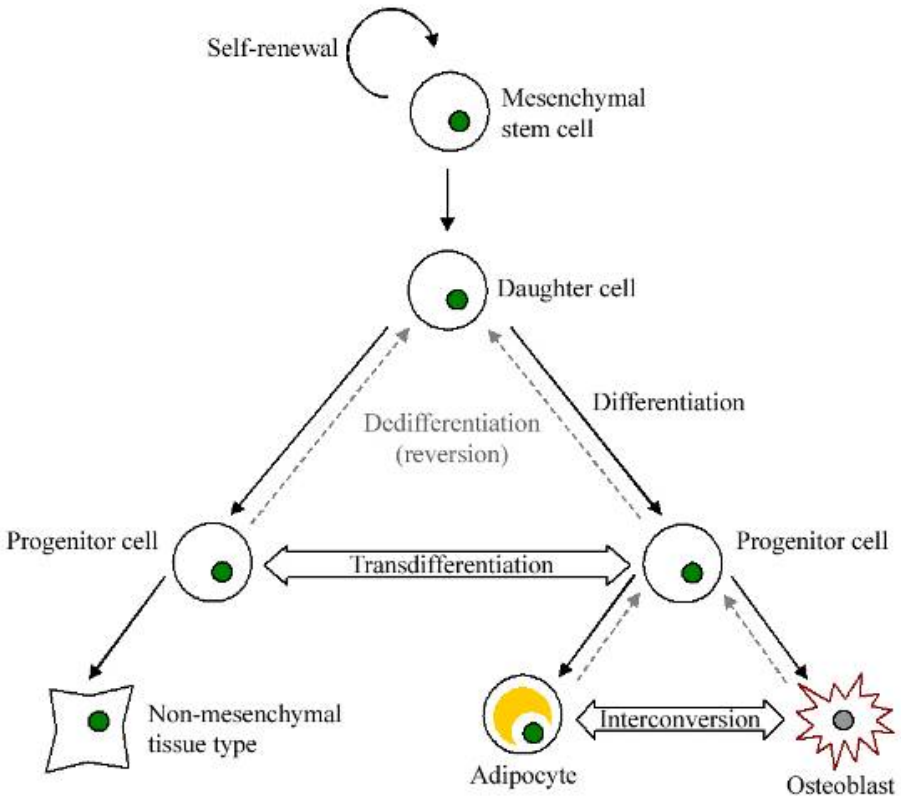

Figure 1-7 Types of Plasticity. As the cells move down the diagram they will differentiate over time and end in a terminal state. The interconversion process may

occur as a direct change in the phenotype of the cell, or through dedifferentiation then by redifferentiation. In transdifferentiation the MSC will switch to a non-mesenchymal linage. Adapted from Aubin, 1998 and Huttmann et al., 2003, Acknowledgment to S.Mirmalek-Sani.

1.3.6 Effects of stem cell plasticity

Plasticity offers tremendous therapeutic potential with numerous tissues induced from MSCs including myocardial, mesangial and endothelial. The plasticity of MSCs will have an impact in injury and repair, transplantations, gene therapy and tissue engineering, as a few examples. The plasticity of MSCs has huge potential for direct therapeutic use and can be used to increase our understanding of established ailments and disease (Nuttall, Gimble, 2004). If the increase of marrow fat and the decrease in calcification (observed in elderly patients) can be described by interconversion and the dedifferentiation of the committed cells to a precursor, therapies to counteract this change would have significant implications for ageing studies. As observed in many of the other studies, however, the progression of cells to a terminal state gave rise to new problems. For Park et al. (Park et al., 1999), cells that had reached a terminal state were significantly less likely to dedifferentiate. This was also confirmed in other studies where the induced cells were unable to form fully functional tissues (Lodie et al., 2002).

1.3.7 Biomaterial scaffolds

Biomaterial scaffolds and their ongoing technological advances remain critical to the discipline of tissue engineering. A number of properties are required for their success. They need to provide a three dimensional support for cell attachment and growth, biocompatibility with seeded cells and the surrounding environment and initial mechanical support. Other desirable properties include osteoinductivity, encapsulation of growth factors and gene delivery. Furthermore these scaffolds have a variable rate of resorption which may affect their mechanical properties and the clinical situations that they may be safe for use. In the field of IBG, the graft plays a major mechanical role and therefore it is crucial the rate of resorption is not only known but is also consistent.

A number of materials have been used for bone regeneration along with mesenchymal progenitors including ceramics, biomimetic scaffolds based upon organic (aliphatic) polyesters, natural biomaterials derived from corals and marine sponges (Green et al., 2003), and natural polysaccharides based upon seaweed derived sources including alginates capsules with peptide coatings (Rowley et al., 1999). Site specific scaffolds are being developed through the use of rapid prototyping, developed from industrial engineering prototypes (Antonov et al., 2004). Considerations that need to be addressed when designing a scaffold for therapeutic use include their effects on the local environment, the mechanism and rate of scaffold degradation (with a fine balance between rapid resorption prior to consolidation against too slow resorption resulting in scaffold encapsulation), and of course, the mechanical properties of the scaffold and how they change with time.

1.3.8 Clinical Applications

The ongoing progress of stem cell biology has led to its interest in many clinical applications. However in orthopaedics, the use of bone marrow to augment allograft is not a new practice (Burwell, 1964). Human bone marrow stromal cells have been isolated from bone marrow and injected percutaneously for the treatment of tibial non-unions (Hernigou et al., 2005) and avascular necrosis of the hip (Hernigou, Beaujean, 2002) with reported success. Outside the clinical domain, a number of animal studies have demonstrated that tissue engineering techniques using autologous MSC seeded onto a scaffold lead to bone regeneration at a defect site (Bruder et al., 1998; Arinzeh et al., 2003; Dai et al., 2005; den Boer et al., 2003). However until recently little work had investigated the potential role that MSC could play in the technique of IBG.

1.4 Aims of thesis

Major Null Hypothesis

"Alteration to the composition of a natural or synthetic scaffold used in Impaction Bone Grafting and the surgical technique of impaction has no effect on biological or mechanical properties of the impacted scaffold."

The study has been divided into four sub-sections

Part I : Tissue engineering & Impaction grafting – *In vitro* study

Part II : Tissue engineering & Impaction grafting – *In vivo* study

Aims of Part I and II

1. Can HBMSC survive the forces of a standard femoral impaction?
2. Can HBMSC differentiate and proliferate along the osteogenic lineage both *in vitro* and *in vivo*?
3. Do HBMSC seeded and cultured on allograft or synthetic graft have an effect on the mechanical properties of the aggregate?
4. Do HBMSC seeded and cultured on allograft or synthetic graft have an effect on revascularisation and incorporation of the aggregate?

Part III : Tissue engineering & Impaction grafting – Clinical study

Aims of Part III

1. Can the tissue engineering principles applied in Parts I & II be translated to the clinical setting to treat bone loss in the femoral head and neck secondary to two different pathological conditions?

Part IV : Modified Impaction grafting technique – Mechanical study

Aims of Part IV

1. Does the use of vibration and drainage to impact bone graft in IBG result in improved graft compaction, prosthetic stability and lower risk of intraoperative fracture?

CHAPTER 2

Materials and Methods

2.1 Reagents, Hardware and Software

Tissue culture reagents including α-MEM, Foetal calf serum (FCS), ascorbate, dexamethasone and all staining agents were purchased from Sigma – Aldrich, UK, unless otherwise stated. Cell Tracker Green^{TM} CMFDA (5-chloromethyl-fluoescein diacetate) and Ethidium Homodimer-1 were purchased from Molecular Probes, Leiden, Netherlands. Collagen I, the polyclonal antibody to type I collagen was a generous gift from Dr Larry Fisher (NIH, Bethesda, Maryland, USA). Morsellised allograft was prepared from banked fresh frozen femoral head (obtained with consent from patients undergoing routine elective total hip replacement surgery, LREC 0091). $P_{DL}LA$ was a kind gift from Professor Kevin Shakesheff in Nottingham. Bench Top CT system for microtomography from X-TEK Systems Ltd, Tring, Hertfordshire, UK.

2.2 Scaffold preparation

2.2.1 Allograft

Highly washed morsellised allograft scaffolds were used in all studies obtained from fresh frozen femoral heads that had been stored at -80^{o}C for greater than 6 months. These had been retrieved with the consent of patients undergoing elective or traumatic hip surgery at Southampton General Hospital. Only tissue that would have been discarded was used, with the approval of the local ethics committee. Under sterile conditions in theatre unmarked femoral heads were defrosted by soaking in warm normal saline, followed by removal of all soft tissue, osteophytes and cartilage using bone nibblers and oscillating saw (Stryker, Howmedica, UK). The heads were cut into halves and milled using the Aesculap 3mm bone mill (A-one Medical B.V., Netherlands). Previous analysis of a variety of bone mills currently in practice revealed the closest to optimum particle size and distribution (i.e. well graded bone graft mix) was produced from this mill (Dunlop et al., 2003), and was therefore used in this thesis for all allograft preparation. Milled bone graft was soaked in 6% Hydrogen peroxide for 10 minutes, removing all fat and marrow (validation Part 1:

3.4.12). The film of fat which collected on the fluid surface was removed along with the Hydrogen peroxide. The graft was then washed repeatedly with Normal Saline (x3), soaked in antibiotic / antimycotic solution for 24 hours, repeat washed in phosphate buffer solution and left to stand in α-MEM prior to use.

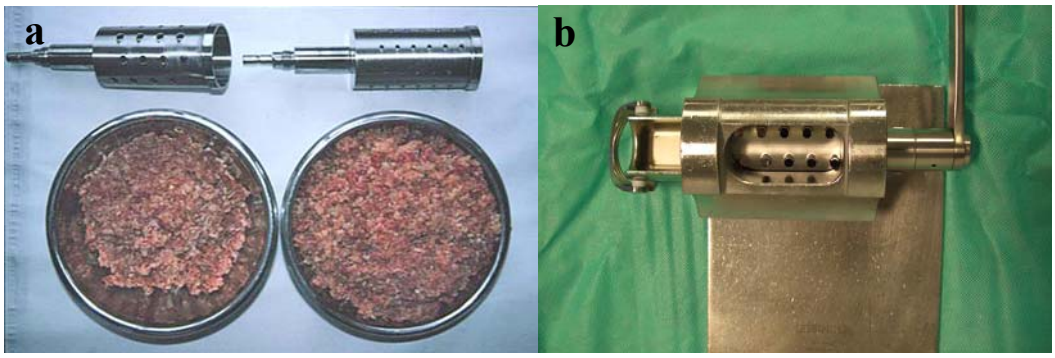

Figure 2-1 Bone mills (a) Aescalup 6 and 3mm graters (A-one Medical B.V., Netherlands) with resultant graft, (b) Leibinger bone mill (Stryker Leibinger GmbH & Co. KG, Germany).

2.2.2 Synthetic graft ($P_{DL}LA$) - Manufacture & Preparation

Poly (D-L lactic) Acid ($P_{DL}LA$) scaffolds were manufactured using high pressure carbon dioxide mixing. The general methodology for production of scaffolds via this method has been previously reported (Barry et al., 2006; Thurecht et al., 2006; Davies et al., 2008). Specific methods for scaffold production for studies performed in this thesis were as follows: 150 mg of $P_{DL}LA$ was weighed into each well of a custom-made 12-well poly(tetrafluoroethylene) (PTFE) collection mould, placed inside a 60 ml pressure vessel and the polymer processed. Conditions used were 24ºC, 230 bar pressure for 30 minutes and rapid decompression over 2 minutes to provide a highly porous foamed structure. Pressure was controlled using a Bronkhorst Hi-Tec BV flow meter (Cambridge, UK) as a back pressure regulator. The scaffolds were cut into 10 mm^3 pieces using a scalpel blade and the whole process repeated until sufficient material for the study was produced.

For micro-CT (μ–CT) analysis, scaffolds were scanned at 55 kV using the Scanco Medical μ–CT 40 machine at a resolution of 12 μm and reconstructed into 3D

models to provide porosity and pore- size data. Porosity of scaffolds was 81% (+/- 4%) with an average pore size of 342μm (+/-174 μm).

$P_{DL}LA$ was provided as chips of approximately $10mm^3$ volumes. Originally the $P_{DL}LA$ chips were morsellised using the same Aesculap 3mm bone mill. However due to the viscoelastic properties of $P_{DL}LA$, the chips did not fragment but simply deformed. An alternative Leibinger spinal bone mill (Stryker Leibinger GmbH &Co. KG, Germany, Figure 2-1b) was used which produced a finer particle range. Ideally the grading of the produced aggregate would have been obtained using sieve towers but this was not possible. Since all morsellised $P_{DL}LA$ used in all the samples (either with or without HBMSC) was obtained from the same mill it was deemed that this information was not an essential requirement for the studies. In Part II, the aim was to compare the shear strength, and its component variables, of $P_{DL}LA$ seeded with HBMSC against $P_{DL}LA$ alone rather than comparing absolute values to other series. Morsellised $P_{DL}LA$ was sterilised in an identical manner to allograft.

2.3 Tissue Culture

2.3.1 Human bone marrow stromal cell culture

Bone marrow samples were obtained from haematologically normal patients undergoing routine total hip replacement surgery with the approval of the local hospital ethics committee. Mesenchymal stem cells were harvested by repeatedly washing the marrow in α-MEM, removing the washed cell population prior to centrifugation at 1100rpm for 5 minutes at 4^oC. The cell pellet was resuspended in 10mls α-MEM and passaged through a 70μm filter. The cell fraction was then plated onto tissue culture flasks (size of which was dependent on yield from sample) and cultured in α-MEM and 10% Foetal calf serum (FCS) under osteogenic conditions (100uM ascorbate-2-phosphate, and 10nM dexamethasone) and incubated at 37^oC in 5% CO_2. The first wash in Phosphate buffer solution (PBS) and media change occurred at day 6 and then was repeated every 3-4 days.

2.3.2 Cell passage

Upon confluence the cells were incubated for 10mins with a 10% Trypsin-EDTA solution in PBS resulting in release from the tissue culture plastic flask. An equal or more volume of α-MEM was added to the lysate to terminate the effect of trypsin. The cell suspension was centrifuged at 1200rpm for 5 minutes at 4^{o}C producing a cell pellet and allowing removal of the solution (containing trypsin). The cells were then resuspended in media (containing 10% serum) and either plated to culture flasks or seeded onto scaffolds.

2.3.3 Cell seeding & agitation

Cells in suspension were counted using a haemocytometer. The volume of suspension required for the desired number of cells was calculated and applied drip wise to the scaffold. Further osteogenic media (containing ascorbate and dexamethasone) was added to ensure complete graft coverage. The seeded scaffolds within an appropriate sterile container were placed on an agitator (Belly dancer) within the incubator for 4 hours, to optimise cell adherence prior to impaction. Passage 1 and Passage 2 cultured cells were used in all studies.

2.4 Impactor design

Previous studies using force plate analysis have determined the total force imparted during a standard femoral impaction bone grafting to be equivalent to a 1.98kg mass falling 65mm onto a circular base plate 60mm in diameter (Brewster et al., 1999). This was appropriately rescaled to produce impactors for both *in vitro* and *in vivo* experiments. Both impactor designs were based on a chamber, into which the graft could be placed and contained, and a piston, applied to the top of the graft with a free sliding drop weight. The weight of the mass and the distance to fall were calculated upon the diameter of the chamber. Calculation of the actual force (i.e. Δ Momentum/Time) imparted on the graft aggregate is problematic due to differing energy absorbing properties of grafts. An "impulse" value was therefore obtained, avoiding the calculation of deceleration time of the impactor onto different densities of

graft. This value provides a momentum change, as a given energy, supplied to a unit area of graft aggregate surface:

Example of calculation (based on *in vivo* impactor (weight 31g, drop height 65mm, pellet 7.5mm diameter)

$$\text{Impulse} = \text{Energy/Unit area} = mgh/\pi r^2$$

$$0.031 \times 9.81 \times 0.065/\pi\ (0.00375)^2$$

$$\mathbf{474\ J/m^2}$$

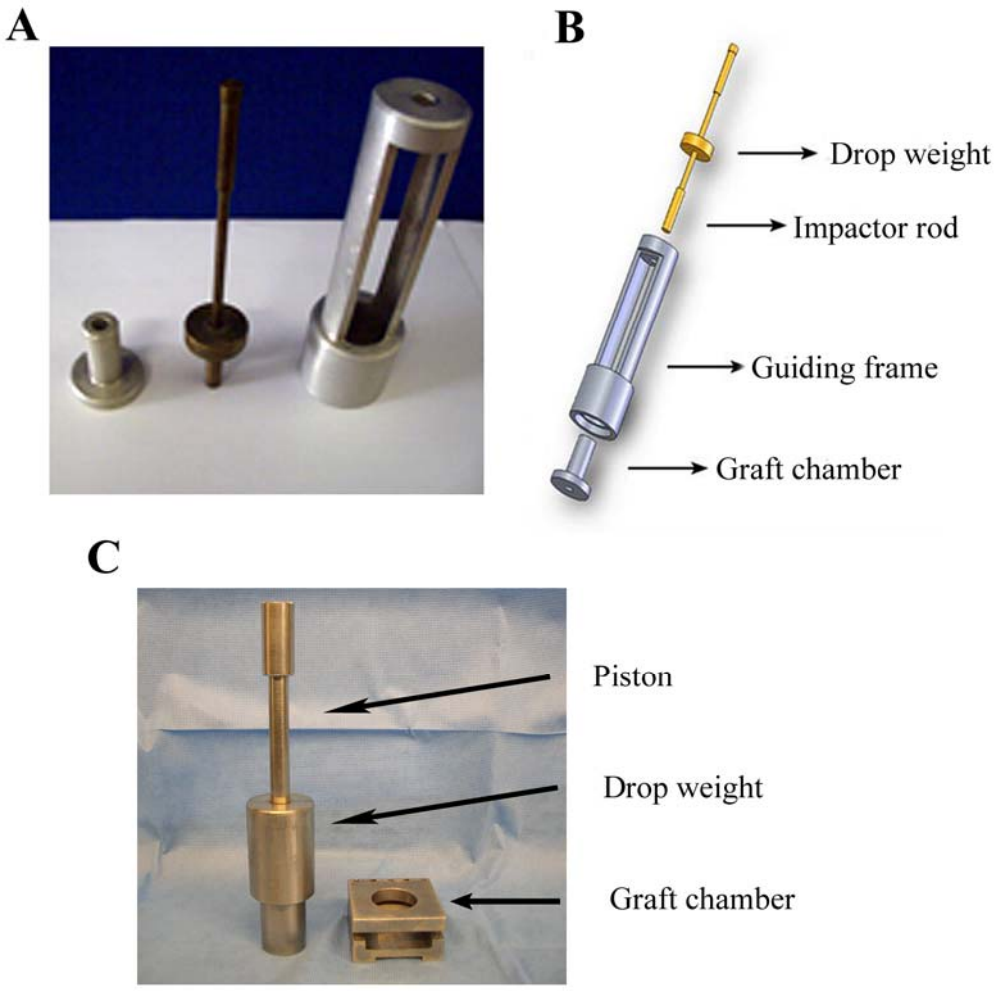

Figure 2-2 Bone Graft Impactors. Photographic and diagrammatic representation of impactor utilised for *in vivo* studies consisting of graft chamber, piston with drop weight and guiding frame and (c) impactor used for *in vitro* studies.

2.5 Scaffold Impaction

Impaction of scaffolds were carried out as described by Dunlop et al (Dunlop et al., 2003). Seeded scaffold was introduced into the top of the impactor in three equal portions, to ensure even compaction. The weight was dropped 24 times from the given height at a rate of approximately 1Hz. The piston was then rotated (to prevent test material adhering to the base of the impactor) and removed. A further portion of scaffold was added and the process repeated, twice, so that the finished pellet received 72 impactions.

2.6 Containment

Following impaction the samples were extruded from the chamber and placed into receivers to ensure complete containment (Figure 2-3 and 2-4). This ensured that the sample remained in the impacted state (refer to *3.4.4*, *4.4.4*. for specific designs)

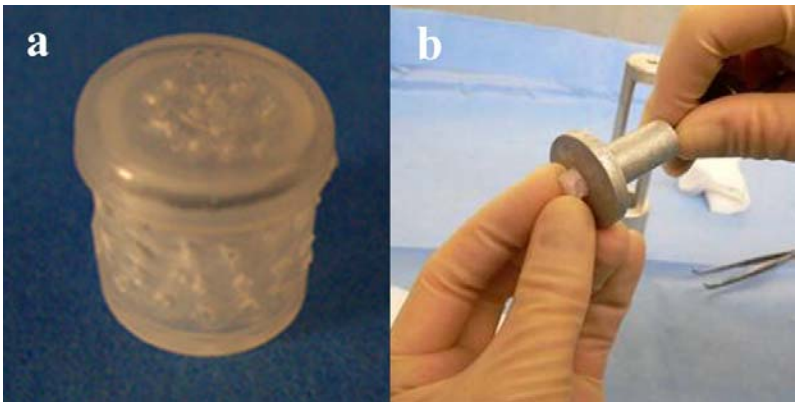

Figure 2-3 Containment apparatus for small impactor samples. Modified perforated electron microscopy pot used for containment of impacted samples during *in vivo* studies. (b) Impacted scaffold pellet extruded from graft chamber into pot.

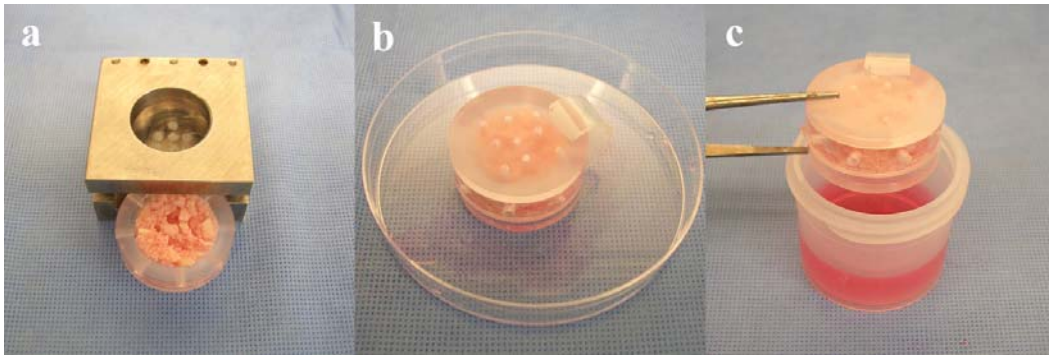

Figure 2-4 Method of containment for large impaction *in vitro* samples. (a) Acrylic ring containing impacted scaffold (b) Application of perforated acrylic discs and clip to maintain sample in impacted state (c) Contained sample placed into polyethylene pot with medium for *in vitro* culture.

2.7 Cell viability

To demonstrate cell viability, the fluorescent probes Cell tracker Green^{TM} CMFDA (10ug/ml) and Ethidium Homodimer-1 (5ug/ml), (CTG/EH-1) were used to label viable and necrotic cells respectively. Prior to fixation, cells were bathed in α-MEM containing CTG/EH-1 at 37^{0}C for 1 hour. Samples were washed twice with α-MEM, bathed for a further 45 minutes (in α-MEM only) repeat rinsed in PBS before fixing in 4% paraformaldehyde for 12 hours. Samples were immersed in PBS and visualised with appropriate fluorescent filters. 3D scaffolds were generally visualised with confocal microscopy using a Leica TCS SP2 laser scanning microscope and software. Alternatively images were captured and processed with Carl Zeiss Axiovision software Version 3.0 via an AxioCam HR digital camera on an Axiovert 200 inverted microscope (Carl Zeiss AG, Germany).

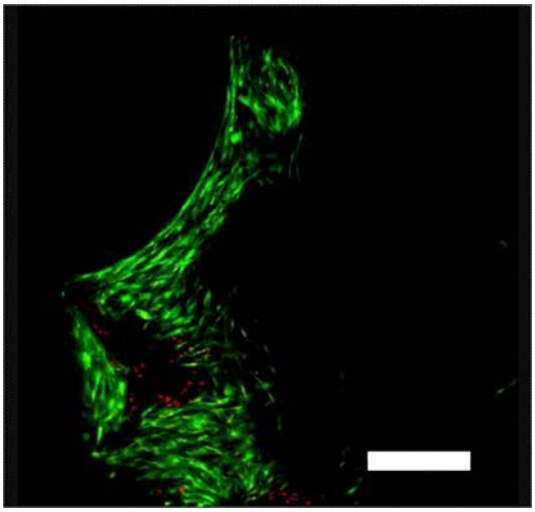

Figure 2-5 Live Dead confocal microscopy imaging. Confocal microscopy image demonstrating viable (green – Cell tracker green immunoflourescent probe) and non viable (red - Ethidium homodimer immunoflourescent probe) cells on impacted allograft scaffold (scale bar = 300μm).

2.8 Biochemical analysis

2.8.1 DNA quantification assay

Allograft: Measurement of DNA concentration was assayed with PicoGreen® dsDNA quantification reagent. Cell lysate samples (10μl) were loaded with 90μl Tris-EDTA (Tris-HCL Ethylenediamine Tetra-acetic acid) buffer and 100μl of 1:200 dilution of PicoGreen® in Tris-EDTA buffer. Flourescence was measured on a Bio-Tek Instruments, Inc. (USA) FLX-800 Microplate Flourescence reader using 480nm excitation and 520nm emission. Results were expressed as ng DNA.

$P_{DL}LA$: Due to crossreactivity of $P_{DL}LA$ with pico green assay, an alternate assay to determine DNA content was used. Samples were frozen in liquid nitrogen at -*70*ºC, followed by freeze drying overnight, until all fluid was removed. 1 ml papain solution was added to the samples and incubated overnight in a waterbath at 60^{o}C. Papain solution was manufactured by dissolving 0.0264g papain in 25ml papain buffer (0.1M dibasic sodium phosphate, 0.005 M cysteine hydrochloride, 0.005 M EDTA). Excess papain was also incubated in identical conditions to act as a blank

control. After allowing the samples to cool to room temperature, triplicate 37.5 µl aliquots of cell lysate from each sample and standard were transferred to a 24 well plate. 0.75 ml Hoechst 33258 working solution and 0.5 ml Hoechst dilution buffer was added to each well and the plate read at excitation λ 360 nm and emission λ 460 nm on a Bio-Tek Instruments, Inc. (USA) FLX-800 Microplate Flourescence reader.

2.8.2 Alkaline phosphatase activity

Allograft: A volume of Trypsin/EDTA (0.05%) sufficient to cover the samples was added and incubated at 37^{o}C and 5% CO_2 for approximately 30 minutes interspersed twice with vigorous vortexing. Following removal of the solution, cells were collected by centrifugation at 13,000rpm for 10 minutes at 4^{o}C, and then resuspended in 1ml 0.05% Triton X-100. Lysis was achieved by freezing –thawing and samples were stored at -20^{o}C until assayed. 10µl of cell lysate from each sample was used to quantify alkaline phosphatase activity. Cell solutions were incubated at room temperature with 90µl of 2-amino-2-methyl-1-propanol buffer containing 100mM p-nitrophenolphosphate (pNPP). The reaction was timed and stopped with 100µl of 1M sodium hydroxide (NaOH). The turnover of pNPP, used to quantify alkaline phosphatase activity, was measured by the absorbance values at 410nm on a Bio-Tek KC4 Kineticalc for Windows Ver.3.01, Rev. & software. Results were expressed as nM pNPP/ng DNA/hr.

$P_{DL}LA$: A volume of 0.02% Sodium dodecyl sulphate (SDS) in saline-sodium citrate buffer sufficient to cover the samples was added and incubated at 37^{o}C and 5% CO_2 for 1 hour. This produced a cell lysate from which 10µl was used to quantify alkaline phosphatase activity, by the method described (*2.8.2*).

2.9 Histological analysis

2.9.1 Fixation and embedding

Samples for alkaline phosphatase staining were fixed in 95% ethanol and all other remaining samples were fixed with 4% paraformaldehyde. All allograft samples were decalcified in EDTA / Tris solution. Imaging using a Faxitron® Specimen Radiography System MX-20 digital with Faxitron® Specimen DR software (Faxitron® X-ray Corporation, USA) was used to determine complete decalcification. Samples were then transferred into PBS solution prior to embedding. For paraffin embedding, samples were first dehydrated for 45 minutes (each) in graded ethanol solutions (50%, 90%, 100%). After being placed in 1:1 ethanol/chloroform solution, samples were placed in chloroform twice for 1 hour, then soaked in paraffin wax at 60^{o}C twice, again for 1 hour. Samples were embedded in hot wax and placed on a cooling surface at 2-4^{o}C to solidify. Embedding of $P_{DL}LA$ required histoclear to be substituted for the chloroform steps as chloroform was found to dissolve the polymer scaffolds. Paraffin wax embedded blocks were stored at 4^{o}C prior to sectioning.

2.9.2 Slide preparation

Paraffin wax embedded samples were removed from cold room storage and trimmed of excess wax. 6μm sections were cut using a Microm 330 microtome (Microm International GmbH, Germany), placed on a water bath at 37^{o}C and allowed to spread. Sections were transferred to pre-heated glass slides on a 37^{o}C hot plate and left for 30 minutes. Slides were moved to a drying oven at 37^{o}C for 2-3 hours and stored at 4^{o}C. Slides were warmed to room temperature prior to staining.

2.9.3 Alcian Blue & Sirius Red staining

After removing excess wax covering the sections with histoclear, the samples were rehydrated by passing through graded methanol solutions. Residual

methanol was removed by submersion of slides in water bath, and followed by nuclear staining with Weigert's haemotoxylin for 10 minutes. Slides were rinsed in water and stained with Alcian blue 8GX for 10 minutes to demonstrate proteoglycan rich cartilage matrix. After 20 minutes pre-treatment with molybdophosphoric acid, sections were stained with 0.1% Sirius red F3B for 1 hour to demonstrate collagen, then dehydrated through reverse graded methanol (50%, 90%, 100%, 100%) and histoclear steps. Sections were mounted mounted with dibutyl phthalate xylene (DPX) under glass coverslips.

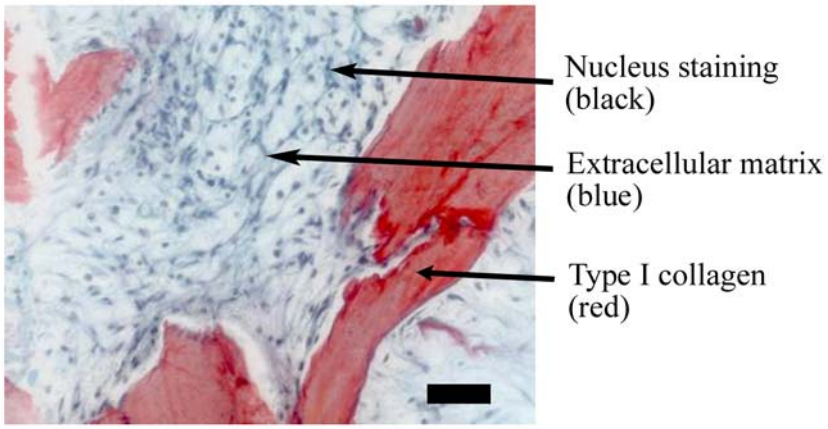

Figure 2-6 Example of Alcian Blue & Sirius Red staining. Demonstrated on a section of allograft seeded with culture expanded HBMSC.

2.9.4 Alkaline phosphatase staining

To demonstrate alkaline phosphatase enzyme activity, samples were incubated with a colourimetric solution reactive to intrinsic alkaline phosphatase. Samples were rinsed in PBS and fixed in 95% ethanol for 15minutes prior to histochemical staining. Naphthol AS-MX phosphate and Fast Violet B salts were combined in accordance with a modified Sigma-Aldrich protocol 104 and applied to culture samples. Reactions were stopped with distilled water following the development of a red-purple stain.

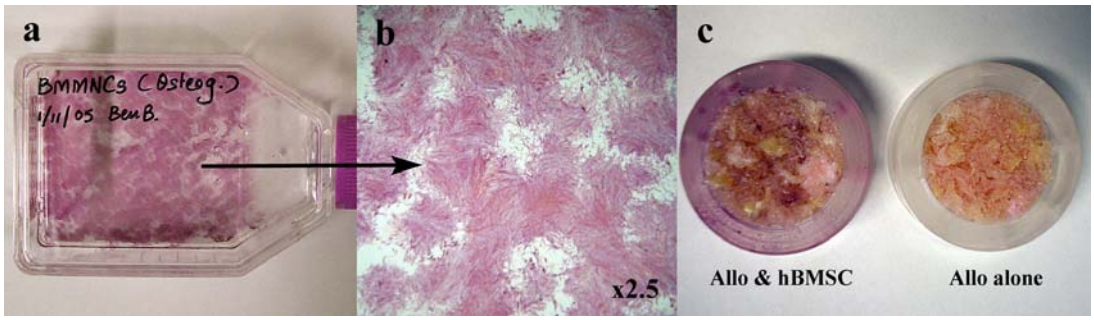

Figure 2-7 Examples of Alkaline Phosphatase staining. (a) 2-D tissue culture plastic (b) magnification of positive stained colonies. (c) Staining on 3-D scaffolds, in this example comparing allograft & HBMSC with allograft alone.

2.9.5 Immunohistochemistry

Excess paraffin wax was removed as previously described (*2.9.3*) and the slides rinsed in a water bath. After quenching endogenous peroxidise activity with 3% H_2O_2 for 5 minutes, sections were rinsed with water and blocked with 1% BSA in PBS for a further 5 minutes. Slides were drained and sections were incubated overnight at 4^{o}C with the primary antibody. Sections were rinsed with water and taken through wash buffers of high salt (1M NaCl, 50mM tris, 0.1% tween), low salt (0.5M NaCl, 50mM tris, 0.05% tween) and tris (0.1M tris, 0.1% tween) for 5 minutes each to remove residual antibody. The appropriate biotin-conjugated secondary antibody was applied for 1 hour followed by further rinses in wash buffers. Streptavidin peroxidise was linked to the secondary antibody complex following 30 minutes incubation and the rinsed again in wash buffers. Samples were developed using 3-amino-9-ethyl-carbazole (AEC) in acetate buffer containing H_2O_2, to yield a reddish-brown reaction product. Nuclear staining with Weigert's haemotoxylin, and a appropriate counterstain was then applied, followed by mounting in glycerol jelly. Negative control slides were always performed by omitting the appropriate primary antibody.
The above method was used to stain for Type I Collagen, Bone Sialoprotein (BSP), Von willebrand Factor (vWF) and tartrate-resistant acid phosphatase (TRAP).

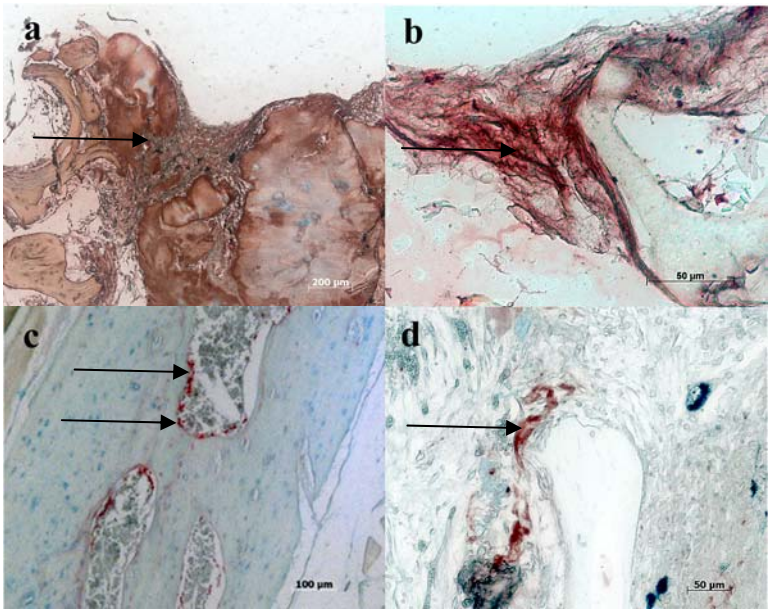

Figure 2-8 Examples of Immunohistochemical staining. Demonstrated on sections of either impacted natural or synthetic graft seeded with HBMSC (a) Type 1 collagen, (b) Bone Sialoprotein, (c) Tartrate resistant acid Phosphatase and (d) von Willebrand Factor (see Part II)

2.10 Micro CT (µ-CT) imaging & analysis

Bench Top CT system for microtomography (Target X-ray source 25-160Kv, 0-100µA, noncontinuous) from X-TEK Systems Ltd, Tring, Hertfordshire was used for all scans. Samples were focused, calibrated and adjusted to prevent X-ray saturation of the sample. The number of frames and the approximate number of angular positions were chosen. The scans were performed with minimised ring artefacts. After the scanning process the raw data was collected and reconstructed using Next Generation Imaging (NGI) software package version 1.4.59 (X-TEK Systems Ltd). The reconstructed images were visualized using Volume Graphics (VG) Studio Max 1.2.1 software package (Volume Graphics, GmbH, and Heidelberg, Germany) and 3D images were created and saved as TIFF & JPEG interchangeable files. The software package allowed segmentation of the scan to allow regions of interest to be analysed.

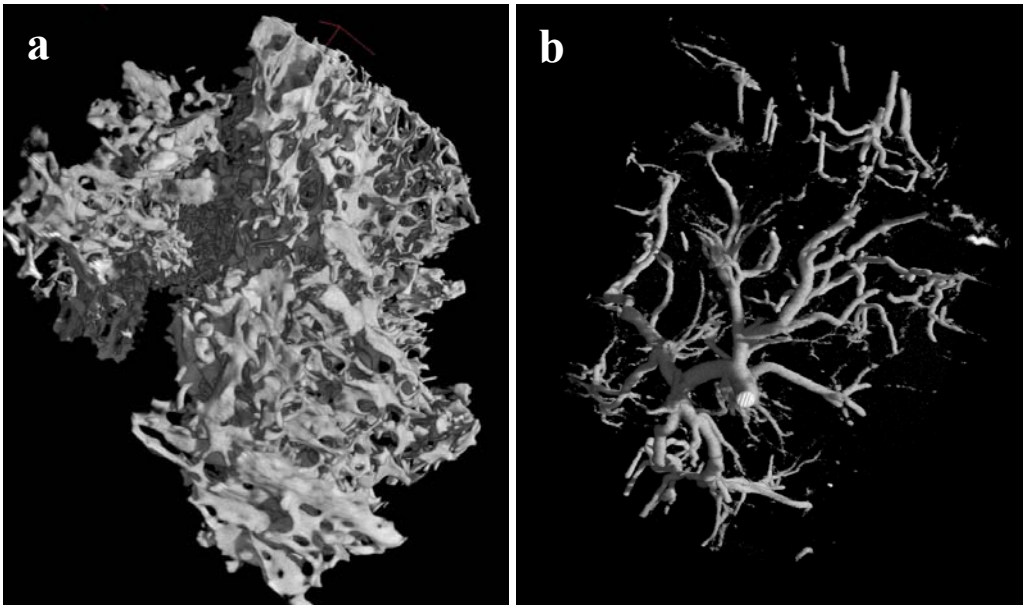

Figure 2-9 Examples of Micro CT imaging. (a) 3D reconstruction of a fragment of morsellised cortico-cancellous bone graft (approximately 10μm resolution); (b) Digital subtraction 3D reconstruction of microvascular network within a tissue engineered living composite.

2.11 Statistical analysis

Statistical significance was assessed with Student's t-test, One-Way Analysis of Variance (ANOVA) with bonferrroni correction or linear regression analysis (GraphPad Software Inc, San Diego, California, USA). All values are expressed as mean ± standard deviation (SD). Multilineage studies were run in triplicate. Graphical representations of P-values were assigned as such; * = $p<0.05$, ** = $p<0.01$ and *** = $p<0.001$.

CHAPTER 3

Part I - In vitro Biological and Mechanical analysis of HBMSC seeded onto Allograft or $P_{DL}LA$.

3.1 Introduction

Tissue engineering is an exciting field that has arisen amidst projections of revolutionizing reconstructive surgery. The fundamental principles involve the combination of living cells within a natural or synthetic scaffold, to produce a three dimensional living tissue construct which is functionally, structurally and mechanically equal to, if not superior to that which it has been designed to replace (Langer, Vacanti, 1993). Currently the use of fresh morsellised allograft in impaction bone grafting for revision hip surgery remains the gold standard offering good mechanical but limited biological support. Bone marrow contains osteogenic progenitor cells that arise from multipotent mesenchymal stem cells and have the potential to differentiate along the osteogenic lineage. Using a simple tissue engineering paradigm, we propose that HBMSC in combination with allograft will produce a living composite with biological and mechanical potential.

3.2 Null Hypothesis

The following null hypotheses were addressed in this study

1. *"HBMSC seeded onto allograft or $P_{DL}LA$ cannot survive the forces of a standard femoral impaction"*

2. *HBMSC seeded onto allograft or $P_{DL}LA$ and impacted and cultured in vitro for 2 or 4 weeks* are unable to continue proliferation and differentiate along the osteogenic lineage"*

3. *"HBMSC seeded onto allograft or $P_{DL}LA$ impacted and cultured in vitro for 2 or 4 weeks* has no effect on shear strength when compared to allograft alone"*

** For $P_{DL}LA$ scaffolds only 4 week study period was tested.*

3.3 Aims

Tissue engineered constructs are dependent upon the cells to grow, differentiate and function on biomaterial scaffolds. In IBG, the scaffold also has an important mechanical role to play in supporting the prosthesis. The primary aim of the study was to establish if HBMSC seeded onto either highly washed morsellised allograft or $P_{DL}LA$, to form a living composite could survive the forces of impaction, and *in vitro* differentiate and proliferate along the osteogenic lineage. The secondary aim was to establish if the living composite thus formed, conferred improved mechanical properties, as measured by shear strength, when compared to the scaffolds alone.

3.4 Study Design

3.4.1 Reagents, Hardware and Software

Impactor, graft chamber, perspex rings, bases and lids were kindly manufactured at Southampton University Bioengineering department and sterilised in 100% ethanol.

3.4.2 Scaffold preparation

Scaffolds (allograft, $P_{DL}LA$) were prepared as described previously (*2.2.1, 2.2.2*). 10cc aliquots of scaffold (volume of graft necessary prior to impaction to produce pellet of correct size) were separated into individual culture containers prior to seeding (7 samples per patient cell line 3 for mechanical testing and 4 for biological analysis).

3.4.3 Cell Culture

Bone marrow samples from 9 patients (including 5 women and 4 men, aged 74-88 years, with a mean age of 80 years) were obtained and prepared as described

(2.3.1.). Cultures were maintained under osteogenic conditions (α-MEM containing 10% FCS, 100μM ascorbate-2-phosphate, and 10nM dexamethasone). $2x10^6$ cells were seeded onto each sample of scaffold (allograft or $P_{DL}LA$) with the addition of media to ensure graft coverage. The sterile pots containing seeded scaffolds were placed on an agitator within the incubator for 4 hours, to optimise cell adherence prior to impaction.

3.4.4 Impactor design

The impactor consisted of a graft chamber 25mm in diameter, a piston with a 344g free sliding weight, and a drop height of 65 mm. During impaction and cell culture, the scaffold was contained in a scaffold chamber consisting of a base, ring and lid machined from cast acrylic rod. When assembled, the three components enclosed a cylinder of scaffold 25 mm in diameter and 10 mm high, a volume of 4.9 cm^3.

The impaction chamber design allowed the easy loading and unloading of the acrylic rings, used to contain the impacted scaffold. In addition, holes within the acrylic rings and in the base of the chamber itself allowed fluid but not particles to escape, so preventing the build up of pressure with its detrimental effect on the degree of impaction.

3.4.5. Impaction

Scaffolds were impacted as described previously (*2.5*). After impaction and removal from the chamber, perforated acrylic discs were place either side of the ring and held with a polyethylene clip. This allowed containment of the impacted scaffold with minimal compressive force. The contained impacted seeded scaffold was transferred into a sterile polyethylene pot with 15mls of osteogenic media and incubated at 37^oC in $5\%CO_2$. Scaffold alone samples were prepared, impacted and cultured under identical osteogenic conditions as a control group. Allograft samples were cultured for either 2 or 4 week periods, with washes in PBS and media changes

every 3-4 days. $P_{DL}LA$ samples were cultured for 4 weeks only due to limited supply of the synthetic graft (Figure 3-1).

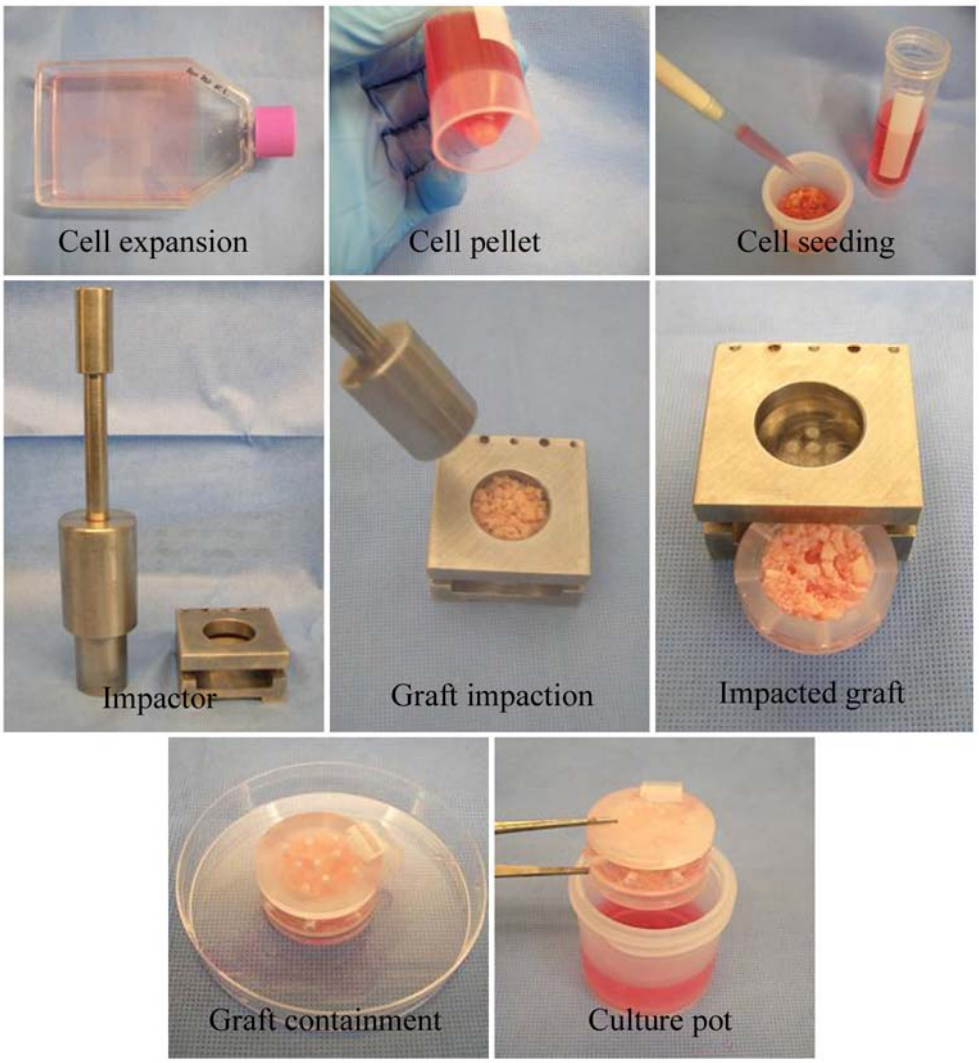

Figure 3-1 Images of cell culture, impaction and containment. Cells were culture expanded on tissue culture plastic, released, pelleted, resuspended, counted and seeded onto washed morsellised allograft or $P_{DL}LA$. This was followed by sequential impaction after which the impacted seeded graft was contained in its impacted state and cultured *in vitro* with osteogenic media.

3.4.6 Analysis of cell viability

Samples from the periphery and centrally within the impacted aggregate were taken from each patient cell line at 2 and 4 week intervals ($P_{DL}LA$ samples - 4

week only) and labelled with CTG/EH-1 as previously described (*2.7*). Confocal microscopy was performed on these samples to look for evidence of viable and non viable cells.

3.4.7 DNA and alkaline phosphatase specific activity

Separate samples were taken for quantitative biochemical analysis. The impacted allograft or $P_{DL}LA$ segments were dissected into equal sized quarters and processed for DNA content and alkaline phosphatase activity using the methods previously described (*2.7.1, 2.7.2*). DNA content was measured as a marker of cell proliferation, and alkaline phosphatase as a marker of the osteogenic activity.

3.4.8 Histological analysis

Samples were fixed in 4% paraformaldehyde, decalcified in EDTA / Tris, processed and paraffin embedded. Cell adherence and proliferation was confirmed with Haemotoxylin and Eosin (H&E) staining. Immunohistochemistry for Type 1 collagen and Bone Sialoprotein (BSP) were performed to confirm cell differentiation along the osteogenic lineage.

3.4.9 Biomechanical testing

In IBG, the mode of failure of the graft or aggregate is shear and therefore shear strength was determined in this study. Soil mechanics studies have demonstrated that shear strength is one of the most important properties of aggregates. It is a measure of their ability to sustain stresses without failure. As mentioned earlier, the shear strength (τ_f) of a granular aggregate, like that of the bone graft or synthetic graft, depends upon the angle of internal friction (Φ) and interlocking (c) of the particles. The frictional resistance varies in proportion with the effective normal stress (σ). The relationship between these parameters can be expressed by the Mohr Coulomb failure law: $\tau_f = c + \sigma \tan\Phi$.

The angle of internal friction (Φ) or angle of shearing resistance is determined mainly by the particle size distribution (grading) of a sample and to a certain extent on the particle shape. Steeper pyramids of aggregates can be made with improved grading, as the particle size distribution is brought closer to a theoretical ('ideal') distribution, which contains particles of all sizes.

Shear strength of a granular aggregate can be measured by a number of different techniques, ranging from basic to highly sophisticated. The ideal method is 3 dimensional (tri-axial) testing (Brodt et al., 1998), as the aggregate is allowed to shear in its weakest plane. Well-compacted aggregate is isotropic (properties equal in all directions) and thus a 2D-testing regime can be applicable. One disadvantage of the 3D method is the large amount of sample material required for each test and complexities of impacting samples in an elastic membrane. The commonest method used by engineers is a direct shear test and was the technique adopted in this study.

The shear strength of all test materials was determined using a Cam shear tester (manufactured at the School of Engineering Sciences, University of Southampton; Figure 3-2). This enabled the mechanical behaviour of particulate materials in combined normal and shear loading to be characterised. It consisted of a fixed upper ring and a mobile lower ring. The normal load was applied by loading weights onto a plunger running in a linear bearing and resting on top of the test material. The normal load was applied five minutes prior to the shear to allow the sample to settle. During the test the mobile lower ring was driven by a hydraulic actuator (Instron Ltd, High Wycombe, Bucks) at a constant rate of displacement of 1.2 mm/min relative to the upper ring, shearing the test sample. The force required to shear the sample and the displacement of the lower ring were recorded using the load and displacement sensors incorporated into the actuator.

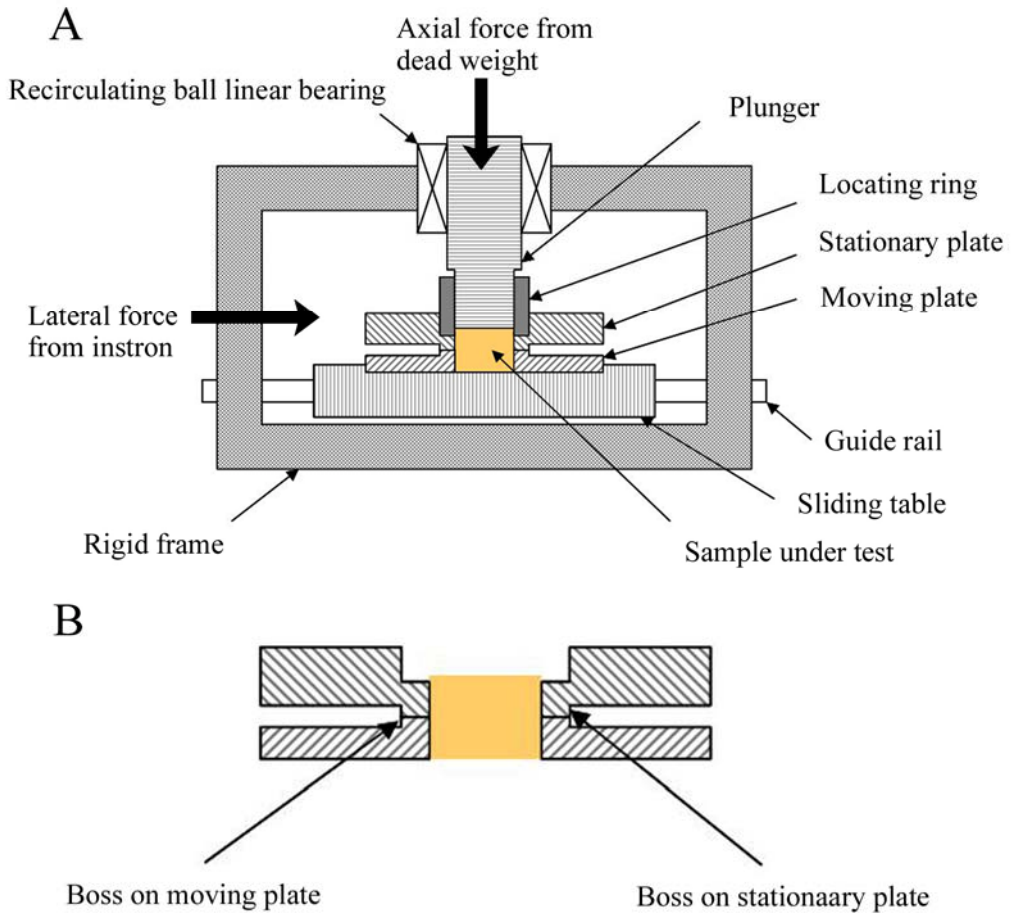

Figure 3-2 Shear tester. (a) Diagram of shear tester design consisting of a fixed upper plate and mobile lower plate in between which the impacted sample is placed. (b) Only contact between the stationary and moving plates is through the sample under test and the contact between the bosses.

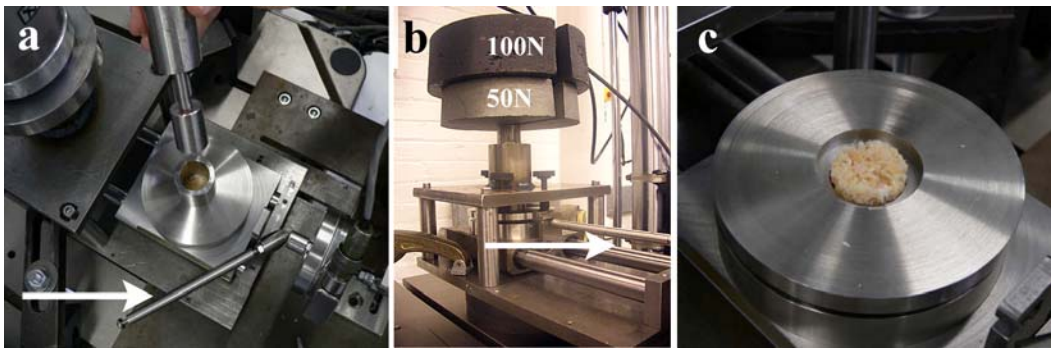

Figure 3-3 Impacted samples in shear tester. (a) Shear tester showing impacted sample between the two plates. The impactor rod was used to extract the sample from the acrylic ring and position the sample accurately between the plates. A rod from the hydraulic actuator (arrow) was attached to the mobile lower ring acting to drive the ring at a constant rate of displacement. (b) Axial compressive force was applied using 50N or 100N weights, (c) Sample within two rings prior to shearing.

Three compressive loads (50N, 150N, 250N) were used on separate samples. These loads generated compressive stresses (102kPa, 306kPa, 509kPa respectively) representative of the lower range of normal physiological stresses. This generated a family of stress-strain curves from which the shear strength at a given shear strain could be determined and plotted against normal stress.

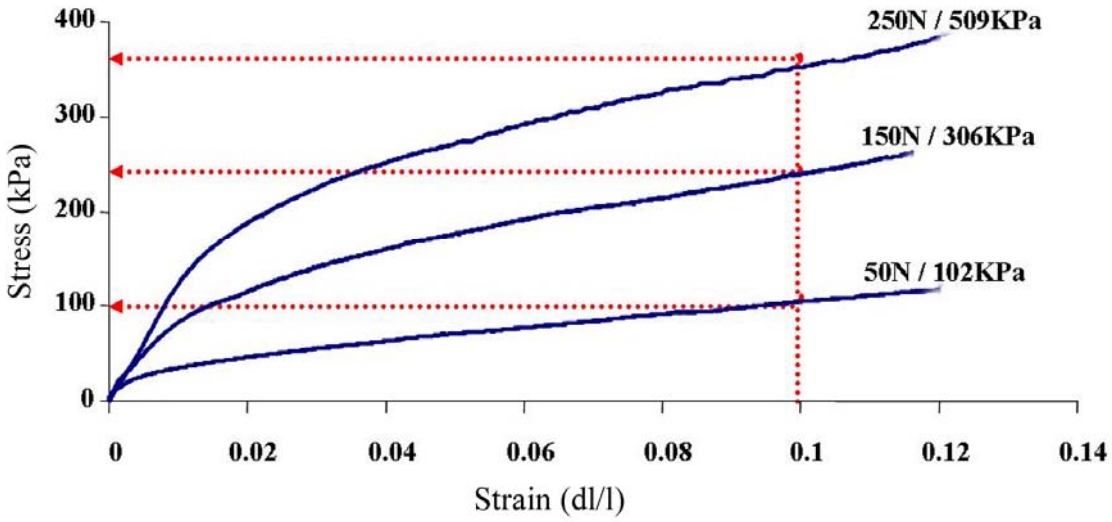

Figure 3-4 Graph of typical family of stress-strain curves. Achieved from shearing samples under increasing axial (compressive) loads.

In this study, shear stress at 9.5% shear strain was taken as shear strength because the stress-strain behaviour of the allograft and $P_{DL}LA$ was such that in most cases there was minimal further increase in shear stress by increasing the shear strain further. The best fit straight line variation between normal stress, (σ), and shear strength, (τ_f), represented the Mohr Coulomb failure envelope.

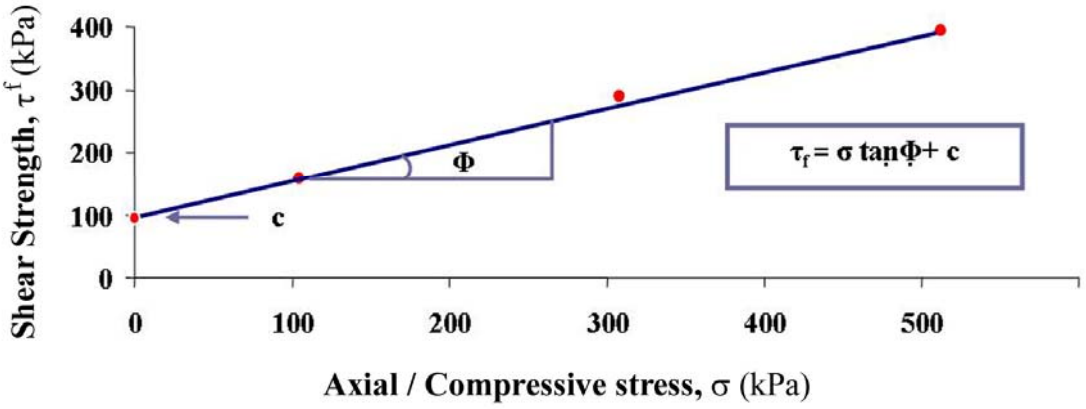

Figure 3-5 Graph of typical Mohr Coulomb failure envelope. The interparticulate cohesion (c), the friction angle (Φ) and the shear strength (τ_f) can be derived from the failure envelope.

From the Mohr Coulomb failure law, it can be seen that (Φ) can be deduced from the slope of the line (cf. y = mx + c. The slope of the line lies around 35 degrees for sandy soils, compared to 55 degrees for gravel). The intersection of this line with the shear stress axis represented the interlocking of the particles (c).

In this study a family of stress strain curves were generated for each cell line (n=3) with controls (n=3) at each time interval (ie 2 & 4 weeks for allograft samples; 4 weeks only for $P_{DL}LA$ samples)

3.4.10 Micro CT analysis

4 week allograft samples from each cell line were imaged at approximately 55 micron resolution using X-Tek micro CT unit (Xtek Systems Ltd., Tring, Hertfordshire,UK). 3D reconstructions using V tech studio MAX 1.2.1 (Volume Graphics GmbH, Heidelberg, Germany) provided a qualititative and quantitative comparison of aggregate density.

3.4.11 Statistics

A general linear model with shear strength as the dependent variable was fitted with axial stress as an independent variable and a categorical term for treatment. SPSS for windows, Version 14 (SPSS UK, Woking, Surrey,UK) was used to conduct the analysis to establish whether there was a linear relationship and whether there was a difference between the control and study groups at both time points. Statistical significance was taken as $p<0.05$. Three patient cell lines were used in all groups and run in triplicate (n=3).

3.4.12 Validation of allograft preparation

Parameters to improve the shear strength of allograft in IBG, include optimum grading, sequential impaction, low state of hydration and washing. Washing is thought to improve the shear strength of allograft by removing the fat and marrow from the interstices of the graft, which both damp the compaction energy applied (as fluids are incompressible) and also remain within the graft, acting as an interparticulate lubricant.

Hydrogen peroxide is an effective defatting agent used in arthroplasty surgery to clean the prepared bone surfaces prior to cementation of the final prosthesis. It was hypothesised that removing all the fat from morsellised allograft would improve the shear strength of the impacted graft when compared to washing in normal saline or no washing. This study was performed to establish a validated protocol for the preparation of all allograft used in all studies.

Three groups were tested. Group 1 – no washing; Group 2 - washed in normal saline, Group 3 – Washed in hydrogen peroxide.

3.4.12.1 Method

Morsellised graft was obtained from 12 femoral heads by the method described and pooled together. Graft was split into three equal volumes by weight.

Graft for group 1 was placed in a sealed bag to prevent drying. Graft for group 2 was washed with 2 litres of pulsed lavage. The surface slurry was removed and the remainder of the fluid and graft was poured over a large swab to allow drainage, before again being place in a sealed bag. Graft for group 3 was soaked in hydrogen peroxide (volume sufficient to cover the graft) and left for 10 minutes. The surface slurry was again removed with the residual hydrogen peroxide. The graft was then washed with 2 litres of normal saline, drained and placed in a sealed bag.

Graft was aliquoted into 20cc volumes prior to impaction. Identical impaction technique and shear testing protocol was used as previously described. 3 samples from each group were tested under 3 axial stresses (102kPa, 306kPa, 509kPa respectively), and by the methods previously described, the Mohr Coulomb failure envelopes for all 3 groups were generated (*3.4.9)*.

3.4.12.2. Results

Interparticulate cohesion, shear strength and aggregate angles were greater in the peroxide group than in the washed and unwashed groups. The values and SD are represented in the table below, along with Mohr Coulomb failure envelopes for all 3 groups (Figure 3-6).

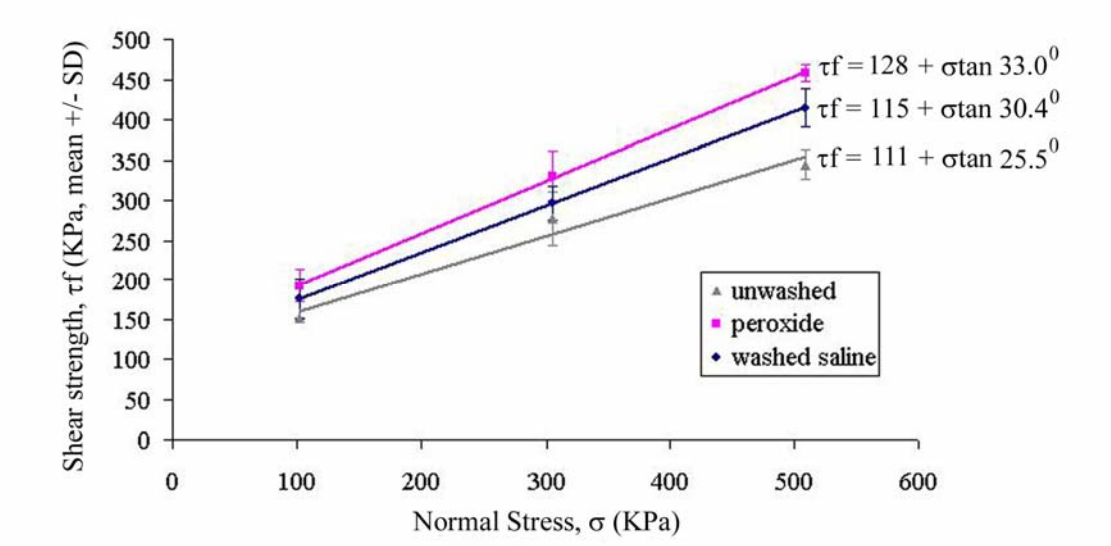

	Interlocking(kPa)	Friction angle (deg)	Shear Strength (kPa)
Unwashed(n=3)	111	25.5	278
Washed	115	30.4	322
Peroxide (n=3)	128	33.0	356

Figure 3-6 Mohr Coulomb failure envelope (unwashed, washed, peroxide). Shear strength envelopes of allograft unwashed, allograft washed in normal saline (washed) and allograft washed in hydrogen peroxide (peroxide), showing regression analysis trend lines and SD error bars. Table demonstrating an increase in shear strength, interparticulate cohesion and friction angle as a result of washing the graft, with the most marked increase seen in the peroxide group (n=3). The values are given as kilopascals at σ = 350kPa.

Washing the graft in hydrogen peroxide and rinsing in normal saline improved the shear strength of the graft when compared to standard techniques of graft preparation. It was postulated that further eradication of fat from the aggregate additionally reduced the damping effect from any residual fat on compaction and reduced interparticulate cohesion. As a consequence of these findings, the graft was prepared in this way for all of the studies described.

N.B These values were generally higher than those observed in later experiments (Part II, IV). This could be due to the following reasons: The graft used was only used in this experiment and therefore this global increase could be as a result of the batch of femoral heads used. The hydration of the graft was likely to be less than the

samples used in the *in vitro* studies, as these samples were immersed in media for either 2 or 4 weeks. A reduction in hydration would result in an increase in shear strength. Finally these samples were impacted and then immediately tested, allowing less time for stress relaxation and disimpaction of the samples. This is in comparison to the *in vitro* samples (Part II), which post impaction, were left in culture for either 2 or 4 weeks prior to testing.

3.5 Results

3.5.1 Cell viability

The survival of cells on impacted allograft and $P_{DL}LA$ was evidenced by fluorescence staining following incorporation of the CTG probe into viable cells and negligible EH-1 staining, a marker of cell death, into non viable cells. In the allograft / HBMSC samples, there was increased number of cells staining with the CTG probe within the 4 week samples when compared to 2 week samples (Figure 3-7).

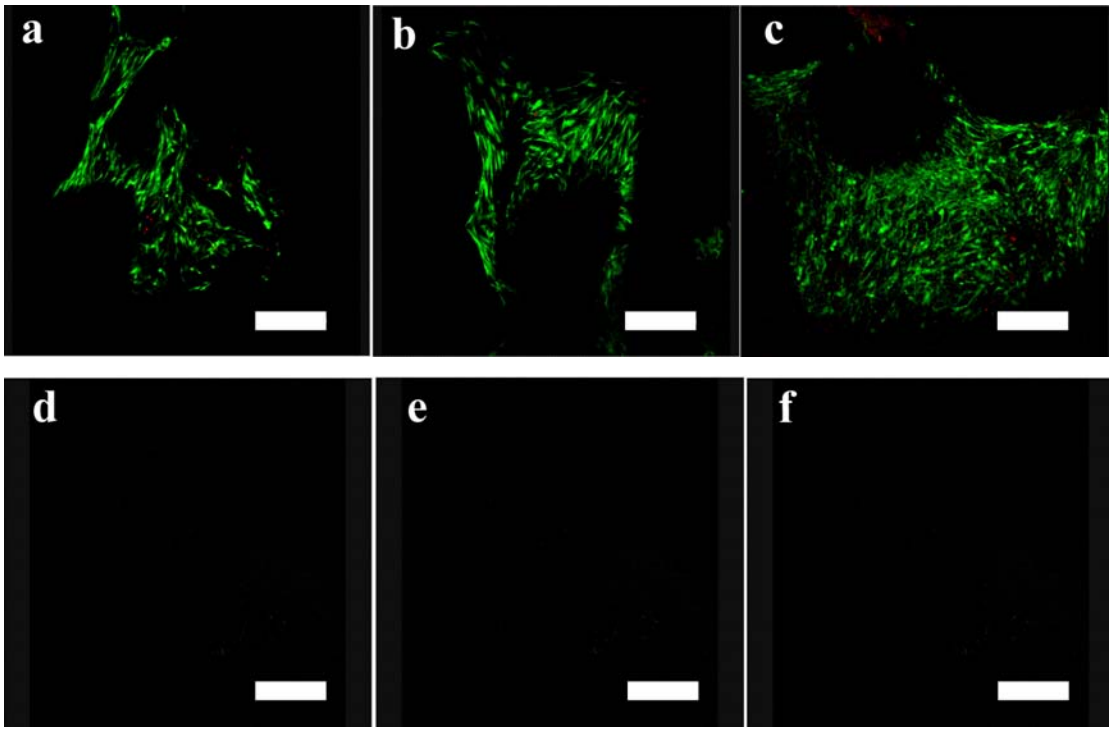

Figure 3-7 EH-1/CTG staining. Confirmation of cell viability with EH-1/CTG staining in (a) Allograft / HBMSC samples at 2 weeks, (b) Allograft / HBMSC samples at 4 weeks and (c) $P_{DL}LA$ / HBMSC samples at 4 weeks using confocal microscopy. Corresponding control images for (d) allograft alone at 2weeks, (e) allograft alone at 4 weeks and (f) $P_{DL}LA$ alone at 4 weeks.

3.5.2 DNA and alkaline phosphatase specific activity

Allograft: There was an increase in the DNA content (2.5-5.3 x 10^3 ngDNA/quarter) and specific alkaline phosphatase activity (0.86-1.48nM pNPP/hr/ngDNA) from impacted allograft seeded with HBMSC compared to allograft alone at 2 weeks. At 4 weeks there was evidence of continued cell viability and proliferation with ongoing rise in DNA content (13.0-21.1 x 10^3 ngDNA/quarter sample) but was associated with a concominant fall in specific alkaline phosphatase activity (0.30-0.55nM pNPP/hr/ng DNA, Figure 3-8 and 3-9). DNA content and specific alkaline phosphatase activity values from allograft alone were negligible at 2 and 4 weeks and were subtracted from the values obtained from the allograft / HBMSC samples.

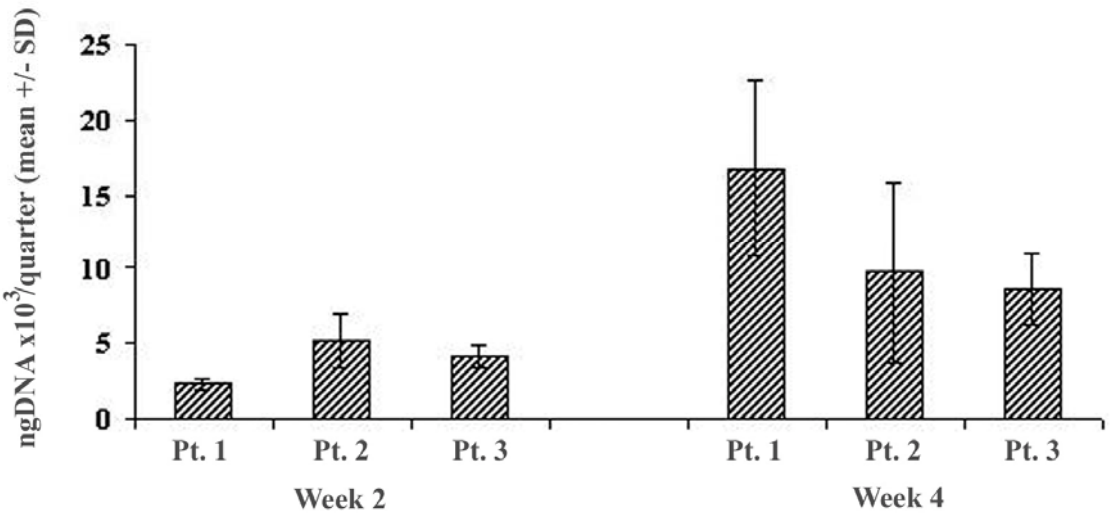

Figure 3-8 DNA content (Allograft). Mean DNA content from three patient cell lines at two and four week time intervals (n=4). An increase in DNA content from 2 to 4 weeks represented ongoing cell survival and proliferation.

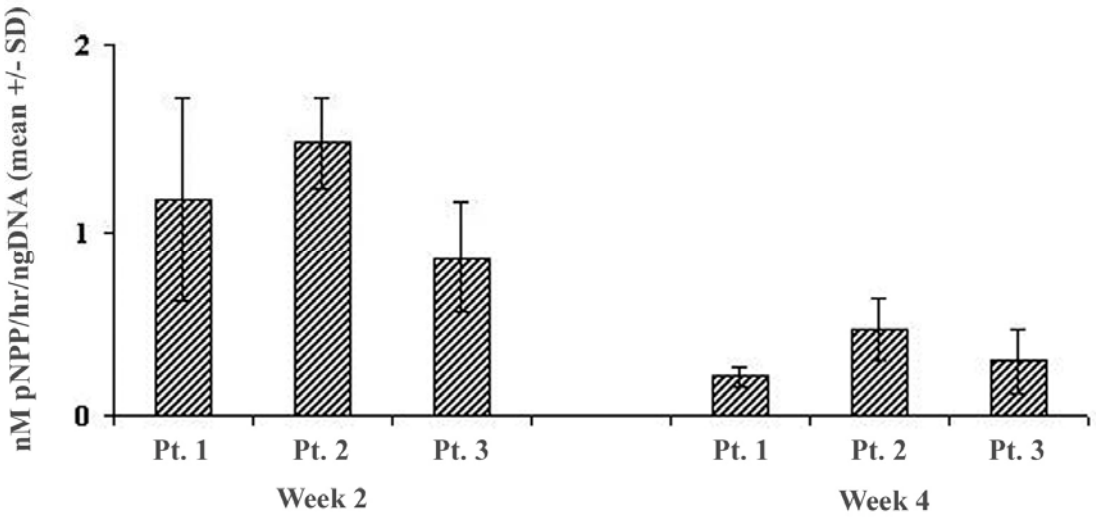

Figure 3-9 Specific Alkaline phosphatase activity (Allograft). Specific Alkaline phosphatase activity from three patient cell lines at two and four week intervals in allograft / HBMSC samples (n=4), demonstrating a fall off in activity with time.

$P_{DL}LA$: There was an increase in the DNA content (9.3-25.6 x 10^3 ngDNA/quarter sample), and specific alkaline phosphatase activity (0.16-1.05nM pNPP/hr/ngDNA) in the impacted $P_{DL}LA$ seeded with HBMSC when compared to

allograft alone. $P_{DL}LA$ alone samples did produce recordable readings of DNA. Since these samples were known not to contain any DNA this was counted as background noise and subtracted from the DNA content values in the $P_{DL}LA$ / HBMSC group.

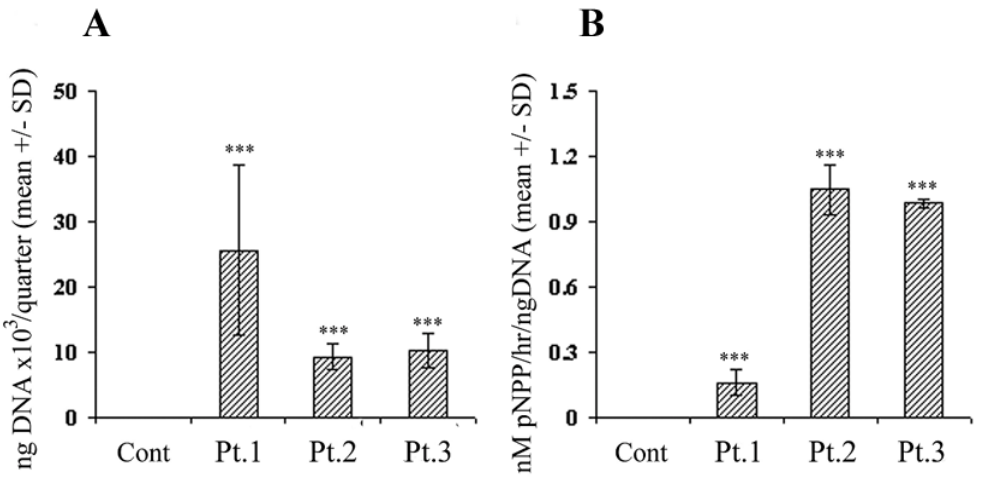

Figure 3-10 DNA content & Specific Alkaline phosphatase activity ($P_{DL}LA$). Graphical representation of mean (A) DNA content and (B) specific alkaline phosphatase activity (n=4, mean +/- SD mean, ***p<0.001). A significant increase in mean DNA content and Specific Alkaline phosphatase activity from three patient cell lines compared to the control ($P_{DL}LA$ alone) indicated cell survival and proliferation in extended cell culture.

3.5.3 Histology & Immunohistochemistry

Haemotoxylin & Eosin and Alcian blue / Sirius red staining confirmed cell presence and adherence (Figure 3-11) with an apparent propensity for the marrow stromal cells to adhere to the fibrous connective tissue layer that remained adherent to the allograft after washing. Strands of developing extracellular matrix and new collagen formation interconnecting $P_{DL}LA$ particles were observed (Figure 3-12). Collagen type 1 and Bone sialoprotein immunostaining confirmed expression of the osteogenic phenotype of the stromal cells both in, $P_{DL}LA$ and allograft / HBMSC groups.

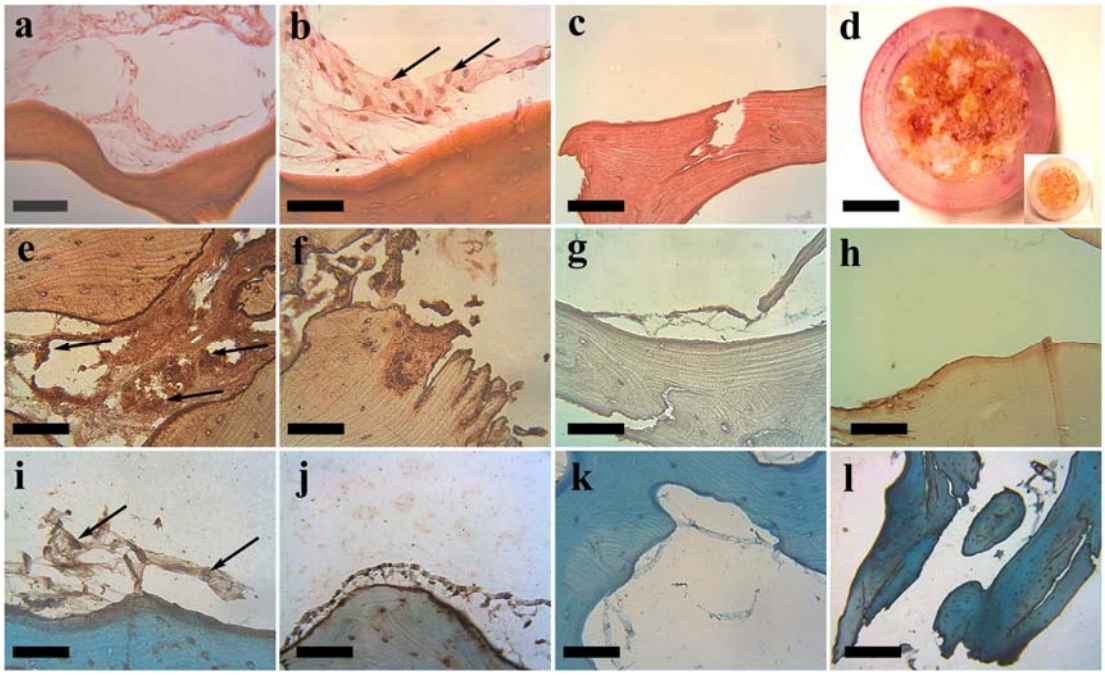

Figure 3-11 Histological & Immunohistochemical staining (Allograft). Haematoxylin and Eosin staining of allograft / HBMSC composite at (a) x10 and (b) x25 magnification demonstrating cells adherent to the allograft surface (arrows) and (c) contrasting bare surface of allograft alone (x10). (d) Alkaline phosphatase positive surface staining on allograft / HBMSC sample (insert: allograft alone, scale bar 10mm). Collagen type 1 staining of allograft / HBMSC composite at (e) x25 and (f) x10 magnification demonstrating the presence of cells with surrounding increased staining (arrows), when compared to (g) negative control (x10) and (h) allograft alone (x10). Increased positive staining for Bone Sialoprotein surrounding a palisade of cells adherent to allograft at (i) x10 and (j) x25 magnification compared with (k) negative control (x10) and (l) allograft alone. (Scale bars = 100μm x10 magnification, 250μm x25 magnification)

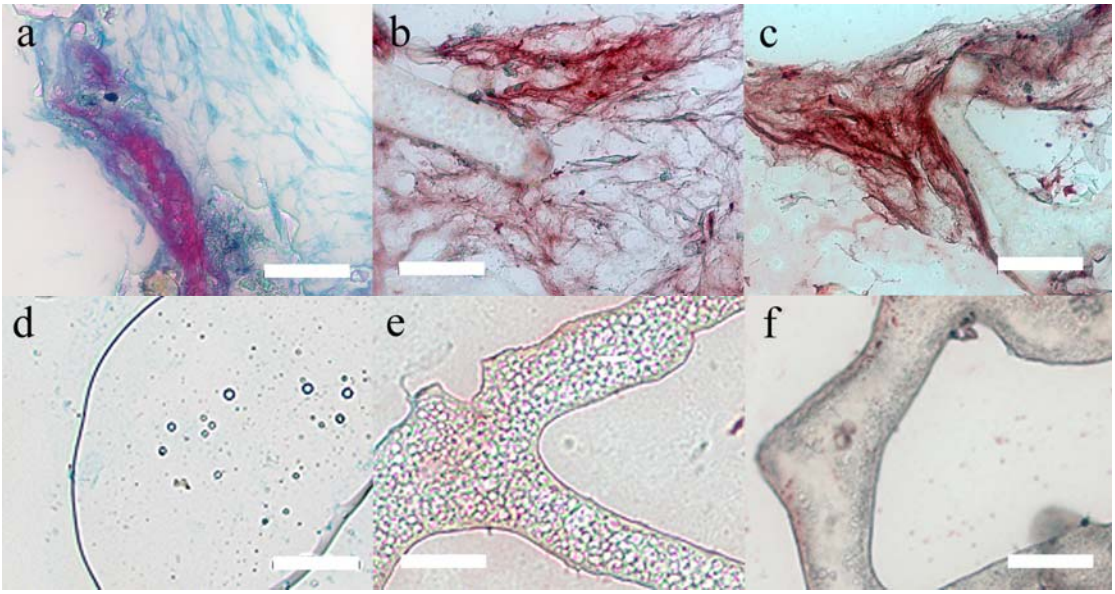

Figure 3-12 Histological & Immunohistochemical staining ($P_{DL}LA$). Alcian Blue and Sirius red staining of (a) $P_{DL}LA$ / HBMSC samples with evidence of collagen and proteoglycan deposition, interspersed with collections of cells adherent to and surrounding the scaffolds. Extensive evidence of staining for Type I collagen (b) and BSP (c) surrounding the $P_{DL}LA$ / HBMSC samples was observed: (all images, x40 magnification; scale bar = 50μm, images (d),(e),(f) = controls).

3.5.4 Shear Testing

Examination of shear strength showed a linear increase with compressive stress (R^2>0.99) for all groups and time intervals, indicating that the grafts satisfied the Mohr Coulomb failure law (Figure 3-13 and 3-14).

Allograft: Interparticulate cohesion (shear strength in the absence of compressive load) and shear strength values, were significantly greater in allograft / HBMSC samples compared to allograft alone at both two and four weeks (n=3, p<0.001, see table in Figure 3-13). There was no difference in aggregate angle between allograft / HBMSC samples and allograft alone at either time point. From 2 to 4 weeks in culture there was no further significant rise in either particle interlocking or shear strength (p=0.7).

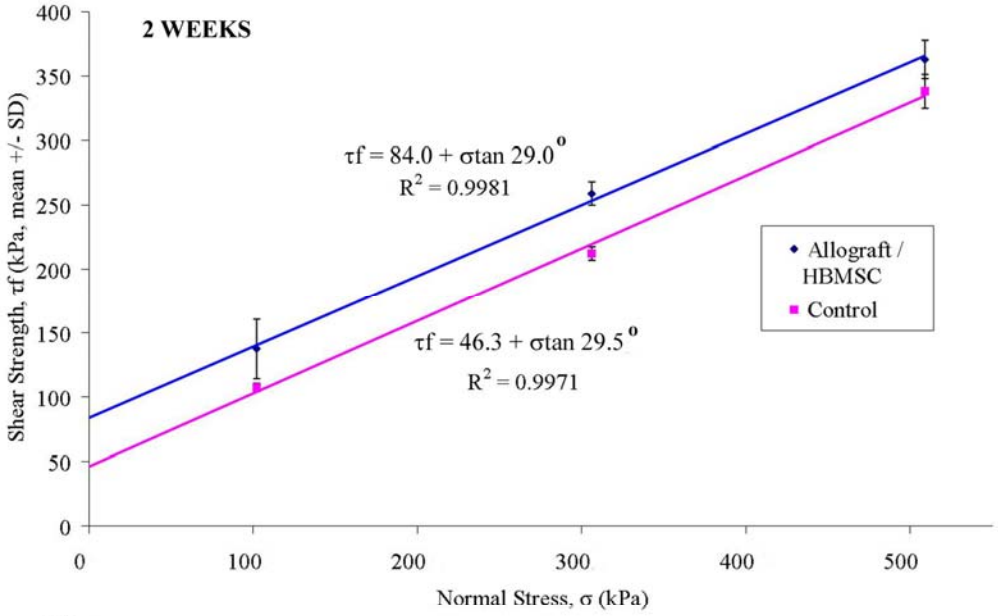

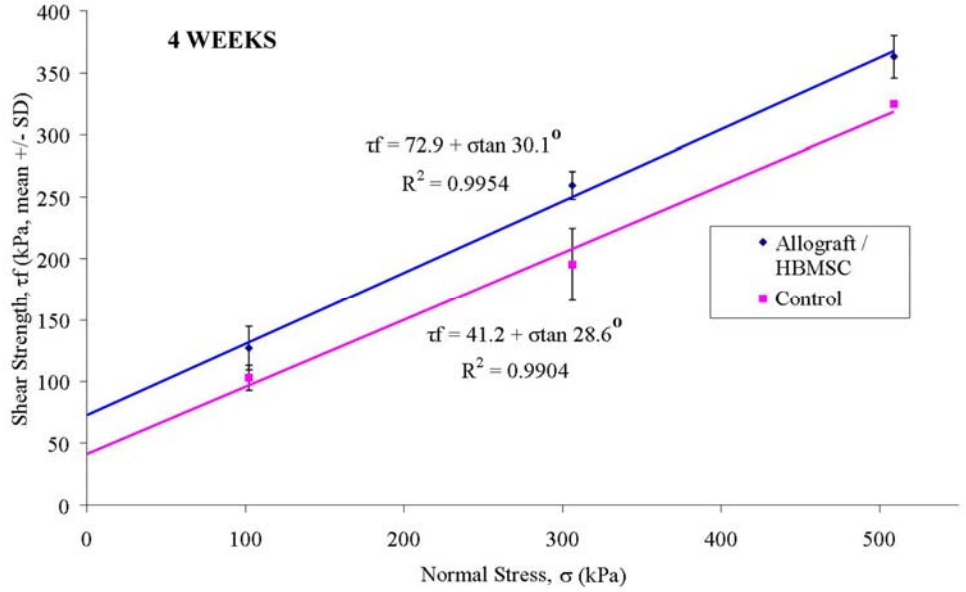

	Interlocking (kPa)	Friction angle (degrees)	Shear strength (kPa)
2 weeks			
Allo & HBMSC (n=3)	84	29	278
Allo alone (n=3)	46.3	29.5	245
4 weeks			
Allo & HBMSC (n=3)	72.9	30.1	276
Allo alone (n=3)	41.2	28.6	232

Figure 3-13 Mohr Coulomb failure envelopes (Allograft). Shear strength envelopes at two and four week time intervals from Allograft / HBMSC composite and Allograft alone, showing regression analysis trend lines and SD error bars. Table depicting an increase in shear strength and interparticulate cohesion at both 2 and 4 weeks in Allograft / HBMSC group compared to Allograft alone (n=3, $p<0.001$). There was no statistical difference in allograft & HBMSC cultured for either 2 or 4 weeks (n=3, $p=0.7$). The values are given as kilopascals at $\sigma = 350$kPa.

$P_{DL}LA$: Interparticulate cohesion and shear strength were significantly greater in $P_{DL}LA$ / HBMSC group compared to $P_{DL}LA$ alone group at 4 weeks (n=3, $p<0.01$). Aggregate angle reduced from 26.4°.in the $P_{DL}LA$ alone group to 21.4° in the $P_{DL}LA$ / HBMSC group.

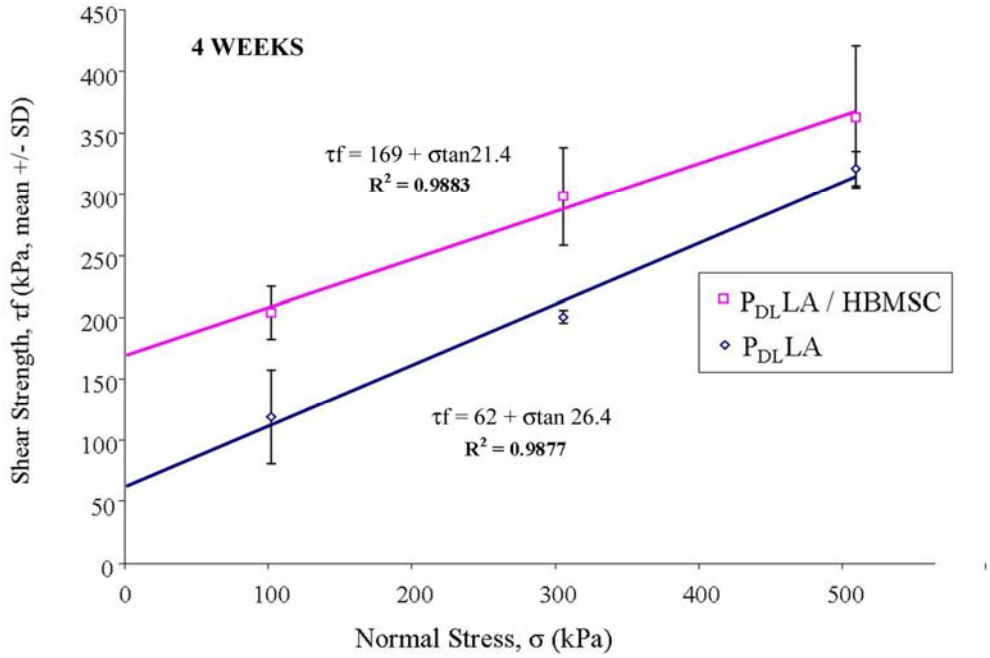

	Interlocking (kPa)	Friction angle (deg)	Shear strength (kPa)
$P_{DL}LA$ / HBMSC (n=3)	169	21.4	306
$P_{DL}LA$ alone (n=3)	62	26.4	236

Figure 3-14 Mohr Coulomb failure envelope ($P_{DL}LA$). Shear strength envelopes at four week time interval from $P_{DL}LA$/HBMSC composite and $P_{DL}LA$ alone, showing regression analysis trend lines and SD error bars. Table depicting an increase in shear strength and interparticulate cohesion with a reduction in aggregate angle in $P_{DL}LA$/HBMSC group compared to $P_{DL}LA$ alone.

3.5.5 Micro CT

Quantitative density analysis confirmed no statistical difference in mean aggregate density, between the two allograft groups at 4 weeks (Figure 3-16). Critically, micro CT analysis confirmed allograft and allograft / HBMSC had similar particulate grading and were exposed to similar degrees of impaction.

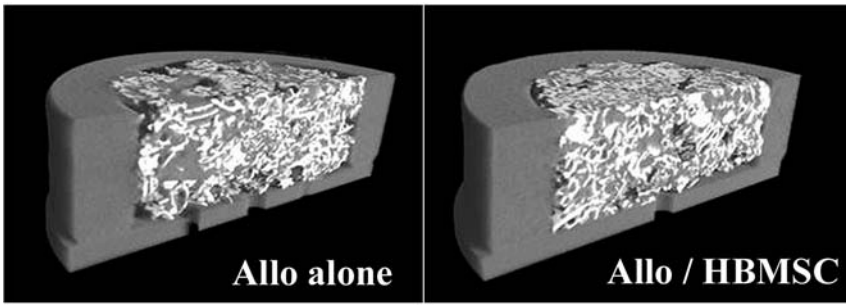

Figure 3-15 3D Micro CT images (Allograft). 3D reconstruction of Allograft & Allograft / HBMSC samples

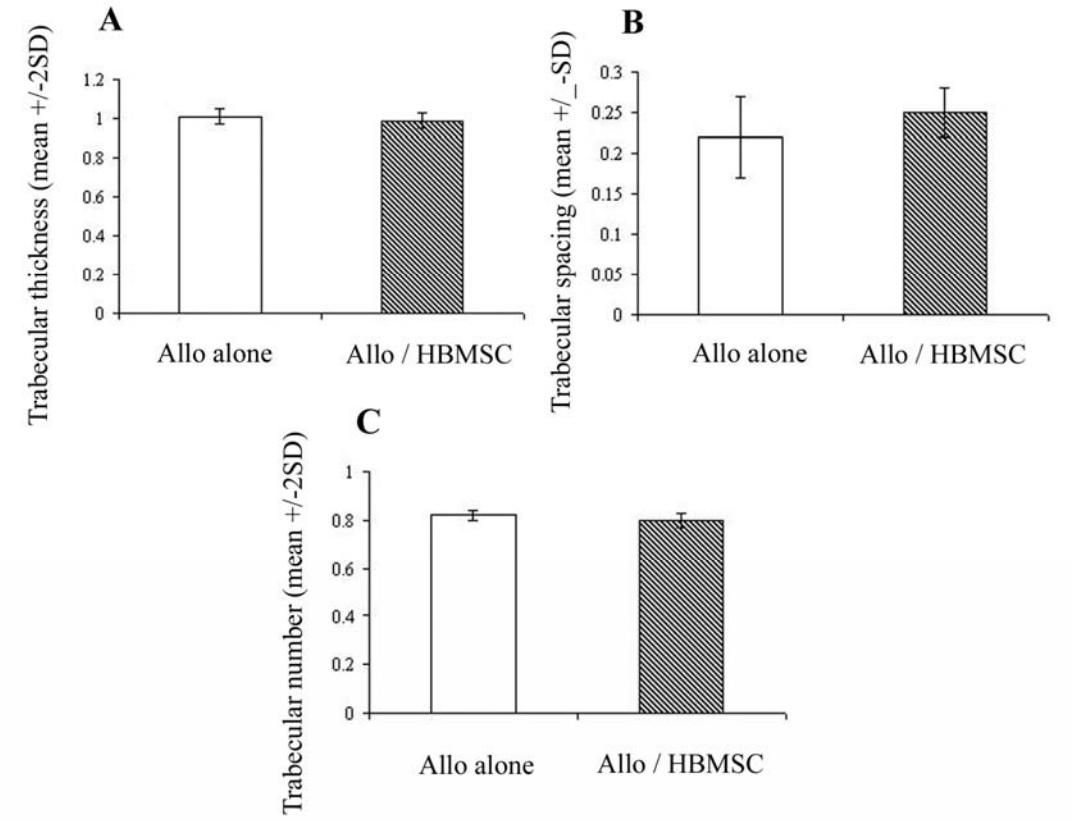

Figure 3-16 Impacted bone graft morphological analysis. Mean (a) Trabecular thickness (mm), (b) trabecular spacing (mm), (c) trabecular number ($x10^6$) in allograft and allograft / HBMSC samples.

3.6 Discussion

This study has demonstrated both biochemically and histologically that HBMSC can adhere to and proliferate on highly washed morsellised bone allograft or $P_{DL}LA$ scaffolds and significantly can withstand the forces equivalent to a standard femoral impaction bone grafting. In addition, the living composite of impacted scaffold and HBMSC, demonstrates a mechanical advantage with increased interparticulate cohesion and increased shear strength when compared to the respective scaffolds alone.

Since the evolution of impaction bone grafting, research has focused on methods to improve the mechanical and to a lesser extent biological characteristics of compacted morsellised allograft. Biological augmentation with osteoinductive agents such as OP-1 has shown mixed results, due to the dual stimulatory effects on both bone regeneration and bone resorption (as a result of osteoclast activation) (McGee et al., 2004; Tagil et al., 2000). Only recently has work been published on *in vitro* studies adding stem cells to scaffolds as a potential technique to augment the biological characteristics of morsellised allograft (Mushipe et al., 2006; Korda et al., 2006). A study by Mushipe et al (Mushipe et al., 2006) has confirmed that a human osteosarcoma cell line (MG63 cells) seeded onto morsellised bovine allograft can survive a limited number of impactions in an acetabular impaction grafting model. Korda *et al* (Korda et al., 2006), investigated the viability of sheep mononuclear cells seeded onto allograft after impaction with a range of forces. These were demonstrated to represent the range of forces encountered by different surgeons performing femoral IBG. The results showed that the cells remained viable in 3kN and 6kN groups but were reduced after 9kN impaction force. The authors concluded that the addition of MSC to allograft could survive normal impaction forces in Revision THR, but recommended avoiding excessively high impaction forces. However, it should be noted that neither of these studies used human (non pathological) cell lines.

In this study, cells were isolated from human bone marrow samples with no cell sorting. This produced a heterogenous population of cells at various stages of

differentiation along the stromal pathway. For HBMSC to play a role clinically in IBG, it would appear more relevant for initial validation studies to be performed using a human non pathological cell line. In addition, cell isolation and culture still involves removal of tissue out of the operating theatre, raising concerns over contamination. Reducing the complexity and number of processing steps during cell culture reduces this risk. For these reasons the cell line and isolation techniques were chosen to enable a safer, less complex translation into the clinical domain.

Morsellised allograft presently remains the gold standard for use in impaction bone grafting. The preparation of this graft is integral to the success of the procedure. Studies have revealed that a well graded mix (proportions of various particle sizes and range) can optimise mechanical strength. In this study the grading of the mixes was identical in both groups (scaffold & HBMSC or scaffold alone), and both were subjected to the same impaction force with the only difference being the presence of HBMSC. There was no difference in the aggregate angle between the allograft / HBMSC and allograft alone samples at either time interval but there was an overall increase in shear strength. This was therefore most likely attributable to the increased cohesion between the particles, and has important clinical implications. Mechanical stability is essential to allow early weight bearing which is important in loading and stimulation of the graft with possible faster graft incorporation (Toms et al., 2004). The increased shear strength provided by an allograft / HBMSC composite could allow not only early mobilisation of our patients but also lead to improved graft incorporation.

Although these results are encouraging, caution must be advocated in advance of validation of mechanical enhancement in an *in vivo* model. The balance between bone resorption and bone regeneration normal seen in fracture healing (and graft incorporation) may be altered when the living composite is subjected to loading and a response from the hosts own cells. This will need to be established to ensure that the augmentation of allograft with HBMSC does not result in a possible accelerated bone resorption prior to bone regeneration, with consequent aseptic loosening and implant failure.

Allograft remains a potential source of retained immunogenicity (and disease transmission) - a risk that may be reduced by the action of washing (Dunlop et al., 2003; Bonfiglio, Jeter, 1972; van der et al., 2003). However, allograft contains important growth factors and cytokines that encourage bone ingrowth and bone formation to replace the morsellised graft. In this study, the graft preparation involved multiple hydrogen peroxide and saline washes, ensuring extensive removal of fat and bone marrow as confirmed on histological analysis (Figure 3-11(c), 3-17) optimising mechanical stability and minimising immunogeneic load.

Figure 3-17 Morsellised allograft. (a) no washing (b) washing in normal saline (c) washing with hydrogen peroxide.

The potential loss of key osteoinductive agents from successive washing protocols would appear to be compensated by the marrow stromal cells, which post impaction continue to proliferate and differentiate along the osteogenic lineage as evidenced by a rise in DNA content and specific alkaline phosphatase activity. Thus a highly washed, well graded aggregate seeded with HBMSC enhances both mechanical and biological potential. Further reduction in the immunogeneic load and risk is provided by the use of freeze dried irradiated bone. It is currently debatable whether this form of preparation is detrimental or indeed enhances mechanical strength (Cornu et al., 2000; Cornu et al., 2003). Either way, the improved shear strength from proliferating HBMSC in combination with a scaffold without the potential for disease transmission or immunological complications is an attractive alternative to the current gold standard.

Further optimisation of mechanical performance along with offloading the already stretched demand on banked allograft, has been shown by the addition of bone

substitutes (van Haaren et al., 2005; Fujishiro et al., 2005; van Haaren et al., 2005). These bone substitutes alone, however, do not add any osteoinductive biological enhancement to the aggregate. In this study, the addition of HBMSC to $P_{DL}LA$ followed by impaction provided osteoinductive potential, confirmed with initial cell viability and ongoing proliferation along a bony lineage at 4 weeks (Figure 3-9). Mechanical analysis demonstrated an improvement in aggregate shear strength and particulate cohesion when compared to $P_{DL}LA$ alone. However, there was a reduction in the aggregate angle in the $P_{DL}LA$ / HBMSC samples. An explanation of these findings could be that when the cells grow, they are creating cohesion between particles at the points of contact which is manifested as an increase in the intercept. When the aggregate sample has undergone a certain degree a shear, these bonds break and the synthetic bone graft is back into aggregate state and friction is again the dominant mechanism that contributes to the shear strength. The small drop in friction angle may be due to lubrication offered by the cell induced deposits on shearing or breakage of angularities. This explanation is also consistent with the fact that 'cohesion' is dominant at low confining compressive stresses. As it is a biological / chemical cementation that is causing the increase in cohesion, this is independent of compressive stress. Therefore, when you test the sample at a larger confining stress, its effect will be small. Frictional resistance to shear on the other hand increases with increasing compressive stress and becomes the dominant factor. This study, however, has only looked at the properties of these living constructs at one time point *in vitro,* in a model that has not been under mechanical loading (unlike in the clinical situation). Therefore before firm conclusions can be made regarding the very exciting potential mechanical enhancement shown from the addition of HBMSC to both allograft and $P_{DL}LA$ scaffolds *in vitro*, the mechanical properties of these living constructs *in vivo* over various time points needs to be established.

3.7 Conclusion

The results in the context of the null hypothesis were examined:

1. "HBMSC seeded onto allograft or $P_{DL}LA$ cannot survive the forces of a standard femoral impaction"

This hypothesis is ***false***

2. HBMSC seeded onto allograft or $P_{DL}LA$ and impacted and cultured in vitro for 2 or 4 weeks are unable to continue proliferation and differentiate along the osteogenic lineage"*

This hypothesis is ***false***

3. "HBMSC seeded onto allograft or $P_{DL}LA$ impacted and cultured in vitro for 2 or 4 weeks has no effect on shear strength when compared to allograft alone"*

This hypothesis is ***false***

** For $P_{DL}LA$ scaffolds only 4 week study period was tested.*

This study has demonstrated that HBMSC when seeded onto either allograft or $P_{DL}LA$ scaffolds can survive the forces of impaction, differentiate and proliferate along the osteogenic lineage and furthermore has an advantageous effect on the mechanical properties of the scaffold.

3.8 Appendix

DNA content: Allograft & Allograft / HBMSC (2 weeks)

	1	2	3	4	Mean (ngDNA)	SD
Pt.1	2.80	2.74	2.71	2.01	2.56	0.37
Pt.2	6.54	6.39	2.73	5.72	5.35	1.78
Pt.3	4.71	4.97	3.28	4.51	4.37	0.75
Control	0.10	0.48	0.31	0	0.22	0.22

DNA content: Allograft & Allograft / HBMSC (4 weeks)

	1	2	3	4	Mean (ngDNA)	SD
Pt.1	16.07	17.02	28.85	22.57	21.13	5.89.
Pt.2	6.83	11.73	19.71	18.48	14.19	6.03.
Pt.3	15.86	13.67	12.64	10.04	13.05	2.42
Control	4.30	4.04	5.14	4.14	4.41	0.50

Summary DNA content: Allograft & Allograft / HBMSC (2 & 4 weeks)

				Minus control	
	Mean (ng DNA)	**SD**		**Mean (ngDNA)**	**SD**
Pt.1 (2/52)	2.57	0.37	**Pt.1 (2/52)**	2.34	0.37
Pt.2 (2/52)	5.34	1.78	**Pt.2 (2/52)**	5.12	1.78
Pt.3 (2/52)	4.37	0.75	**Pt.3 (2/52)**	4.15	0.75
Control (2/52)	0.22	0.22	**Control (2/52)**		
Pt.1 (4/52)	21.13	5.90	**Pt.1 (4/52)**	16.72	5.90
Pt.2 (4/52)	14.19	6.03	**Pt.2 (4/52)**	9.79	6.03
Pt.3 (4/52)	13.05	2.42	**Pt.3 (4/52)**	8.65	2.42
Control (4/52)	4.41	0.50	**Control (4/52)**		

Specific Alkaline phosphatase activity: Allograft & Allograft / HBMSC (2 weeks)

	1	**2**	**3**	**4**	**Mean (nM pNPP/hr/ng DNA)**	**SD**
Pt.1	0.54	0.88	1.63	1.63	1.17	0.55
Pt.2	1.53	1.73	1.15	1.50	1.48	0.24
Pt.3	0.53	0.78	1.25	0.87	0.86	0.30
Control	0	0	0	0	0	0

Specific Alkaline phosphatase activity: Allograft & Allograft / HBMSC (4 weeks)

	1	2	3	4	Mean (nM pNPP/hr/ng DNA)	SD
Pt.1	0.27	0.25	0.38	0.61	0.38	0.17
Pt.2	0.69	0.33	0.51	0.68	0.55	0.17
Pt.3	0.43	0.54	0.49	0.37	0.46	0.07
Control	0	0	0	0	0	0

DNA content: P_{DL}LA & P_{DL}LA / HBMSC (4 weeks)

	1	2	3	4	Mean (ngDNA)	SD
Pt.1	22.24	27.13	50.52	24.35	31.06	13.13
Pt.2	14.04	17.61	13.66	13.66	14.74	1.92
Pt.3	18.42	13.34	13.56	17.66	15.74	2.67
Control	3.05	7.02	6.76	5.12	5.49	1.83

Summary DNA content: P_{DL}LA & P_{DL}LA / HBMSC (4 weeks)

				Minus control	
	Mean (ngDNA)	SD		Mean (ngDNA)	SD
Pt.1	31.06	13.13	**Pt.1**	25.57	13.13
Pt.2	14.74	1.92	**Pt.2**	9.25	1.92
Pt.3	15.74	2.67	**Pt.3**	10.25	2.67
Control	5.49	1.83	**Control**		

Specific Alkaline Phosphatase activity: $P_{DL}LA$ & $P_{DL}LA$ / HBMSC (4 weeks)

	1	2	3	4	Mean (nM pNPP/hr/ngDNA)	SD
Pt.1	0.29	0.19	0.08	0.20	0.19	0.09
Pt.2	1.26	0.76	1.05	1.26	1.08	0.24
Pt.3	1.26	0.38	0.35	0.31	1.00	0.08
Control	0	0	0	0	0	0

Shear Stress Vs Normal Stress (Hydrogen peroxide experiment.)

	Normal Stress (kPa)	Shear Stress at 10% Strain (Av)	Shear Stress at 10% Strain (SD)
Unwashed	101.9	150.3	1.4
	305.6	277.1	32.8
	509.3	344.4	18.4
Peroxide	101.9	192.8	20.8
	305.6	330.5	30.9
	509.3	457.6	11.0
Saline	101.9	175.4	23.8
	305.6	296.5	21.3
	509.3	414.8	23.5

Shear Stress Vs Normal Stress (Allo 2 weeks)

	Normal Stress (kPa)	Shear Stress at 10% Strain (Av)	Shear Stress at 10% Strain (SD)
Allo control	101.9	107.5	3.3
	305.6	211.9	5.2
	509.3	338.2	13.1
Allo & HBMSC	101.9	137.4	23.3
	305.6	259.1	8.9
	509.3	363.0	14.9

Shear Stress Vs Normal Stress (Allo 4 weeks)

	Normal Stress (kPa)	Shear Stress at 10% Strain (Av)	Shear Stress at 10% Strain (SD)
Allo control	101.9	102.9	10.1
	305.6	195.3	29.2
	509.3	325.0	1.5
Allo & HBMSC	101.9	127.2	17.7
	305.6	259.4	11.0
	509.3	363.2	17.3

Shear Stress Vs Normal Stress (PLA 4 weeks)

	Normal Stress (kPa)	Shear Stress at 10% Strain (Av)	Shear Stress at 10% Strain (SD)
P_{DL}LA control	101.9	119.0	38.1
	305.6	200.6	5.1
	509.3	321.2	14.0
P_{DL}LA & HBMSC	101.9	214.6	3.0
	305.6	295.1	48.1
	509.3	375.9	63.4

CHAPTER 4

Part II - In vivo analysis of Biocompatibility, Neovascularisation and New bone formation in impacted Allograft and $P_{DL}LA$ scaffolds seeded with HBMSC.

4.1 Introduction

The success of tissue engineered constructs not only depends on the ability of organ or tissue-specific cells to grow, differentiate and function on biomaterial scaffolds but, in most cases, they are dependent on successful vascularisation post implantation. Cells cannot survive greater than a distance of 200 μm from a blood supply (Brey, Patrick, Jr., 2000). The formation of a blood vessel network, which extend into the implant material will support and supply the metabolic needs of the developing tissue mass, and a cell population capable of responding to the chemical cues to grow new tissue. Hence, a key important design constraint to providing clinically translatable engineered tissue is the development of a microvascular network with properly structured geometry (Brey et al., 2002). This microvascular network will control the mass transport of nutrients, ensure tissue viability, control tissue differentiation, and allow long-term tissue maintenance. For example, in impact bone grafting, the blood supply will be a significant distance away from the central regions of the tissue. The proximity of this vascular supply will become critical when this technique is combined with mesenchymal stem cells to help reconstitute and regenerate bone in both acetabulum and femur (Bolland et al., 2007). Conversely, upregulation of angiogenesis can result in undesirable outcomes such as tumor angiogenesis, and yet, very little is understood about the development, growth-kinetics and structure of the microvasculature in soft-tissue tumours or in bone tissue engineered constructs.

A complete understanding of angiogenesis in any system is limited with current assays and imaging modalities. Many techniques have been developed to study angiogenesis and microvascular architecture. These include histology, immunohistochemistry (Peng et al., 2005), animal perfusion (Langheinrich, Ritman, 2006), vascular casts (Djonov et al., 2001) and micro-computer tomography (μCT) (Langheinrich, Ritman, 2006).

Microvascular networks are complex, exhibiting wide variation among environments and can be greatly complicated due to various pathologies. These assays require broad assumptions with oversimplification of the network microarchitecture.

Angiogenesis can be adequately understood only with a high resolution, three-dimensional, quantifiable assay, where resulting images allow measurement of many parameters, including vascular network density, vessel diameters, void space, and tortuosity.

One technique that has been used over the past 15 years to quantify complex geometries at small resolutions is micro-computed tomography (micro-CT, μCT). Micro-CT works by scanning a subject with high-powered X-rays and rendering the dense regions in a volume. The scan head is rotated 360 degrees around the subject, creating a series of planar slices. Voxel sizes less than 10μm are readily achievable with micro-CT (Guldberg et al., 2004) which is superior to those currently achievable with ultrasound (30μm) and magnetic resonance imaging (100μm). Micro-CT has mainly been used for visualizing and quantifying bone architecture and development (Guldberg et al., 2004) and several studies have been conducted using this technique to quantify trabecular structures (Chappard et al., 2006). More recent studies using radio-opaque contrast agents have enabled the visualization of microvascular structures, such as those associated with bone fracture healing (Duvall et al., 2004), distraction osteogenesis (Moore et al., 2003), coronary artery vasa vasorum (Malyar et al., 2004) and tumour angiogenesis (Kindlmann et al., 2005). However, the detection and quantification of neovascularisation in tissue engineered constructs by micro-CT has not been studied. This led to the development of a novel technique to visualise and quantify neovascularisation using micro-CT along with evidence of biocompatibility and new bone formation in allograft and $P_{DL}LA$ scaffolds seeded with HBMSC in a nude mouse subcutaneous *in vivo* model.

4.2 Null Hypothesis

The following null hypotheses were addressed in this study:

1. HBMSC seeded onto allograft or $P_{DL}LA$ impacted and implanted into the subcutaneous tissue of a nude mouse for 4 weeks are unable to continue to proliferate and differentiate along the osteogenic lineage and commence bone regeneration"

2. "HBMSC seeded onto allograft or $P_{DL}LA$ impacted and implanted into the subcutaneous tissue of a nude mouse for 4weeks do not stimulate neovascularisation when compared to allograft or $P_{DL}LA$ alone."

4.3 Aims

The aim of this study was to establish if HBMSC seeded onto either highly washed morsellised allograft or $P_{DL}LA$, impacted with forces equal to a standard femoral impaction, and implanted into the subcutaneous tissue of nude mice could differentiate and proliferate along the osteogenic lineage and commence new bone formation. The secondary aim was to establish if there was evidence of increased neovascularisation and new bone formation within the living composites, when compared to the scaffolds alone.

4.4 Study Design

4.4.1 Materials and Methods

Polyclonal rabbit anti-human Von Willebrand factor and donkey anti-rabbit IgG-FITC were obtained from Dako, Denmark and Santa Cruz, USA respectively. Recombinant human vascular endothelial growth factor-165 (VEGF) was purchased from Tebu-bio, Peterborough, UK. Microfil MV-120 Blue was purchased from FlowTech, Inc Carver, MA, USA. Electron microscopy pots, impactor and graft chamber were kindly manufactured at Southampton University Bioengineering department.

4.4.2 Scaffold preparation

Scaffolds (allograft, $P_{DL}LA$) were prepared as described previously (*2.2.1, 2.2.2*). $2cm^3$ aliquots of scaffold (volume of graft necessary prior to impaction to produce pellet of correct size) were separated into bijoux containers prior to seeding.

4.4.3 Isolation and culturing of HBMSC

Bone marrow samples from 4 patients (3 women and 1 man, aged 62-85 years, with a mean age of 79 years) were obtained and prepared as described (2.4). Cultures were maintained under osteogenic conditions (α-MEM containing 10% FCS, 100uM ascorbate-2-phosphate, and 10nM dexamethasone). Cells were labelled with long term CTG (Invitrogen) as according to the instructions of the manufacturer. $1x10^6$ cells were seeded onto each sample of scaffold (allograft or $P_{DL}LA$) with the addition of media to ensure graft coverage. The sterile pots containing seeded scaffolds were placed on an agitator within the incubator for 4 hours, to optimise cell adherence prior to impaction.

4.4.4 Impactor design and scaffold containers

The impactor consisted of a graft chamber 7.5mm in diameter, a piston with a 31g free sliding weight, and a drop height of 65mm. The design allowed the generation of an impacted pellet which could be extruded through the base of the graft chamber. Electron microscopy pots were adapted by being cut in half to create a pot volume of $0.7cm^3$ and perforated throughout with a dissection needle.

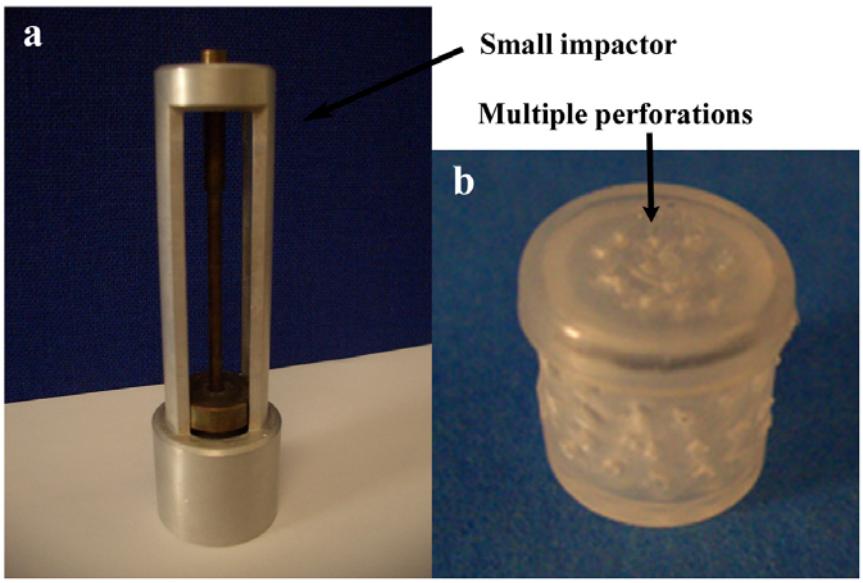

Figure 4-1 Small impactor and container. (a) Image of small impactor with drop weight, piston, guiding frame and graft chamber. (b) Perforated modified electron microscopy pot used to contain impacted samples.

4.4.5 Impaction of samples

Scaffolds were impacted as described previously (*2.5*). After impaction, scaffolds were extruded through the base of the graft chamber directly into perforated electron microscopy pots and placed in osteogenic media prior to implantation into the subcutaneous tissues of nude mice.

4.4.6 Subcutaneous implants of impacted $P_{DL}LA$, allograft and HBMSC

For all *in vivo* studies male MF-1 nu/nu immunodeficient mice were purchased from Harlan, Loughborough, UK and acclimatized for a minimum of 1 week prior to experimentation. Animals had ad libitum access to standard mouse chow and water at all times, and all procedures were performed with prior received ethical approval and carried out in accordance with the regulations as laid down in the Animals (Scientific Procedures) Act 1986. The animals were anaesthetised with fentanyl-fluanisone (Hypnorm), (Janssen-Cilag Ltd) and midazolam (Hypnovel), (Roche Ltd) in sterile water at a ratio of 1:1 and a dose of 10ml kg^{-1} intraperitoneally. Perforated pots containing the impacted allograft / HBMSC or $P_{DL}LA$ / HBMSC composites were inserted subcutaneously into male MFI-nu/nu (SCID) mice (Harlan, Loughborough, UK; 28-32g) (Yang et al., 2003). After 28 days the mice were perfused with microfil (MV-120 Blue FlowTech, Inc Carver, MA, USA).

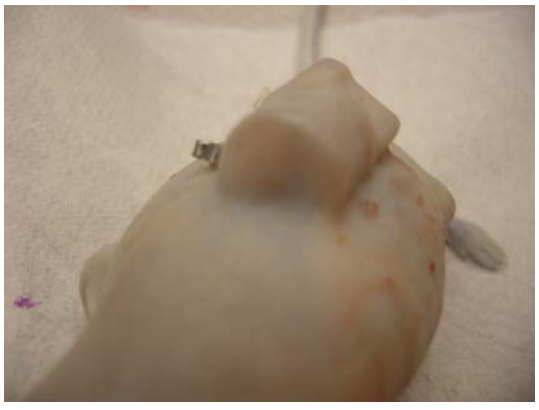

Figure 4-2 Capsule under subcutis in SCID mouse.

4.4.7 Perfusion of Microfil

The mice were anaesthetised with 1:1 and a dose of 10ml kg^{-1}hypnorm/ hypnovel and laid supine to gain access to both mediastinal and abdominal cavities. The skin was prepared with chlorhexidine solution. A midline incision extending across the thorax and abdomen was made. The abdominal cavity was opened with dissection scissors and the bowel loops swept to one side. This allowed visualisation of the right kidney, renal vein and inferior vena cava). 0.01mg of low molecular weight heparin (LMWH) was injected into the IVC after which the abdominal cavity was packed and attention turned to the thorax.

The sternum was split in the midline, and the left side of the diaphragm taken down. The pericardium was incised allowing the left side of the heart to be elevated and visualised. The left ventricle was then perforated with a 22G cannula onto which a 20ml syringe containing 0.5% Normal Saline was attached. A perforation was made in the right atrial appendage and the saline infusion commenced. A steady constant flow rate allowed the infusion pressure to be maintained at a physiological range. Complete exsangination was determined with blanching of the liver along with clear fluid exiting the right atrial appendage.

Pre-prepared solution of Microfil (MV-120 Blue FlowTech, Inc Carver, MA, USA) consisting of a lead chromate-containing radio-opaque polymer, Microfil MV-120 blue and MV-dilutent solutions (1:1) along with MV-curing agent (10% of total volume) was then infused via syringe at a constant sustained rate and pressure. This was continued until the dye was visualised at the right atrial appendage, and within the tail and ear veins.

Packs were applied around the heart to prevent leakage of dye from the cardiac perforations and both thoracic and abdominal cavities closed with clips. The mice were then stored at 4^0C for 30 minutes to stimulate polymerisation of the silicone rubber. The capsules along with a cuff of soft tissue were dissected from the subcutis and fixed in 4% paraformaldehyde.

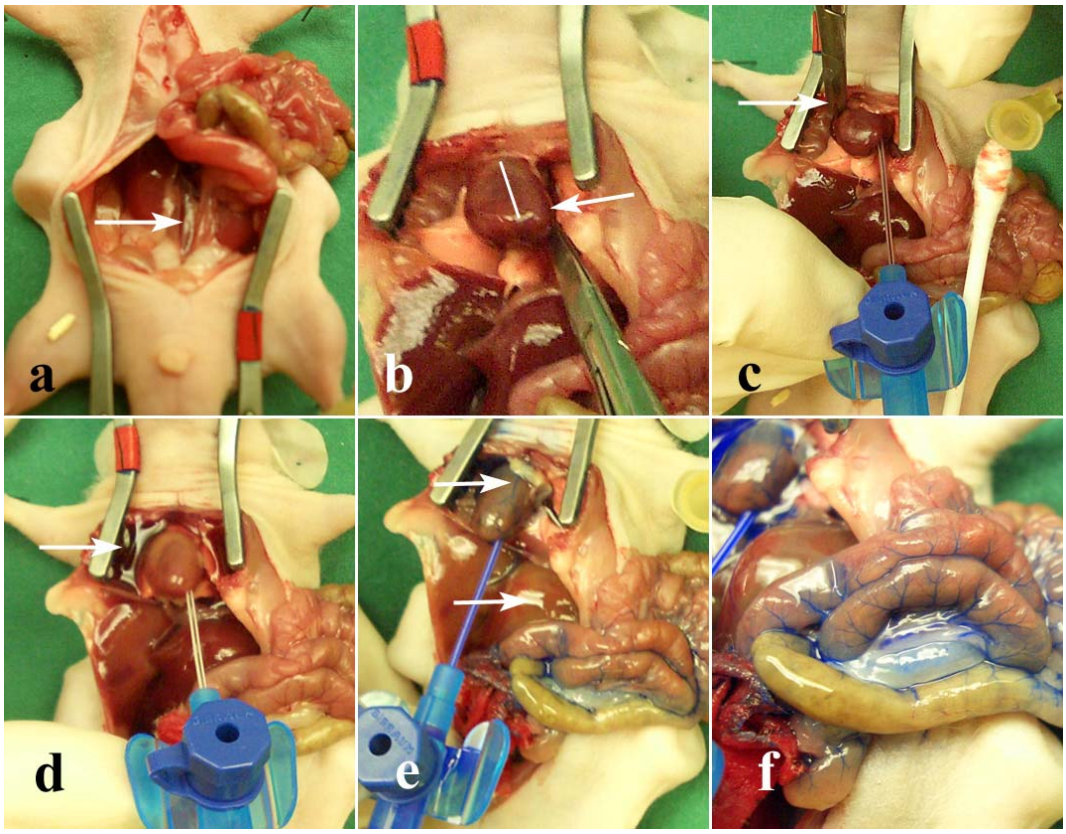

Figure 4-3 Surgical technique for radio-opaque dye infusion. (a) Exposure of the IVC (arrow) for cannulation and injection of heparin. (b) Exposure of heart and visualization of left ventricle (arrow) through midline sternotomy. (c) Perforation of left ventricle with 22G cannula and incision to the right atrial appendage (arrow). (d) Normal saline flushed through the circulation, exiting through the right atrial appendage (arrow), with blanching of the liver (e, arrow) indicating complete exsangination. Slow infusion of microfil contrast agent visualized in coronary (e, arrow) and mesenteric vessels (f).

4.4.8 Micro CT:

The capsules were held securely in a 5ml Bijoux tube and were centred in the middle of the micro CT X-TEK machine. Samples were scanned using settings between 45Kv and 215µA with the number of frames at 16 and the approximate number of angular positions at 1600. After the scanning process the raw data was collected and reconstructed using Next Generation Imaging (NGI) software package version 1.4.59 (X-TEK Systems Ltd) with an average voxel size of 14µm. The reconstructed images were visualized using Volume Graphics (VG) Studio Max 1.2.1 software package (Volume Graphics, GmbH, and Heidelberg, Germany) providing

qualitative 3-D reconstructions along with axial, sagittal and coronal slices. Segmentation tools within the software package allowed the isolation of a volume representing the inside of the capsule only. A region corresponding to a vessel perfused with microfil was selected and the binarisation threshold for that region determined (Figure 4-4). This was taken as the range corresponding to density of microfil only and therefore, the quantification of the total voxel number within this range, represented the total volume of microfil and hence vessel volume within each sample. The scanning parameters and binarisation threshold were kept constant for all samples in all groups. Algorithms developed for bone structural material parameters by VG studio max based on the calculations of Gunnewig (1996) and Parfitt (1987) were applied to the analysis of the microfil based on the gray scale values defined for the radio-opaque dye. All voxels counted in the specified microfil range represented the vessel volume (VV). Vessel volume / Total volume was defined as the ratio of the vessel structure to the total volume analysed. Vessel thickness (VTh) was determined by the ratio of vessel surface (VS) to the vessel volume (VV) and was calculated using the Cauchy-Crofton Theorem from differential geometry. i.e. VTh = 2 / BS/BV. The mean number of vessel structures per unit length was calculated using the formula VN = (VV/TV) / VTh and finally the vessel spacing (VSp) between vessel structures which depends on VN and VTh was calculated using the formula VSp = 1 / VN – VTh. Furthermore, axial slices through the capsules were sequentially visualized and the number of vessels (main trunk only) penetrating the capsules was collated.

The data range corresponding to cortico-cancellous bone (100-450) was used to quantify new bone formation in samples which had not been previously infused with microfil. As a consequence of the volumes of new bone formation representing only a small proportion of the total scaffold volume, small differences in the bone volume of the individual aliquots of morsellised allograft (selected prior to seeding and impaction), rendered it impossible to determine or quantify new bone formation in this group. Likewise comparison of qualitative reconstructions was not useful for the same reason.

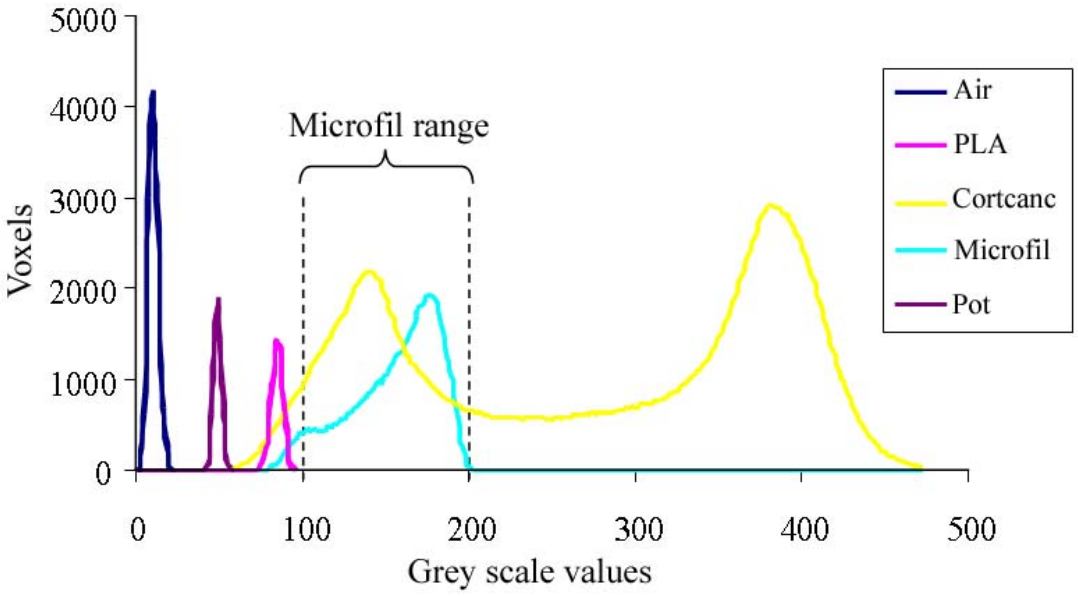

Figure 4-4 Micro CT calibration histogram. Histogram showing the grey scale ranges of all the individual components contained within the impacted samples.

4.4.9 Histology / Immunohistochemistry:

Samples were fixed in 4% paraformaldehyde, decalcified in EDTA / Tris, processed and paraffin embedded. Sections were cut and stained for the nuclear counter-stain Weigert's haematoxylin, followed by staining with 0.5% Alcian blue 8GX for proteoglycan-rich cartilage matrix and 1% Sirius red F3B for collagenous matrix. Immunohistochemistry for new type 1 collagen formation, von Willebrand Factor (vWF), a marker of endothelial cell formation and TRAP, a marker of osteoclast activity were performed.

Histological analyses of the capsules were additionally used to quantify neovascularisation, enabling a comparison to the trends observed using micro-CT quantification. On each slide, blood vessels immuno-positive for vWF in five randomly selected standardised regions of interest (ROI) were photographed at 100x magnification using a Carl Zeiss Axiovert 200 microscope and counted using Axiovision 3.1 software package. A total of 15 representative slide sections across the impacted scaffolds were analysed per group and the mean numbers of vessels/mm^2

were collated. Correlation coefficients, comparing vessel number with positive immunostaining for vWF in each of the groups, and vessel number measured by the micro-CT were calculated.

4.5 Results

4.5.1 Macroscopic appearance

Visual inspection of blue dye within the tail, ear veins and mesenteric vessels, confirming good penetration, was observed in all mice. Dissection of the capsules from the subcutis again allowed direct visualisation and confirmation of a homogenous distribution of radio-opaque dye within all visible vessels.

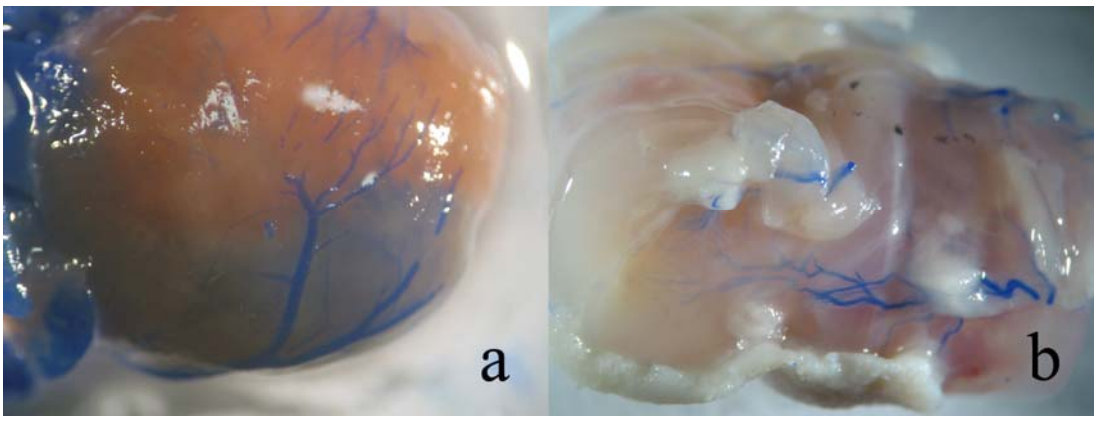

Figure 4-5 Perfusion of vessels with radio-opaque dye. (a) Coronary vasculature (b) subcutaneous tissue surrounding capsule containing impacted sample.

4.5.2 Penetrating vessel number:

The average number of vessels penetrating the capsules were 22.33 ±3.21 (range 20-26) in the allograft / HBMSC constructs compared to 3.67 ±1.53 (range 2-5) in the allograft alone samples and 32.67 ±8.33 (range 26-42) in the $P_{DL}LA$ / HBMSC constructs compared to 7.67 ±3.06 (range 5-11) in the $P_{DL}LA$ alone samples

(Figure 4-6). The difference between the HBMSC and control samples for both allograft and $P_{DL}LA$ was significantly different (**p<0.01, *p<0.05 respectively).

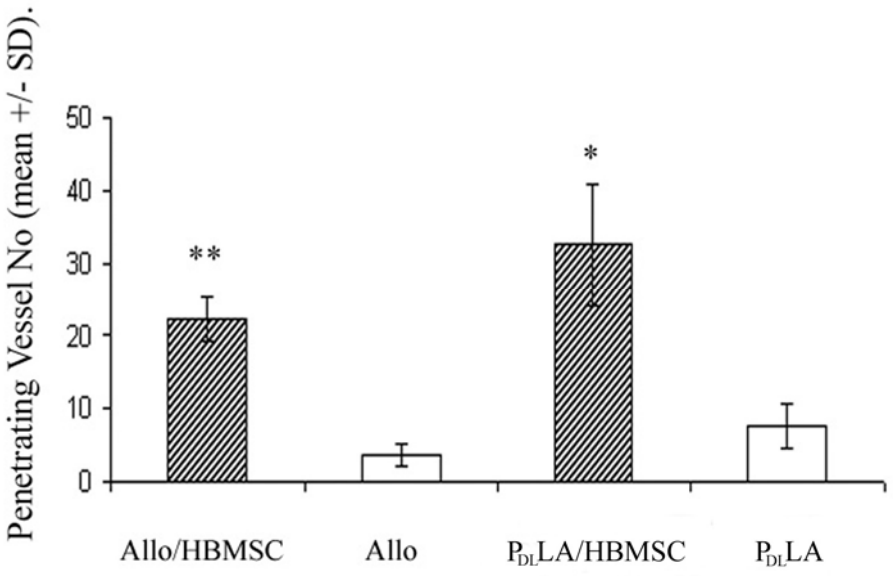

Figure 4-6 Graph representing mean number of penetrating vessels. Mean number of blood vessels penetrating impacted allograft / HBMSC, $P_{DL}LA$ / HBMSC, and control samples. Values are means ± SD; n = 3).

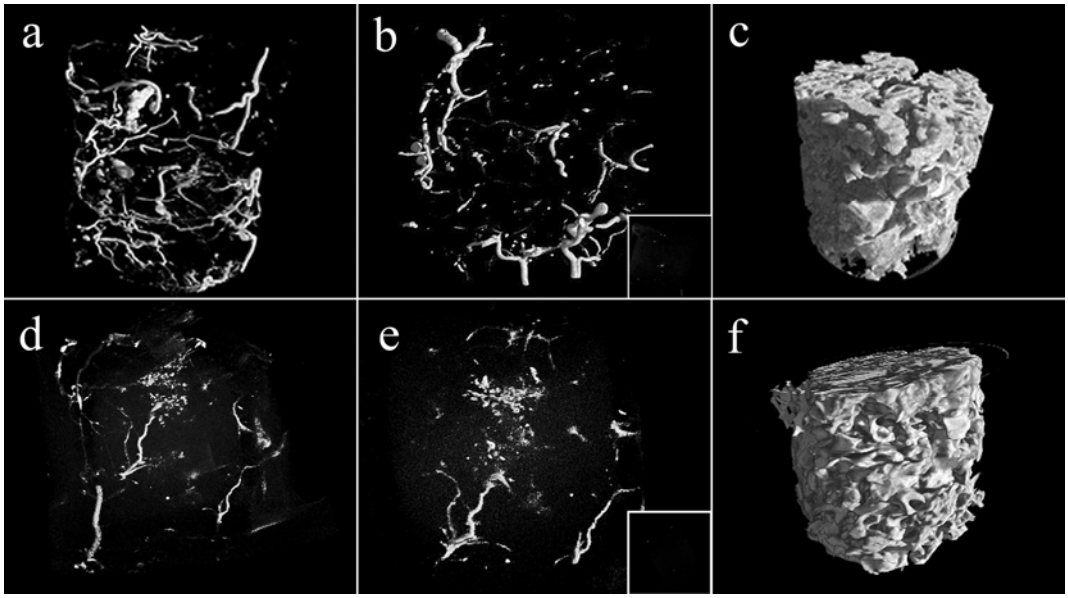

Figure 4-7 3D Micro-CT visualisation of vessel networks. 3D reconstructions demonstrating new vessel formation outside and inside the capsules in impacted $P_{DL}LA$ / HBMSC (a,b) and allograft / HBMSC (d,e) samples compared to allograft (e,

insert) and $P_{DL}LA$ (b insert) alone. 3D reconstructions of the impacted scaffolds: (f) allograft, (c) $P_{DL}LA$.

4.5.3 Vessel volume:

The average total vessel volume within the capsules was 0.57mm^3 ±0.19 in the allograft / HBMSC constructs compared to 0.04mm^3 ±0.04 in the allograft alone samples and 1.19mm^3 ±0.31 in the $P_{DL}LA$ / HBMSC constructs compared to 0.12mm^3 ±0.01 in the $P_{DL}LA$ alone samples (Figure 4-8). The difference between the HBMSC and control samples for both allograft and $P_{DL}LA$ was significantly different (*p<0.05, ***p<0.001 respectively).

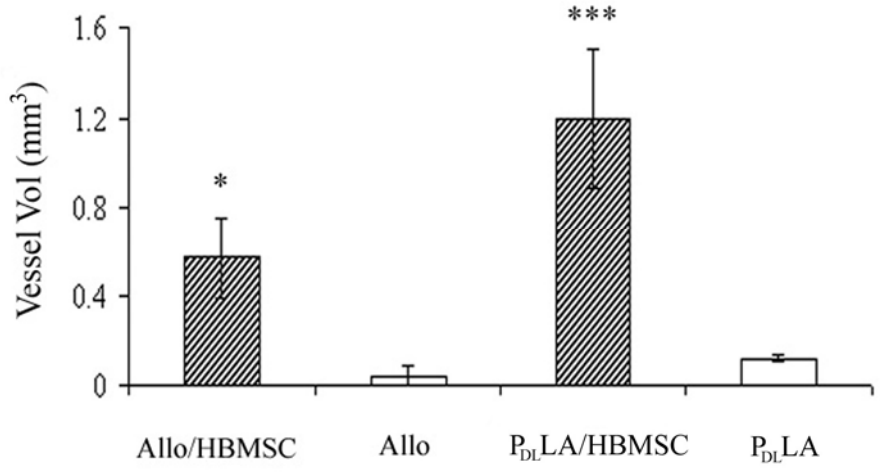

Figure 4-8 Graph representing mean volume of vessels (mm^3). Mean volume (mm^3) of vessels inside the capsules of impacted allograft / HBMSC, $P_{DL}LA$ / HBMSC, and control samples. Values are means ± SD; n = 3.

4.5.4 Vessel volume / Total volume (VV/TV):

The mean ratio of blood vessel volume to total volume (represented by the inside of the capsule only) was 0.005 ±0.003 in the allograft / HBMSC constructs compared to 0 ±0 in the allograft alone samples and 0.01 ±0.001 in the $P_{DL}LA$ / HBMSC constructs compared to 0 ±0 in the $P_{DL}LA$ alone samples (Figure 4-9). The

difference between the HBMSC and control samples for both allograft and $P_{DL}LA$ was significantly different (**p<0.01, ***p<0.001 respectively)

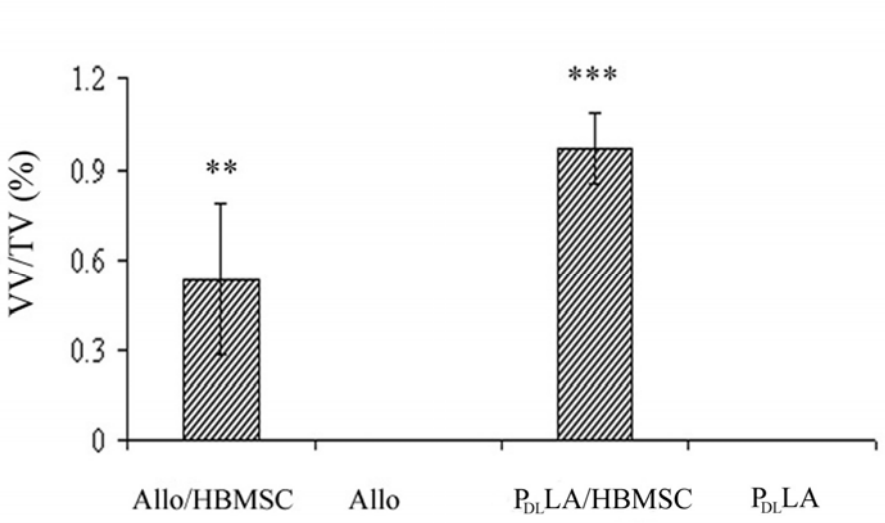

Figure 4-9 Graph representing ratio of vessel volume to total volume. Ratio of vessel volume to total volume in impacted allograft / HBMSC, $P_{DL}LA$ / HBMSC, and control samples. Values are means ± SD; n = 3.

4.5.5 Mean thickness:

The mean vessel thickness was 0.013mm ±0.005 in the allograft / HBMSC constructs compared to 0.01mm ±0.003 in the allograft alone samples and 0.024mm ±0.008 in the $P_{DL}LA$ / HBMSC constructs compared to 0.031mm ±0.05 in the $P_{DL}LA$ alone samples (Figure 4-10) There was no significant difference between the HBMSC and control samples for both allograft and $P_{DL}LA$.

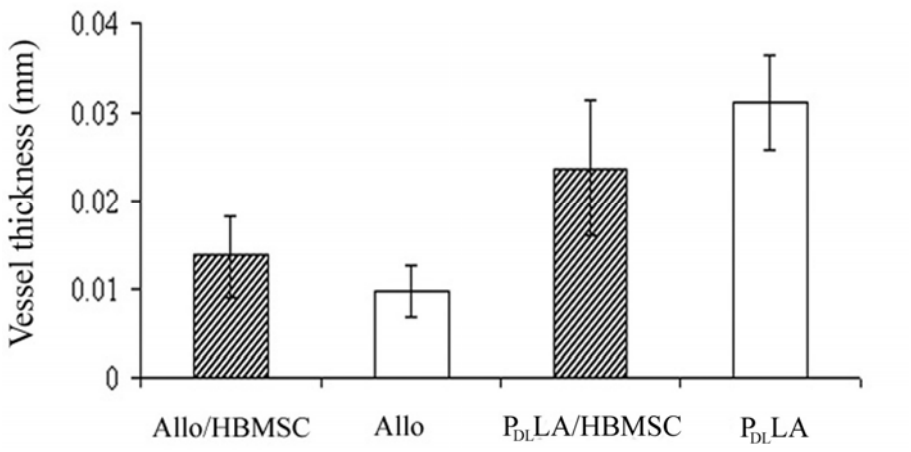

Figure 4-10 Graph representing mean vessel thickness (mm). Mean vessel thickness in impacted allograft / HBMSC, $P_{DL}LA$ / HBMSC, and control samples. Values are means ± SD; n = 3.

4.5.6 Mean spacing:

The mean vessel spacing was 3.91mm ±2.81 in the allograft / HBMSC compared to 2.39mm ±0.85 in the $P_{DL}LA$ / HBMSC constructs (Figure 4-11). Values were not recordable in the controls due to the extremely small number of vessels present within the analysed volume. There was no significant difference between allograft / HBMSC and $P_{DL}LA$ / HBMSC groups.

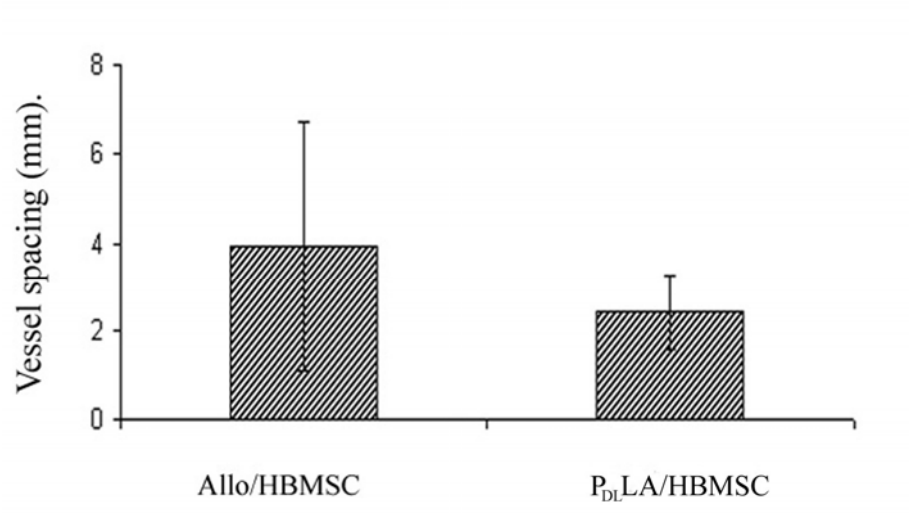

Figure 4-11 Graph representing mean vessel spacing (mm). Mean vessel spacing in impacted allograft / HBMSC and $P_{DL}LA$ / HBMSC. Values are means ± SD; n = 3.

4.5.7 Immunohistochemical analysis of blood vessel ingrowth:

The mean number of vessels per region of interest was 19.29/mm^2 ±2.33 in the allograft/HBMSC constructs compared to 4.95/mm^2 ±1.52 in the allograft alone and 11.91/mm^2 ±5.42 in the $P_{DL}LA$/HBMSC constructs compared to 2/mm^2 ±0.65 in the $P_{DL}LA$ alone samples (Figure 4-12). The difference between the HBMSC and control samples for both allograft and $P_{DL}LA$ was significantly different (***p<0.001, *p< 0.05 respectively). A significant correlation was found between the blood vessels positively staining for vWF counted in the histological sections and the number of vessels calculated by the micro-CT analysis. Correlation: r^2 = 0.502 (significance **p<0.01).

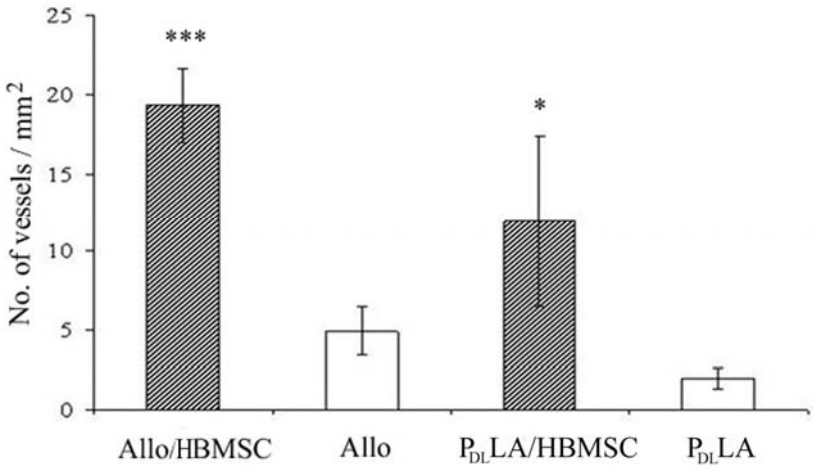

Figure 4-12 Histological quantification of vessel ingrowth. Histological quantification of vessel ingrowth in impacted allograft / HBMSC, $P_{DL}LA$ / HBMSC, and control samples. Values are means ± SD; n = 3.

4.5.8. New bone formation

The average relative total volume of new bone formation in the $P_{DL}LA$ / HBMSC constructs compared to the $P_{DL}LA$ alone groups was 0.47mm^3. In the $P_{DL}LA$ alone samples there was an average reading of 0.02mm^3. This was postulated to be a combination of background noise and contamination in the samples (fine stainless steel particles from the bone mill). This was subtracted from the mean $P_{DL}LA$ / HBMSC value to give relative new bone formation.

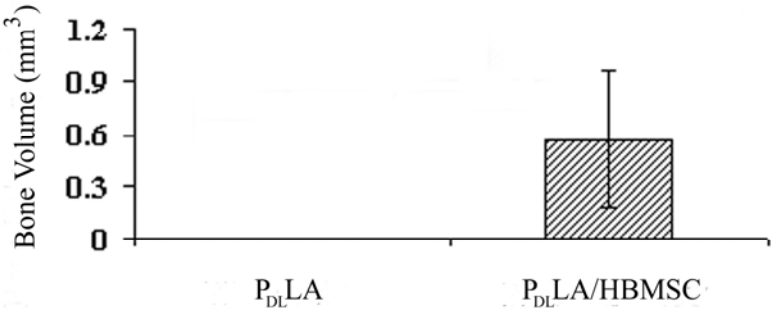

Figure 4-13 Graph representing relative new bone formation (mm^3). Quantification of new bone formation in impacted $P_{DL}LA$ / HBMSC, and $P_{DL}LA$ alone samples. Values are means ± SD; n = 3.

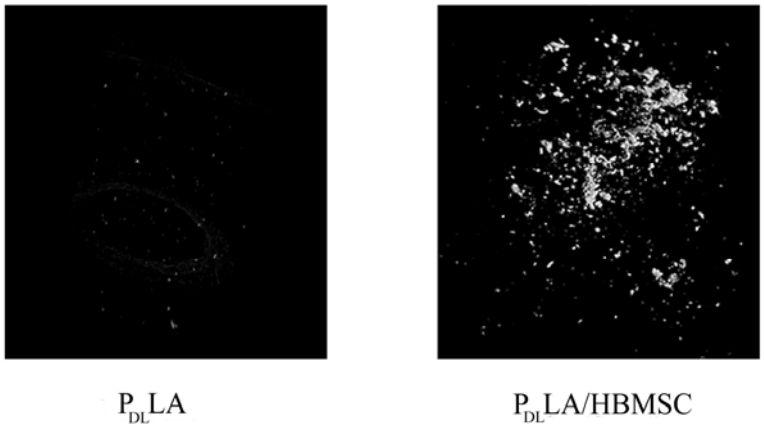

Figure 4-14 Micro CT images of new bone formation. Representative 3D images of new bone formation in impacted $P_{DL}LA$ / HBMSC and $P_{DL}LA$ alone samples.

4.5.9. Cell viability

The survival of cells on impacted allograft or $P_{DL}LA$ was evidenced by fluorescence staining following incorporation of the long term CTG probe into viable cells.

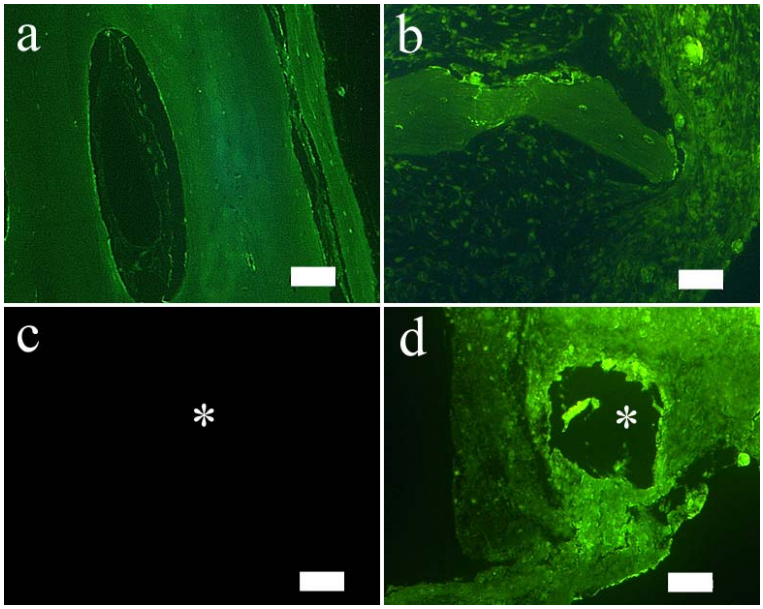

Figure 4-15 Cell tracker green staining. Confirmation of cell viability with CTG immunoflourescent staining in allograft / HBMSC (b), $P_{DL}LA$ / HBMSC (d), control allograft (a) control $P_{DL}LA$ (c) samples. (*represents $P_{DL}LA$ scaffold. Scale bar = 100μm).

4.5.10. Histological and immunohistochemical staining

Alcian Blue and Sirius red staining in the periphery and centre of the capsules confirmed abundance of cells surrounding and adjoining regions of scaffold with interposed areas collagen and proteoglycans in both the allograft and $P_{DL}LA$ / HBMSC samples when compared to allograft / $P_{DL}LA$ alone. Collagen type 1 immunostaining confirmed expression of the osteogenic phenotype of the stromal cells. Multiple discrete areas staining positive for vWF were observed in both the periphery and centre (but to a lesser extent) of the allograft and $P_{DL}LA$ / HBMSC samples. In addition to immunostaining, the dye within the vessels also acted as a method of vessel staining / labelling post sectioning. No staining was observed in the control groups. No positive staining for TRAP was observed in either the periphery or centre of the allograft and $P_{DL}LA$ / HBMSC.

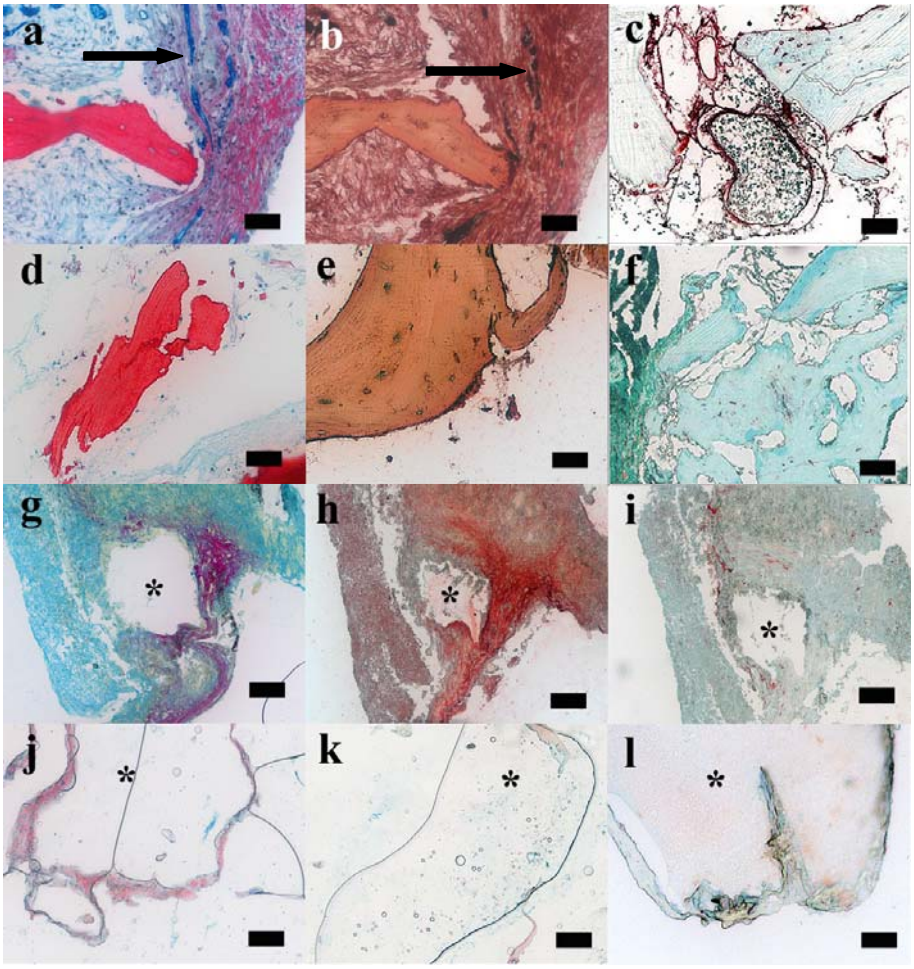

Figure 4-16 Histological & Immunohistochemical staining (Allograft, $P_{DL}LA$). Alcian Blue, Sirius red and Type I collagen staining confirmed positive nuclear staining for cells with surrounding regions of extracellular matrix and type I collagen production in allograft / HBMSC (a,b) and (g,h) $P_{DL}LA$ / HBMSC samples when compared to allograft (d,e) $P_{DL}LA$ alone (j,k). Multiple discrete areas staining positive for von Willebrand factor (vWF) were observed in the periphery and centre of allograft / HBMSC (c) and $P_{DL}LA$ / HBMSC (i) samples. No staining was observed in the control groups (allograft (f) and (l) $P_{DL}LA$ controls). In addition, coloured contrast agent within the vessels provided a facile method of staining and labelling the vessels post sectioning (demonstrated in (a) and (b), black arrow). Scale bar = 100μm.

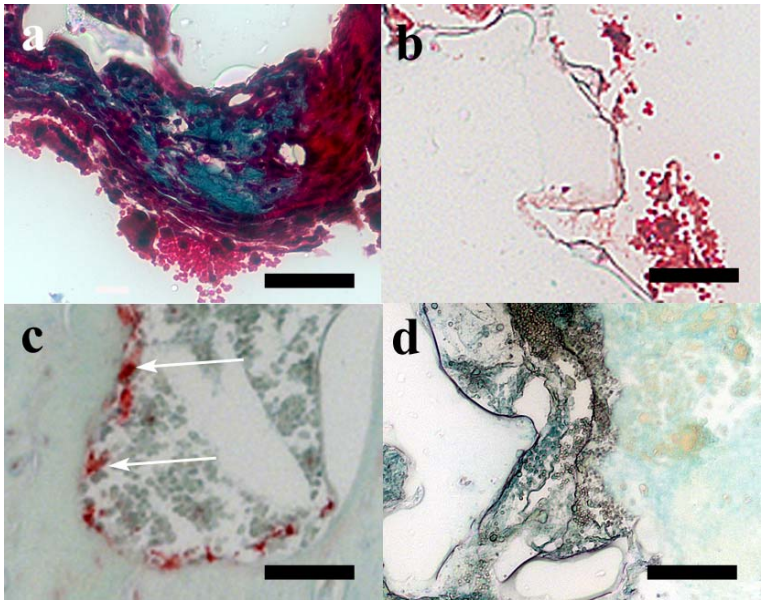

Figure 4-17 Goldners Trichome & TRAP staining ($P_{DL}LA$). Goldners Trichome staining demonstrated abundant regions positive for new osteoid formation in $P_{DL}LA$/HBMSC samples (a); (b) representative staining for Goldners Trichome from $P_{DL}LA$ alone sample. (c) positive staining for TRAP (positive control); (d) negative staining for TRAP from $P_{DL}LA$ HBMSC sample. Scale bar = 50μm.

4.6 Discussion

The current study details a novel technique, using contrast enhanced micro-CT imaging, to visualise and quantify new blood vessel formation in tissue engineered scaffolds with further validation through the *in vivo* demonstration of neovasularisation in impacted bone graft constructs. The emerging discipline of tissue engineering has developed rapidly with novel scaffold technology and improved cell isolation techniques. However, fundamental to the survival of these living constructs remains the development of a new vascular network. To date, vascularisation has received relatively little attention in the context of tissue engineering due in part to the difficulty in quantifying vessel formation within 3-D constructs. Traditionally approaches to measure vessel formation and structure have relied on 2-D qualitative strategies.

A number of applications have utilised contrast-enhanced micro-CT to assess tissue microvasculature networks (Duvall et al., 2004; Toyota et al., 2002; Plouraboue

et al., 2004; Heinzer et al., 2006; Malyar et al., 2004; Kindlmann et al., 2005; Lu et al., 2006; Moore et al., 2003; Zhang et al., 2005). Clear definition of microvasculature is generated when the density of the scaffold is significantly less than the radio-opaque dye. Preliminary imaging confirmed an overlap between the allograft and microfil densities, resulting in the necessity to decalcify the allograft samples prior to CT scanning. This also precluded quantifying new bone formation in samples perfused with microfil dye. A previous study has used a similar technique to visualise both new bone and neovascularisation in the same enhanced allograft samples in a murine segmental defect model (Zhang et al., 2005). A caveat with this study is the potential exaggeration of new bone formation due to the inclusion of the volume of microfil within these samples.

This is a highly promising technique for visualisation and quantification of neovascularisation but it remains important to highlight potential challenges. These include the difficulty at the microscopic levels to determine whether blood vessels in certain areas appear as “dead ends”. These areas may represent physiologically relevant processes where blood vessels have sealed up, sustained damage or undergone angiogenic morphogenesis, or regions in which penetration of the contrasting agents was limited due to fluctuating perfusion pressures at the microscopic level. Furthermore, threshold definition for binarization and scanning resolution can result in a reduction of the number of visualised vessels or artefactually increase the size of vessels respectively emphasising the need to maintain constant optimal thresholds for all samples to prevent either over or under estimation of vessel number and size. In this study the binarisation thresholds were kept constant for all samples. Despite this however, the combination of a limitation to the size of vessel which the dye will penetrate, with an average resolution of 14μm will undoubtedly have resulted in some of the microvasculature not being visualised.

Despite the outlined limitations / potential pitfalls, the use of contrast enhanced 3D micro-CT is significantly superior to current alternatives. Quantification of new vessel formation using immunohistochemistry with analysis of a selected number of slides (due to the practicalities of cutting and staining the entire sample), lends itself to significant subjective bias as a consequence of only analysing a fraction of the entire sample. This not only distorts the microarchitecture of the samples but

fails to provide any information into the 3D geometrical arrangements of these networks – a fundamental source of novel information for future scaffold micro-architectural developments. This study has demonstrated a correlation between using micro-CT and immunohistochemistry for quantification of vessel formation in tissue engineered constructs, but for the reasons outlined above do not believe that immunohistochemistry can provide as accurate a representation of the sample as a whole, when compared to micro-CT.

This study has validated the use of contrast enhanced micro-CT imaging using an *in vivo* subcutaneous impaction bone grafting model. Previous *in vitro* studies have demonstrated that HBMSC can survive the forces of impaction, differentiate and proliferate along the osteogenic lineage *in vitro* (Mushipe et al., 2006; Korda et al., 2006; Bolland et al., 2006). However if in the future living composites, combining natural or synthetic graft with HBMSC populations, are to be used *in vivo* in IBG, their long term survival will be dependent on the development of a vascular network. This is particularly pertinent when one considers the hostile, relative avascular environment, the graft / cell composite would be placed into, and the large distance it is from the reduced host blood supply. To date, we have been unable to visualise neovascularisation and therefore it has remained unclear how allograft (a non vascularised graft) is successfully incorporated in IBG. Histology from biopsy samples has shown viable tissue ingrowth into the graft (Ling et al., 1993), although confirmation of new bone formation within the defects remains limited and, at best, inconsistent (Mikhail et al., 1999; Nelissen et al., 1995; Ullmark, Obrant, 2002).

This study demonstrated a significant increase in blood vessel volume, penetrating vessel number and mean vessel number in the scaffold/HBMSC groups compared to the scaffolds alone. VV/TV values matched blood vessel volume for all groups excluding the potential bias from any variation in the volume under analysis. The mean vessel thickness (and spacing) was greater in both $P_{DL}LA$ groups compared to allograft groups, but was not found to be significant. The potential voids between compacted morsellised $P_{DL}LA$ were greater than compacted morsellised allograft which may attribute to the increase in vessel thickness and spacing observed. In addition to vessel quantification, this study has also demonstrated qualitatively 3-D

reconstructions of vessel networks and quantitatively morphological data on the newly developed vessels. This morphological and 3-D network patterning of neovascularisation within scaffolds and tissue engineering constructs will provide invaluable data for future new scaffold design in IBG to encourage and stimulate neovascularisation. Furthermore qualitatively with histology and quantitatively with micro-CT we observed new bone formation in the scaffold / HBMSC groups when compared to the controls. With the long term success of IBG reliant on the restoration of living bone stock by bone ingrowth, an impacted biological scaffold / HBMSC composite that stimulates the ingrowth of vessels coupled with new bone formation appears to be a promising and attractive composite to provide long term support and therefore survivorship of the revision prosthesis than the present day gold standard.

The use of a synthetic graft or bone extender has immediate advantages over the gold standard with regard to disease transmission, immunogeneic response, cost and availability, but lacks the provision of an osteoinductive stimulus. These studies have successfully demonstrated that the production of a biological living composite of $P_{DL}LA$ augmented with HBMSC has the osteoinductive potential post impaction, previously lacking in both allograft and synthetic graft substitutes. In addition the versatility offered in the processing of $P_{DL}LA$ allows further biological augmentation prior to HBMSC application with the potential incorporation of growth factors and BMPs with controlled release mechanisms. With the additional advantage of avoiding an immunogenic reaction or disease transmission, $P_{DL}LA$ is a promising alternative to the current gold standard, allograft. However, it is important to bear in mind that $P_{DL}LA$ and the biological living composites thus formed may differ to allograft in their handling properties during the impaction process and therefore may alter the way in which the graft is impacted (van Haaren et al., 2005). Furthermore, in these studies the impacted living composites were not subjected to physiological loading, which stimulates graft incorporation and bone remodelling. Therefore, despite their being no histological evidence of increased bone resorption, (represented by negative staining for TRAP) caution must be advocated until further *in vivo* studies, using large *in vivo* models, in which the impacted living composites are also subjected to representative physiological loads, have been performed.

Finally, the combination of contrast based 3D micro-CT, histology and immunohistochemistry, has enabled enhanced assessment of blood vessel morphological development, and although micro-CT is limited to anatomical evaluation, inferences regarding physiological function may be deduced. Ultimately a combination of histological analysis and Laser Doppler perfusion imaging will provide detailed functionality and structure of the micro-vasculature.

The development of a novel vascular supply is integral to the long term incorporation and remodelling of impacted allograft in IBG, and it would appear HBMSC play an important role although the exact mechanisms, remains unclear. Recent studies by Wang et al (Wang et al., 2007) have highlighted the hypoxia inducible factor α (HIF α) pathway as an important coupler of angiogenesis and osteogenesis during skeletal development. They have demonstrated that osteoblasts use the HIF α pathway to sense reduced oxygen tension and transmit signals that impinge on angiogenic and osteogenic gene programs. The activation of this pathway resulted in increased vEGF levels in osteoblasts resulting in promotion of both angiogenesis and osteogenesis. In this study, a heterogenous population of stromal cells were used. These cells could act directly via signalling pathways to activate / recruit osteoblasts or could themselves differentiate along the osteogenic lineage to become osteoblasts, and so could therefore play an important role in both the angiogenic and osteogenic pathways. In the field of IBG where alternatives to allograft are being sought due to limited stocks, this is an exciting area of research but requires further characterisation and development.

4.7 Summary

These studies have demonstrated a facile approach, utilising a radio-opaque dye and micro-CT, for the quantification and visualisation of neovascularisation in tissue engineered constructs. The knowledge of 3D vascular networks will prove highly beneficial to scaffold microstructural design to potentially promote neovascularisation in tissue engineered constructs. Micro CT is a highly versatile and powerful imaging modality which should find wide application in the field of regenerative medicine.

4.7 Conclusion

The results in the context of the null hypothesis were examined:

1. HBMSC seeded onto allograft or $P_{DL}LA$ impacted and implanted into the subcutaneous tissue of a nude mouse for 4 weeks are unable to continue to proliferate and differentiate along the osteogenic lineage and commence bone regeneration"

This hypothesis is ***false***

2. "HBMSC seeded onto allograft or $P_{DL}LA$ impacted and implanted into the subcutaneous tissue of a nude mouse for 4weeks do not stimulate neovascularisation and new bone formation when compared to allograft or $P_{DL}LA$ alone."

This hypothesis is ***false***

4.8 Appendix

Number of penetrating vessels

VESSEL NUMBER	Allo	Allo/HBMSC	$P_{DL}LA$	$P_{DL}LA$/HBMSC
Sample 1	2	21	7	30
Sample 2	5	26	11	42
Sample 3	4	20	5	26
Mean	3.67	22.33	7.67	32.67
SD	1.53	3.21	3.06	8.33

Mean vessel volume

VESSEL VOLUME	Allo	Allo/HBMSC	$P_{DL}LA$	$P_{DL}LA$/HBMSC
Sample 1	2543	290435	39452	491667
Sample 2	8754	164501	48428	525428
Sample 3	32764	179882	44113	310640
Mean (voxel)	14687	211606	43998	442578
Mean (mm^3)	0.04	0.57	0.12	1.19
SD	0.04	0.19	0.01	0.31

Ratio Vessel volume / Total volume (VV/TV)

VV/TV	Allo	Allo/HBMSC	$P_{DL}LA$	$P_{DL}LA$/HBMSC
Sample 1	0	0.003	0	0.011
Sample 2	0	0.008	0	0.009
Sample 3	0	0.005	0	0.009
Mean	0	0.005	0	0.010
SD	0	0.003	0	0.001

Mean Vessel thickness.

THICKNESS	Allo	Allo/HBMSC	$P_{DL}LA$	$P_{DL}LA$/HBMSC
Sample 1	0.008	0.019	0.029	0.026
Sample 2	0.008	0.012	0.027	0.015
Sample 3	0.013	0.010	0.037	0.030
Mean (mm)	0.010	0.014	0.031	0.024
SD	0.003	0.005	0.005	0.008

Mean Vessel spacing

SPACING	Allo/HBMSC	$P_{DL}LA$/HBMSC
Sample 1	6.948	2.215
Sample 2	1.397	1.646
Sample 3	3.372	3.311
Mean (mm)	3.906	2.391
SD	2.814	0.846

CHAPTER 5

Part III - Clinical translation: Implantation of impacted Allograft seeded with HBMSC for the treatment of bone defects in two case studies.

5.1 Introduction

5.2 Case 1 (Introduction, Case History, Surgical technique)

5.3 Case 2 (Introduction, Case History, Surgical technique)

5.4 Materials & Methods

5.5 Results

5.6 Discussion

5.7 Summary

5.1 Introduction

Historical studies by Burwell (Burwell, 1985; Burwell, 1964) using an animal model, demonstrated that bone allograft seeded with autogenous marrow as a composite graft resulted in considerably more new bone than either of the components of the graft transplanted separately. While this technique has yet to become standard clinical practice autologous marrow is increasingly being used in conjunction with synthetic grafts in spinal fusion, (Korovessis et al., 2005; Vaccaro et al., 2002) and maxillofacial reconstructive facial surgery (Feinberg et al., 2005). A number of clinical studies have evaluated the separate use of bone marrow to augment osteogenesis (Hernigou, Beaujean, 2002; Gangji et al., 2004; Khanal et al., 2004; Hernigou et al., 2005) but little work has been performed on its combination with morsellised allograft. We have examined in two cases the application of the principles of a tissue engineering paradigm and translation techniques modified from Burwell's original work to allow transfer from the laboratory to the operating theatre. Marrow-derived stromal cells, which include osteoprogenitor cells, were seeded onto washed morsellised allograft and the resulting composite impacted *ex-vivo* forming a solid construct with which to fill pathological defects in the proximal femur. In addition to its space filling ability, the osteogenic, osteoinductive and osteoconductive properties of the graft was examined.

5.2 Case 1

5.2.1. Introduction

Benign tumours are commonly found in the proximal femur (Jaffe, Dunham, 1990). Clinical presentation is variable depending on the pathology, site and size of the lesion. The spectrum of presentation varies from asymptomatic incidental x-ray findings to those with acute proximal femoral fracture. Most however, present with pain, limp and leg-length inequality (Shih et al., 1996).

Qualitatively, indications for surgery include progressive lesions causing pain or deformity and quantitatively, when over 2·5 cm or more than 50% of the cortex is involved (increases risk of fracture significantly) (Mirels, 1989; Jaffe et al., 2002). Principles of prophylactic treatment remain contentious and may involve curettage of the lesion, void filling either with bone graft or marrow injection and mechanical stabilisation. The process of reconstitution of the defect is often difficult due to the degree of bone loss. In addition, reconstruction may be associated with significant blood loss, donor site morbidity, infection, restriction of activity and recurrence (Roposch et al., 2004).

5.2.2 Case History

A sixty two year old male presented with a one year history of right hip pain. The patient described a dull ache around the lateral trochanter, passing down the anterior thigh with significant deterioration in the months leading up to the procedure. The patient reported difficulty in walking and was beginning to experience night pain, although otherwise, was systemically well with no significant past medical history. On examination, he walked with an antalgic gait. There were no other positive findings and no restriction of hip movements.

Plain radiographs of the right hip (Figure 5-1) showed early degenerative changes along with a well circumscribed focal lesion was seen in the anterior portion of the femoral neck on the right side. The lesion was expansile with slight distortion of the anterior femoral neck cortex (though this remained intact) and diagnosed as representing a benign non-ossifying fibroma.

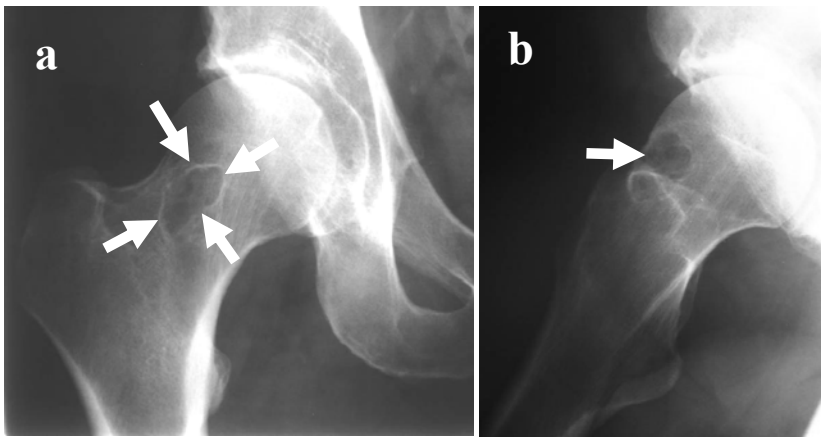

Figure 5-1 Pre-op radiographs (Case 1). Anterior – Posterior (AP) (a) and Lateral (b) radiographs of the right hip, Case 1. The lesion is seen residing in the anterior third of the femoral neck, distorting the anterior cortex.

Exacerbation of the patient's pain and proximity of the lesion to the anterior cortex indicated the potential of impending fracture through the lesion. Surgical intervention was recommended with appropriate counselling with informed consent, including the risks of intra-operative femoral neck fracture.

5.2.3 Surgical Technique

Morsellised allograft was prepared from a banked fresh frozen femoral head. After denuding the femoral head of articular cartilage, fibrous tissue, osteophyte, cystic areas and calcar, the remaining bone was milled using the large and small cylinders of a Noviomagus bone mill. This combination of mill sizes ensured optimal particle size distribution (grading) most resistant to shear strength (Dunlop et al., 2003). The morsellised aggregate was serially washed with pulsed lavage and 6% Hydrogen Peroxide until no further fat or blood was visible. The graft was then finally washed with normal saline and mixed with 500mg Vancomycin powder.

Figure 5-2 Prepared morsellised allograft. Morsellised allograft after washing with hydrogen peroxide and normal saline.

Bone marrow aspiration was performed with the patient in the lateral position in the operating theatre under strict aseptic conditions. A single incision was made over the posterior superior iliac spine and multiple passes were made with a trephine to prevent dilution of the aspirate with haemopoietic cells (Figure 5-3). A total aspirate volume of 36 mls was obtained, 2mls were retained for *ex-vivo* analysis and the remainder immediately seeded onto the graft and covered.

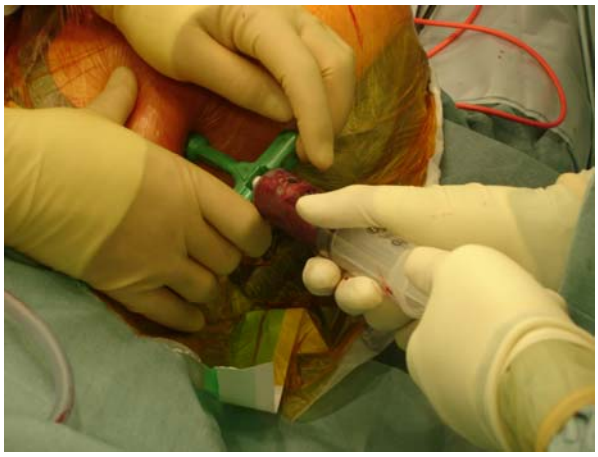

Figure 5-3 Bone marrow aspirate. Bone Marrow Aspirate being taken in theatre from the post superior iliac spine.

The patient was then positioned supine on the operating table with standard lateral preparation and draping. Image intensification was used to determine the incision point. A 3cm incision was made in the skin over the lateral thigh followed by sharp dissection to bone. A guide Kirschner wire was introduced through the lateral cortex and under image intensification directed towards and through the cystic lesion. A 10mm cannulated femoral canal corer (Stryker Int. IBG kit) was passed over the Kirschner wire (Figure 5-4), removing a tunnel which included the contents of the cyst, which was used for histological analysis. Aggressive curettage using a serrated spoon was performed to the cyst walls under image intensification.

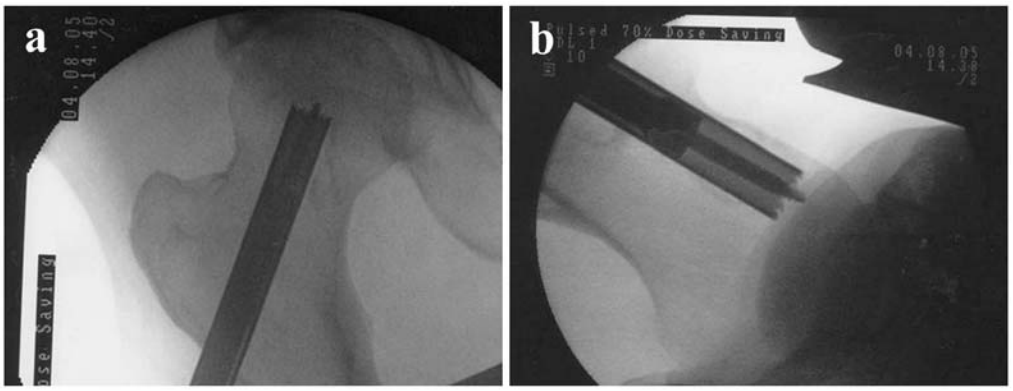

Figure 5-4 Intra-op radiographs (Case 1). Image intensifier images demonstrating technique using apple corer railroaded over guide wire to enucleate the cyst.

Graft was introduced into the corer (Figure 5-5) and impacted ex-vivo to produce a solid core. This was extruded with further impaction in a retrograde fashion into the tunnel defect under image intensified control. This process was repeated with grafting to the lateral femoral cortex. The wound was closed following haemostasis and washout.

Figure 5-5 Seeded graft in corer. Graft loaded into corer followed by impaction prior to filling of tract.

Representative samples including bone marrow aspirate, impacted allograft seeded with bone marrow stromal cells and allograft alone were taken for biochemical and histological analysis with local ethics committee approval (LREC 0091).

5.3 Case 2

5.3.1 Introduction

Avascular necrosis of the femoral head is a potentially devastating complication of intracapsular femoral neck fracture in the young patient. Surgical options for early disease (Ficat stage I and II, see Figure 5-6) (Ficat, 1985) include core decompression and more recently implantation of autologous bone marrow cells (Hernigou, Beaujean, 2002; Gangji et al., 2004; Gangji, Hauzeur, 2005; Gangji et al., 2005). Salvage procedures for advanced disease including the use of vascularised fibular grafts (Leung, Chow, 1984) are technically demanding. Alternatives include the Bonfiglio strut graft (non-vascularised), proximal femoral osteotomy to alter the pattern of stress transfer and vascularised pedicle flaps. Each procedure has substantial morbidity and to date there are no studies indicating the optimal procedure in the treatment of advanced disease. We present the first reported combination of

these procedures, utilising the positive attributes of each: decompression, osteoinduction, osteoconduction and structural support.

Stage	Pain	Findings	X-ray	Bone Scan	MR scan	Treatment
0 (Preclinical)	None	None	Normal	Normal	Normal	None
I (Preradiological)	Minimal	decreased. internal rotation	Normal	Non-diagnostic	Early changes	Core decompression
II	Moderate	decreased. ROM	Osteopenia/ sclerosis; spherical head	Positive	Positive	Core decompression Strut graft
III	Moderate/ Severe	decreased. ROM	Flattened head/ crescent sign	Positive	Positive	Strut graft THR
IV	Severe	Pain	Secondary degenerative changes	Positive	Positive	THR

Figure 5-6 Ficat Classification of AVN of the hip (1985).

5.3.2 Case History

A thirty nine year old male presented with a six month history of pain and stiffness in his left groin and buttock. Eighteen months earlier he had fallen off his bicycle sustaining an intracapsular fracture of his left femoral neck. He was treated within twelve hours with a Dynamic Hip Screw (DHS), two hole plate and de-rotation screw, and had made an uncomplicated post operative recovery remaining pain free for one year. The resultant pain was mechanical in nature, did not disturb him at night, but was becoming progressively more intrusive. On examination, there was no obvious muscle wasting. Trendelenberg test was negative. There was no bony tenderness. Hip movements revealed reduced internal rotation on the left.

Pelvis and left hip radiographs showed two defined areas of lucency in the left femoral head with apparent disruption of the articular surface and a degree of collapse of the femoral head (Figure 5-7).

Due to the intrusive nature of the symptoms and the radiological evidence of advanced avascular necrosis, it was decided to remove the metalwork and bone graft the femoral head and neck using morsellised allograft, seeded with autologous

marrow stromal cells. The patient underwent full informed consent including the benefits and risks of the procedure.

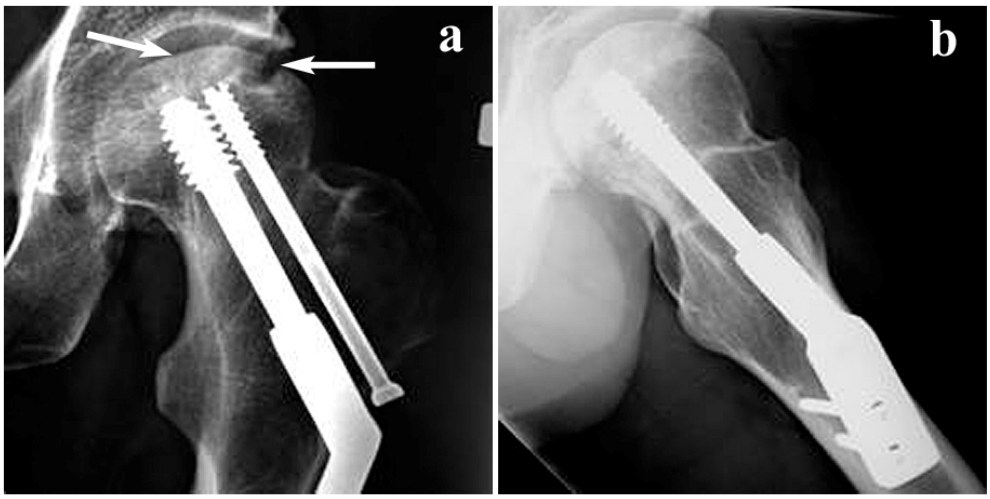

Figure 5-7 Pre-op radiographs (Case 2). Radiographs taken 18 months post fixation of intracapsular femoral neck fracture demonstrated evidence of advanced AVN.

5.3.3 Surgical technique

A similar procedure to Patient 1 was performed. The patient was placed in the lateral position, prepared and draped. 50mls of bone marrow was aspirated from the posterior superior iliac spine and seeded onto prepared highly washed morsellised allograft obtained from 1 donated fresh frozen femoral head. The previous incision was used to expose and remove the dynamic hip screw and derotation screw. The screw tracks were curetted and under image intensification, the sclerotic bed was drilled. The seeded allograft was then impacted into the femoral neck using the 10mm cannulated femoral corer as before, without disruption to the articular cartilage. Samples were taken for biochemical and histological analysis.

5.4 Materials & Methods

5.4.1 Biochemical and histological techniques

5.4.1.1 Assay of Alkaline Phosphatase-Positive Colony-Forming Units

Bone marrow aspirate (2mls) taken intraoperatively was immediately plated, in theatre, into tissue culture flasks (75cm^3, n=3). 8mls of α–MEM, 10% foetal calf serum, 100uM ascorbate-2-phosphate, and 10nM dexamethasone was added to each flask. The plates were incubated at 37^{o}C in 5% CO_2. The media was changed including two washes with PBS on the seventh day. On day 9, the samples were stained in situ for alkaline phosphatase activity. The number of alkaline phosphatase-positive colony forming units – fibroblastic (CFU-F) (colony is defined as containing more than 32 cells), were counted in each flask.

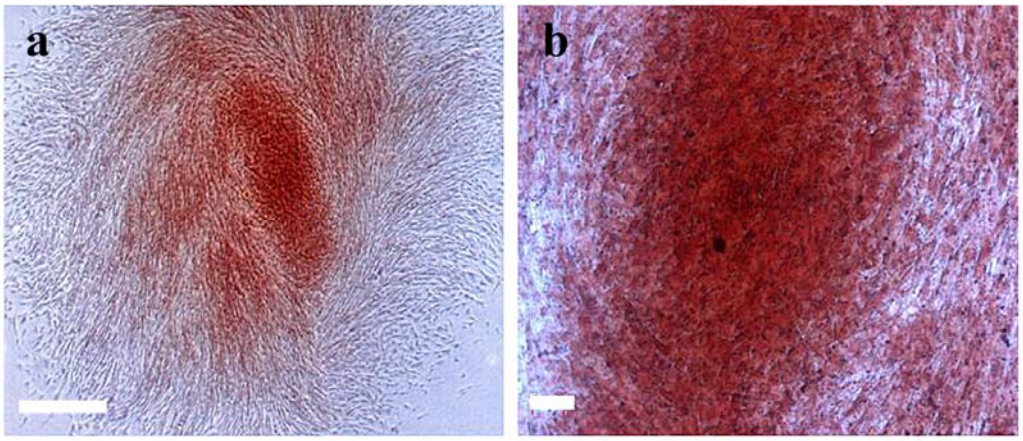

Figure 5-8 Alkaline phosphatase positive stained CFU-F. Alk phos. +ve CFU-F after 9 days in culture under osteogenic conditions (a) x2.5 (b) x10 magnification (Scale bar represents 50μm).

5.4.1.2 DNA and alkaline phosphatase-specific activity.

Samples taken in theatre of impacted seeded allograft, were transferred to two, six well plates and media added. The plates were incubated at 37^{o}C in 5% CO_2 and media changed every 4 days. Control samples of highly washed morsellised allograft were also cultured under identical conditions. At 1 week, constructs were washed with PBS, then incubated with 0.05% Trypsin / EDTA at 37^{o}C and 5% CO_2 interspersed twice with vigorous vortexing. Cells were collected by centrifugation (13,000rpm for 10 minutes at 4^{o}C), and then resuspended in 1ml 0·05% Triton X-100. Lysis was achieved by freezing –thawing and samples were stored at -20^{o}C until assayed. Lysate was measured for alkaline phosphatase activity using *p*-nitrophenyl phosphate as substrate in 2-amino-2-methyl-1-propanol alkaline buffer solution (1·5M, pH 10·3 at 25^{o}C (Sigma, Poole, UK). DNA content was measured using PicoGreen according to manufacturer's instructions (Molecular Probes, Paisley, UK). Alkaline phosphatase-specific activity was expressed as nM pNPP/hr/ng DNA.

5.4.2 Degree of graft compaction

A load cell of 5 kN capacity taken from an Instron 1173 materials testing machine (Instron Ltd., High Wycombe, Bucks) was used in the laboratory to measure the forces imparted to the morsellised graft during graft compaction. The 10mm bone corer was loaded with representative amounts of wet washed allograft and the graft compacted by means of repeated blows to the plunger in the same fashion as in theatre (Figure 5-9). For each graft sample, three groups of ten blows were applied to the plunger and the peak and mean forces recorded. The mean and standard deviation of the force delivered per blow for three different surgeons are represented by Figure 5-10.

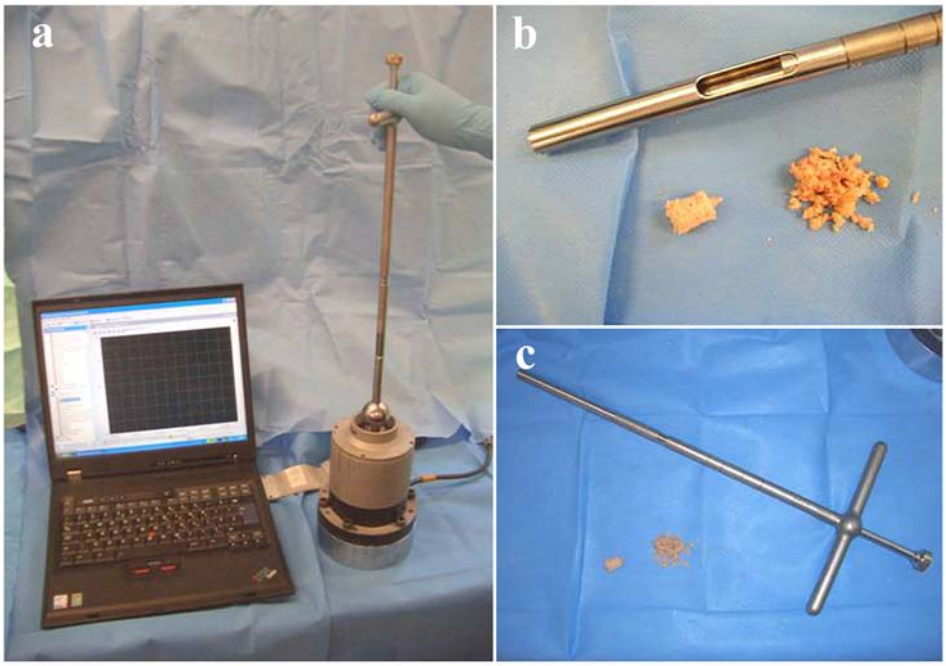

Figure 5-9 Surgical impaction forces. Apparatus used to determine the estimated forces transferred to the graft during impaction of the graft within the corer device. (a) Load cell with corer and guiding piston. (b,c) Corer, piston and graft pre and post impaction.

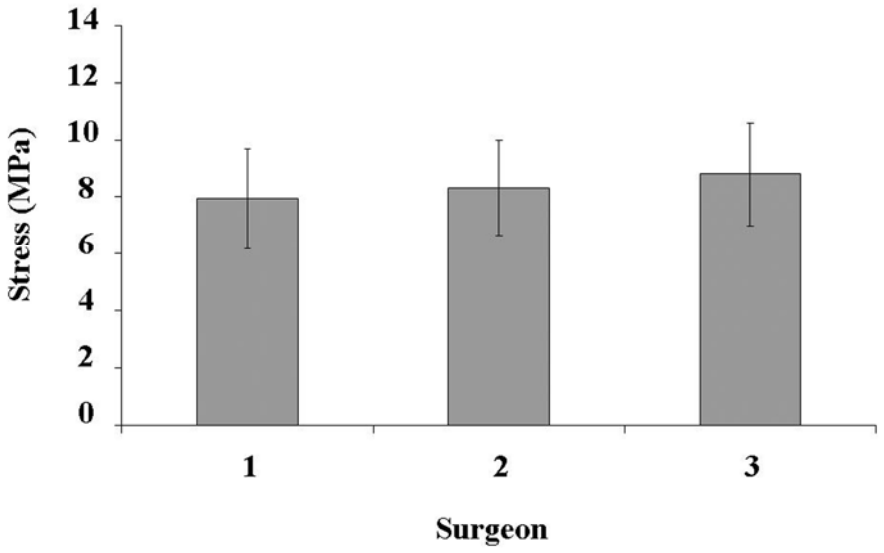

Figure 5-10 Mean peak stresses. Mean peak stresses per strike imparted to the bone graft from three surgeons.

5.5 Results

5.5.1 Clinical & Radiological

Both patients left hospital on day 1 post-operatively with simple analgesics and mobilised with protective weight bearing for 6 weeks, with two crutches whereupon both patients were reviewed and were both found to be asymptomatic. In case 1 radiographs (Figure 5-12) and computerised tomography slices (Figure 5-13) at 6 months, showed satisfactory appearances of bone graft incorporation. In case 2, at 6 month follow up, there was no progression of AVN both clinically and radiologically (Figure 5-15 radiographs at 18 months post op). Current follow up is at 2 years in Case 1 and 18 months in Case 2. Case 1 remains asymptomatic. CT images show good graft incorporation in the track with partial resolution of the cyst. The previously thin walled anterior cortex in the femoral neck has remodelled. In Case 2 at 18months radiologically there was evidence of remodelling and healing of the avascular segment with filling in of the defect in the superolateral portion of the femoral head (Figure 5-15). Although his symptoms had not progressed they remained intrusive affecting his lifestyle and activities as a keen young sportsman. As a result he has recently undergone a total hip replacement. Intraoperatively, macroscopically one could see the site of the previous defect which had filled in with the appearance of cartilagenous tissue.

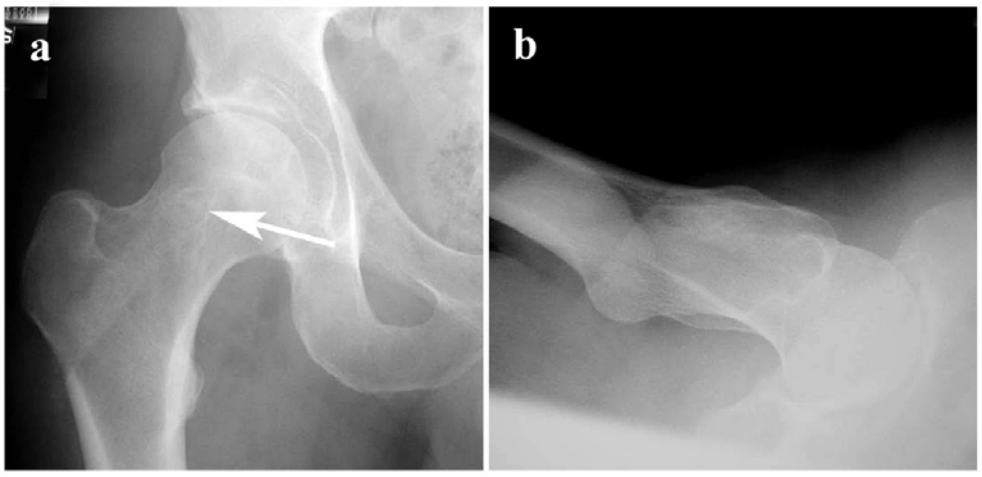

Figure 5-11 Post-op radiographs (Case 1). AP and Lateral radiographs of case 1 (a, b). Increased density seen in cored out tract filled with impacted seeded graft (arrow = site of previous body of cyst).

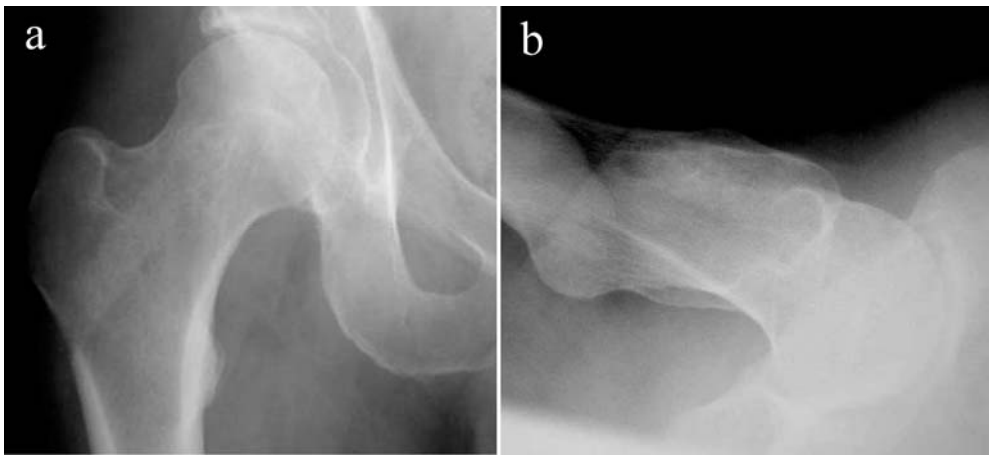

Figure 5-12 Follow up radiographs (Case 1). AP and (b) lateral radiographs taken at 6 month follow up. Radiographically the lesion has been replaced by bone at a higher density than the surrounding cancellous bone.

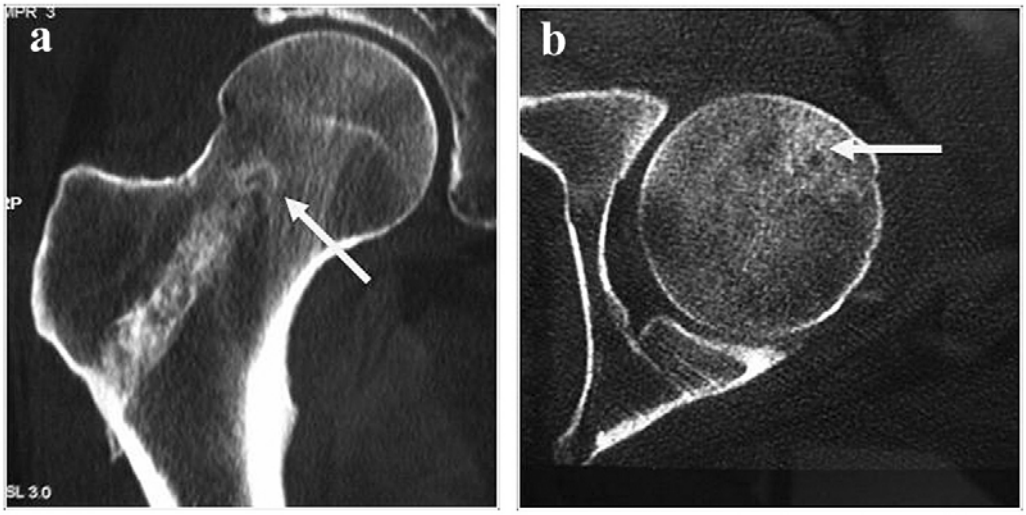

Figure 5-13 Follow up CT images (Case 1). CT imaging also at 6 month follow up. (a) Coronal and (b) Axial slices at the midsection of the site previously occupied by the cyst.

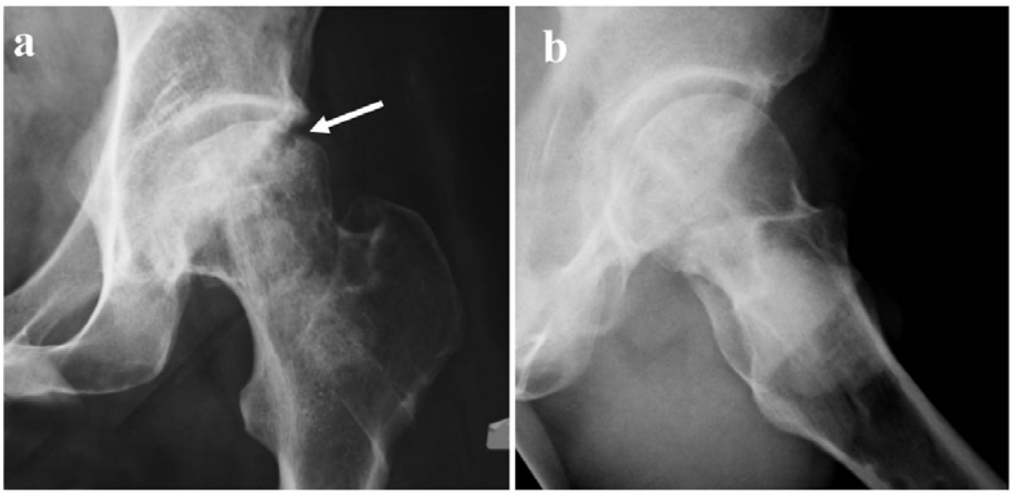

Figure 5-14 Post-op radiographs (Case 2). AP and Lateral radiographs of case 2 (a, b) demonstrating impacted graft within the old DHS tract. Note the "rat bite" lesion on the antero-superior aspect of the femoral head (arrow).

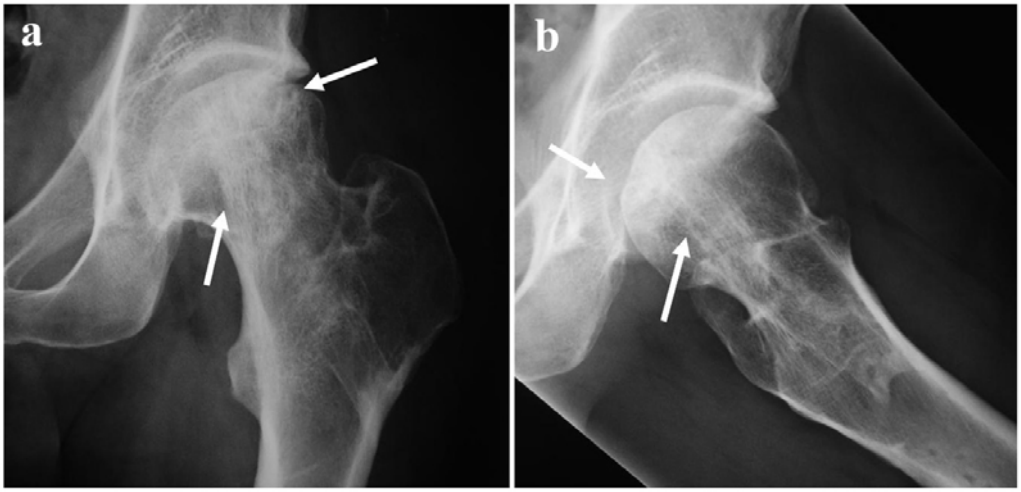

Figure 5-15 Follow up radiographs (Case 2). (a) AP and (b) lateral radiographs taken at 18 month follow up with evidence of bone graft incorporation and trabeculation. Note the filling in of the previous more defined rat bite lesion in the antero-superior aspect of the femoral head

5.5.2 Impaction Forces

The mean of the peak force delivered per strike to the graft was 0·7+/-0·13kN (SD) corresponding to average peak stresses within the graft of 8·3+/-1.5MPa (SD). There was no statistical difference between the three operators (Figure 5-10). This stress was greater in magnitude to our estimated peak stresses imparted in a standard femoral impaction bone grafting in revision hip surgery (0·8MPa). This was an expected finding as the pellet of allograft produced from the apple corer both in theatre and in the laboratory appeared more compact than impacted graft from a femoral impaction bone grafting.

5.5.3 Alkaline Phosphatase-positive CFU-F and enzyme activity

The bone marrow aspirate from case 1 yielded 4 x 10^5 nucleated cells/ml of aspirate and 2·75 x 10^6/ml from the patient in case 2. The average number of alkaline phosphatase-positive CFU-F formed was 2·18 (range 1·64–2·54) CFU-F/10^6 nucleated cells. The presence of large numbers of erythrocytes, in the absence of fractionation in

the theatre, resulted in a reduced surface area and suboptimal conditions for adherence and proliferation of the nucleated stromal cell population with a lower CFU-F yield. The exact mechanisms of reduced proliferation are not currently understood although expansion in the presence of high erythrocyte number appears a factor.

5.5.4 Biochemical

Samples from both cases of allograft seeded with bone marrow showed increased DNA content and specific alkaline phoshatase activity. Specific alkaline phoshatase activity in Case 1 at day 0 was 0·05nM pNPP/hr/ngDNA and in Case 2 at day 7: 23·7nM pNPP/hr/ngDNA compared to 0nM pNPP/hr/ngDNA in allograft alone samples.

5.5.5 Histological

The histological analysis of the sample of tissue containing the cyst from theatre showed macro and microscopic appearances consistent with a non-ossifying fibroma. Immediate live / dead staining confirmed cell viability post impaction in allograft / HBMSC samples (Figure 5-16b), with no corresponding cell activity in the allograft alone samples (Figure 5-16a). Repeat staining at 1 week demonstrated increased live cell numbers on the graft (Figure 5-16c). Staining with Haemotoxylin & Eosin showed dark staining marrow stromal cells adherent to the graft surface (Figure 5-17b). No cells were visible adherent to or surrounding the allograft alone (Figure 5-17a). Immunohistological staining demonstrated a proportion of the marrow stromal cells at the allograft surface and in the surrounding haematoma positive for Bone Sialoprotein (Figure 5-17d).

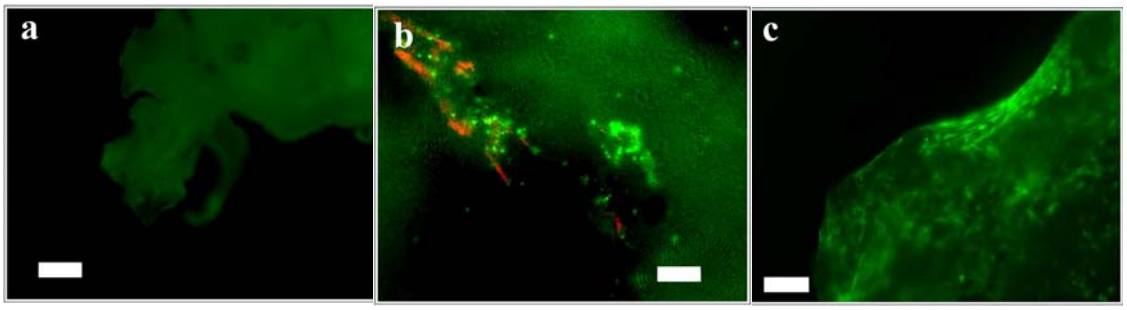

Figure 5-16 Ethidium Homodimer / Cell tracker Green staining. (a) Allograft alone (x5), (b) Immediate viability of allograft seeded with autologous bone marrow aspirate (x5), and (c) at 1 week (x5). Scale bar represents 50μm.

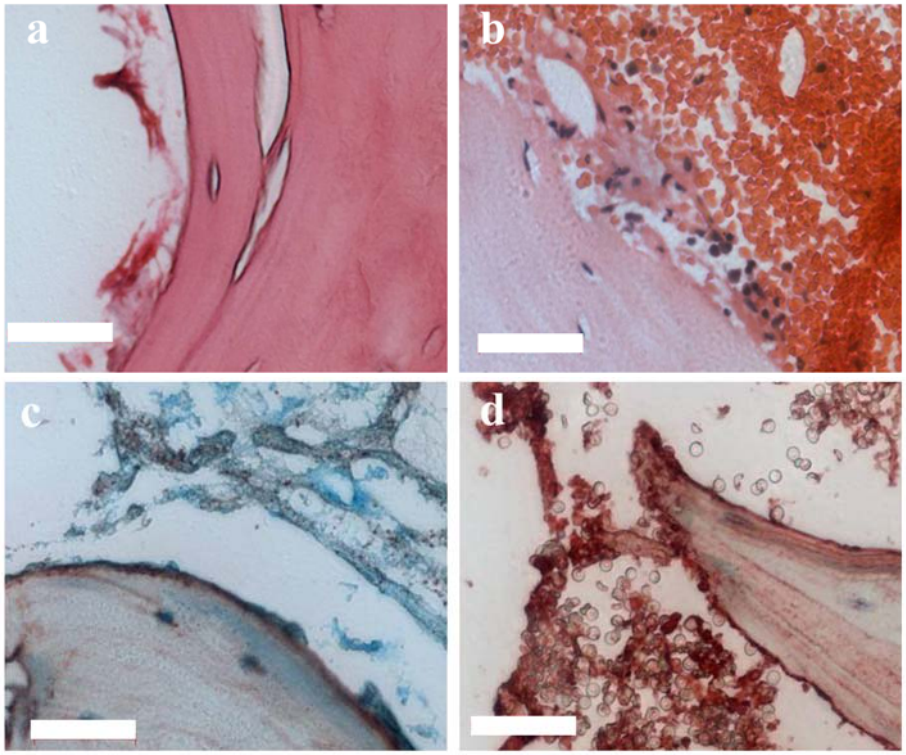

Figure 5-17 Histological & Immunohistochemical staining. Haematoxylin and Eosin staining of (a) washed allograft alone (x40) and (b) seeded allograft (x40). (d) Bone Sialoprotein immunostaining of seeded allograft (x40) and negative control (x40) (c). Scale bar represents 100μm.

5.6 Discussion

This study demonstrates the potential to use autogenous human bone marrow stromal cells for bone impaction and clinical potential therein. This study has demonstrated that autologous human bone marrow stromal cells can adhere to highly washed allograft, proliferate and express a bone phenotype after impaction into a contained defect. In both cases, bone marrow aspirate alone was used in the absence of cell selection.

Central in this impaction procedure is the correct preparation of allograft. Sequential hydrogen peroxide washing followed by quenching in normal saline were used to remove the majority of lipid contaminants. Banked allograft remains a potential source of retained immunogenicity (and disease transmission). This can be attenuated by the process of freezing, however, the marrow elements within the cancellous bone, attributed to raising an immune response remain. In addition, removal of lipid and marrow fluid results in a stronger, compacted graft that displays greater resistance to shear (Part I: section *3.4.12* – Validation of washing technique using hydrogen peroxide). Histological analysis of washed allograft samples taken from theatre confirmed negligible or no bone marrow remnant within the graft infrastructure. Soil mechanical engineering principles have shown that a carefully graded and impacted aggregate will exhibit greater load carrying capacity than a poorly graded impacted aggregate (Smith, 1990; Lambe, 1979). Morsellised allograft has been combined with bone marrow to produce a living composite (Burwell, 1964) but provides little structural support. However as seen in revision hip surgery, impacted bone graft can withstand significant loading. In the current studies, bone marrow stromal cells were observed not only to adhere to allograft but were able to withstand the forces of impaction and continue to proliferate offering significant potential in orthopaedic practice particularly in the field of revision hip surgery with impaction bone grafting. Improvements with bone marrow fractionation to remove contaminating erythrocyte numbers will undoubtedly improve CFU-F yield, as was observed in the laboratory.

Advantages: This innovative impaction approach has a number of advantages: i) the procedure fulfils the triad of osteogenesis, osteoinduction and osteoconduction with immediate effect, ii) the procedure can be performed under a single anaesthetic without removal of tissue from the operating theatre thus avoiding issues of sterility associated with further expansion of marrow stromal cells and iii) the procedure provides a rapid, cost-effective, facile approach applicable to a number of clinical orthopaedic scenarios.

Disadvantages: Banked allograft is expensive, and despite the robust septic screens and the aggressive intraoperative cleansing cycles, there remains the potential for immune or septic reactions. However, the procedure, as advocated, carries minimal risk of donor site morbidity from the marrow aspiration. If multiple punctures of the cortex and small volume aspirations are performed, there is also the risk of diluting the yield of osteoprogenitor cells (Muschler et al., 1997). Current studies are centred on i) improvements in the fractionation process to remove contaminating erythrocytes and improve CFU-F numbers, ii) determination of the rate of bone incorporation and, iii) whether the living composite confers an advantage in reaching maximum strength in comparison to allograft alone. This latter issue will ultimately depend on the successful development of a local infiltrative vascular system.

5.7 Conclusion

This pilot study has demonstrated an innovative technique to aid the reconstitution of substantial bone loss when the volume of graft needed exceed volumes provided by autograft alone. These studies combine marrow stromal cells including progenitor cells committed to the osteogenic lineage onto prepared allograft to create a living composite, as verified by laboratory analysis. Critically, the augmentation of graft with mesenchymal populations has been shown to survive the impaction process converting a loose aggregate into a viable cell composite graft with comparable density to the cancellous bone that it has replaced without the need for additional fixation.

This facile versatile technique can be tailored to a variety of orthopaedic situations and in particular offers an exciting potential role in the augmentation of allograft or synthetic graft, used in acetabular and femoral impaction bone grafting.

CHAPTER 6

Part IV - A Vibration assisted IBG technique to reduce fracture risk and improve graft compaction and prosthetic stability

6.1 Introduction
6.2 Null Hypothesis
6.3 Aims
6.4 Study design
6.5 Results
6.6 Discussion
6.7 Summary
6.8 Appendix

6.1 Introduction

IBG is a technically demanding procedure with a steep learning curve. Determining when the graft is adequately compacted is potentially one of the most difficult factors for the surgeon to judge intra-operatively. Initial success of the technique requires the morsellised allograft to be adequately compacted to provide initial stability for the prosthesis and in addition induce bone remodelling, the absence of which is thought to be key in graft collapse and subsequent implant failure (Nelissen et al., 2002; Nelissen et al., 1995). In revision of the femoral component, a thin walled ectatic proximal femoral cortex is often encountered and intraoperative fractures are common given the high forces that must be applied to the graft in order to gain adequate graft compaction (though this risk is reduced somewhat reduced with prophylactic cables). The risk of intraoperative femoral fracture rates during revisions with impacted allograft bone and cement fracture has been identified as a concern in a number of series (Pekkarinen et al., 2000; Knight, Helming, 2000; Meding et al., 1997; Ornstein et al., 2002) with rates ranging from 12% (Meding et al., 1997) to as high as 27% (Ornstein et al., 2001). The risk of inducing fracture is balanced against underimpaction leading to high degrees of subsidence and implant failure. Achieving this delicate balance is also compounded by the fact that with current instrumentation there is still no specific indicator or guideline to enable the surgeon to determine when the graft is adequately compacted. Since the development of the technique, there have been few modifications to either the technique itself or the instrumentation used for impaction.

There are many examples in everyday situations whereby aggregates are impacted. Examples include the laying of tarmac roads or the building of foundations. Morsellised allograft shares many characteristics with these common aggregate materials such as soils, sands and ballasts used in civil engineering applications (Smith, 1990). The behaviour of these aggregates under load has been studied extensively and this knowledge can be applied to improve the mechanical characteristics of other aggregates such as bone graft. To produce the strongest aggregate, the following characteristics are required:

i) The aggregate should have a well graded particle size distribution (a mixture of bone chips of different sizes in appropriate proportions).

ii) The aggregate should have a low state of hydration.

iii) The aggregate should be well compacted using an appropriate quantity of applied compaction effort, preferably by sequential compaction of layers of aggregate.

iv) The aggregate should be adequately contained during compaction. (Dunlop et al., 2003; Brewster et al., 1999)

v) Vibration should be applied to the aggregate.

Common practice today employs points i – iv, to prepare and impact the bone graft in IBG. However, as yet, vibration has not been introduced.

Vibration applied to the aggregate is commonly used in civil engineering applications in order to improve the compaction (assembly) of the aggregate particles and hence to increase the aggregate's compressive and shear strengths (Smith, 1990). If the aggregate is subjected to vibration in an unconfined space then the particles forming the aggregate will be moved into a denser packing improving its shear strength. When the aggregate is saturated in the fluid phase and as the aggregate is moved into a denser packing, the interstitial fluid needs to be drained out. This is often not a problem in an unconfined space. However, in a contained environment such as the space between the prosthesis and femur the increase in fluid pressure generated by the vibration can lead to an increase in pressure in the fluid phase that will be exerted on the solid particles forming the aggregate. Under strong vibration, the fluid pressure can become large enough to push the solid particles apart causing an eventual loss of contact. This type of phenomena called "liquefaction" is often witnessed in saturated granular media during earthquake loading and is known to result in the sinking of large buildings or bridges (Coelho et al., 2007). The phenomenon of liquefaction can be avoided if adequate drainage is provided for the fluid phase precluding fluid pressure build up.

Figure 6-1 Images of liquefaction. Examples of "liquefaction" phenomenon post earthquake. Note the increase in pressure has forced the water drain out from the surrounding pavement surface.

6.2 Null Hypothesis

The following null hypotheses were addressed in this study:

1. *"The use of vibration coupled with a drainage system to impact bone graft does not reduce the peak forces and hoop strains created during impaction"*

2. *"The use of vibration coupled with a drainage system to impact bone graft does not improve graft compaction"*

3. *"The use of vibration coupled with a drainage system to impact bone graft does not result in less subsidence of the prosthesis under cyclical loading"*

6.3 Aims

The aim of this study was to establish if the use of vibration and drainage to compact bone graft, when compared to the standard technique, could reduce the risk of fracture (represented by hoop strain and load measurements transmitted to the femur) and improve graft compaction and subsequent prosthetic stability (represented by subsidence measurements under cyclical loading), using an in vitro femoral IBG model.

6.4 Study Design

6.4.1 Bone Graft Preparation

The bone graft used in this study was prepared from fresh frozen femoral heads defrosted in warm saline solution. Following removal of articular cartilage and residual soft tissues, the heads were milled using a Noviomagus bone mill (OrthoLink Ltd., Scotland), washed with hydrogen peroxide solution to remove most of the fat from the graft, cleaned using pulsed lavage with normal saline solution and drained through a sieve (300micron). The graft was placed in a polythene bag, sealed and wrapped in moist swabs to maintain constant graft hydration. Approximately three femoral heads were required in each experiment. For each femur the weight of bone graft used was determined.

6.4.2 Instrumentation

A polished collarless tapered tamp (phantom) from the "X-change" Stryker impaction bone grafting kit was modified by drilling multiple holes through the flanks of the tamp into the central guide wire hole.

Figure 6-2 Stryker X-change instrumentation. Standard femoral impaction bone grafting X-change Stryker instrumentation.

The "Woodpecker" vibration device (Minnesota Bramstedt Surgical Inc, St. Paul, MN, USA) was used to apply vibration to the phantom. The Woodpecker is a pneumatic hammer developed for broaching of the femoral canal, and initial trials in the present application indicated that the energy imparted per blow was too great when the device was operated at air supply pressures recommended by the manufacturer for broaching applications. For this reason, a pressure regulator was fitted in the air supply line and preliminary experiments established a working pressure of 2.4 bar with the control on the body of the vibration hammer set in the maximum (+) position, to be optimum.

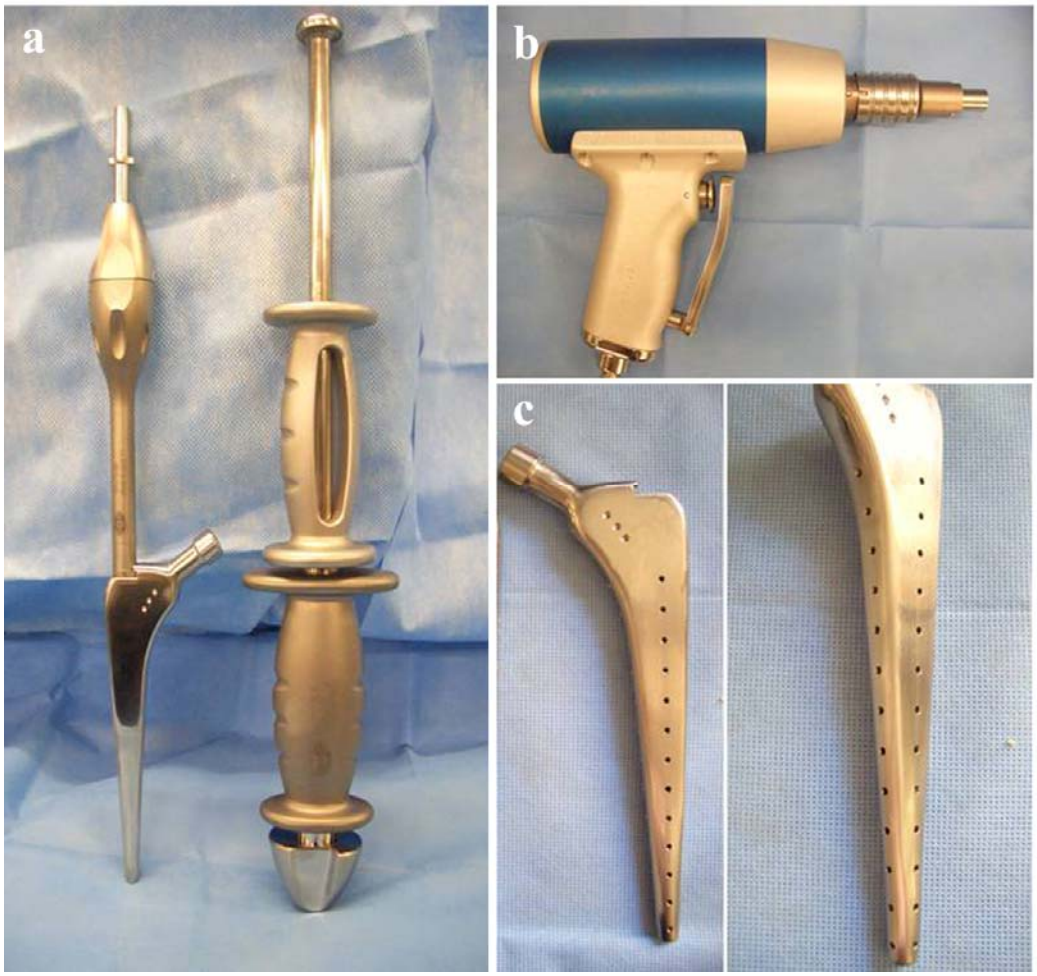

Figure 6-3 Standard & Vibration impaction instrumentation. Instrumentation used for impaction (a) Standard slap hammer and phantom used in the control group (b) Vibration hammer was coupled to the perforated phantom (c) in the experimental group.

The apparatus and experimental set up is shown in Figure 6-3. The Vibration hammer (1) is coupled to the phantom (2) such that vibration generated is transmitted to the morsellised allograft (5), with the coupling between the vibration hammer and tamp disengaging on hammer retraction.

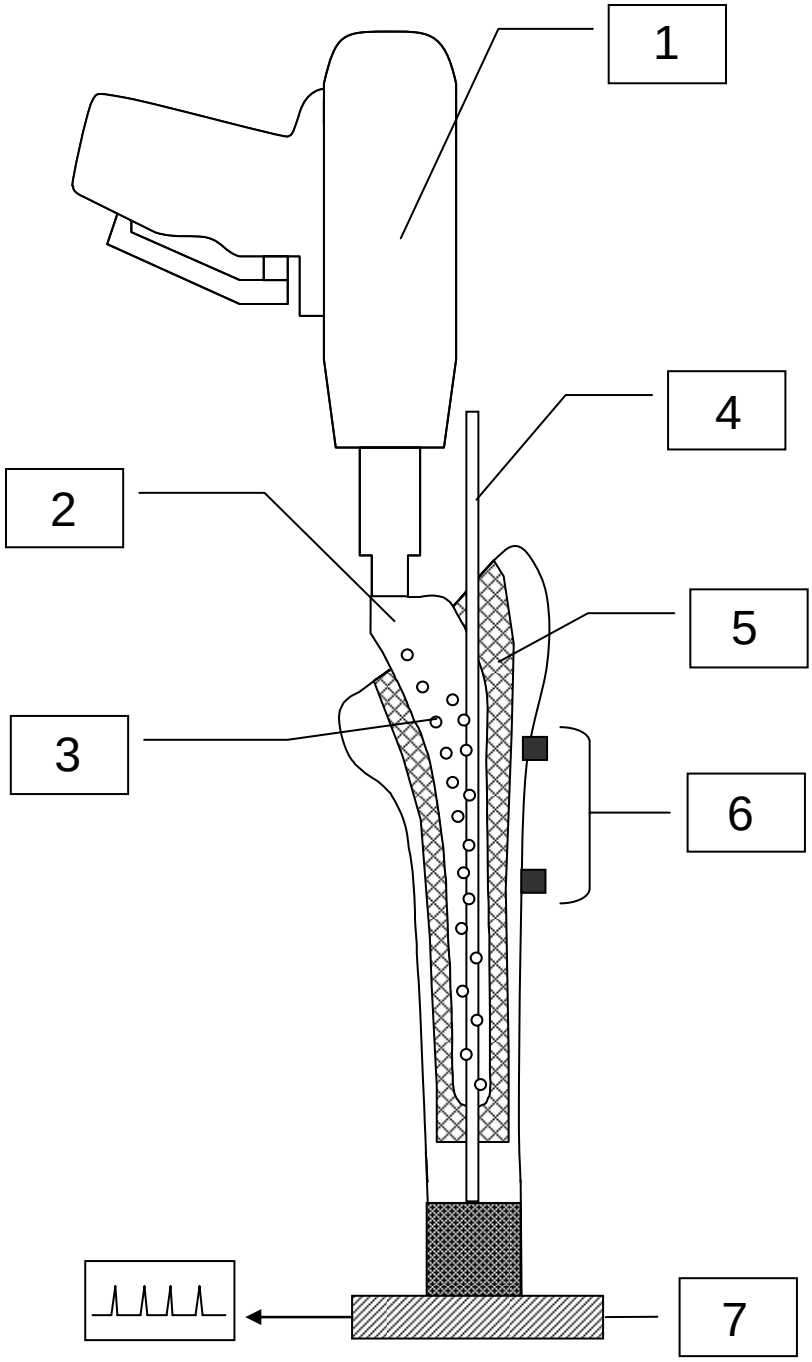

Figure 6-4 Sketch of vibration IBG device & set up. (1-Vibration hammer, 2-phantom / tamp, 3-holes in phantom / tamp, 4-centralising rod, 5-bone graft, 6-strain gauges, 7-load cell)

Twelve biomechanical models of the femur were prepared; six in each group (Standard femoral compaction with slap hammer – Control group. Vibration assisted compaction – Vibration group). Medium left third-generation composite femurs

manufactured from short glass fibre reinforced epoxy resin were used as the basis of the biomechanical model (Model number 3303, Sawbones Europe AB, Malmo, Sweden). These models have been shown to approximate the mechanical properties of the human femur, but with much less variability than that found in cadaveric material (Heiner, Brown, 2001).

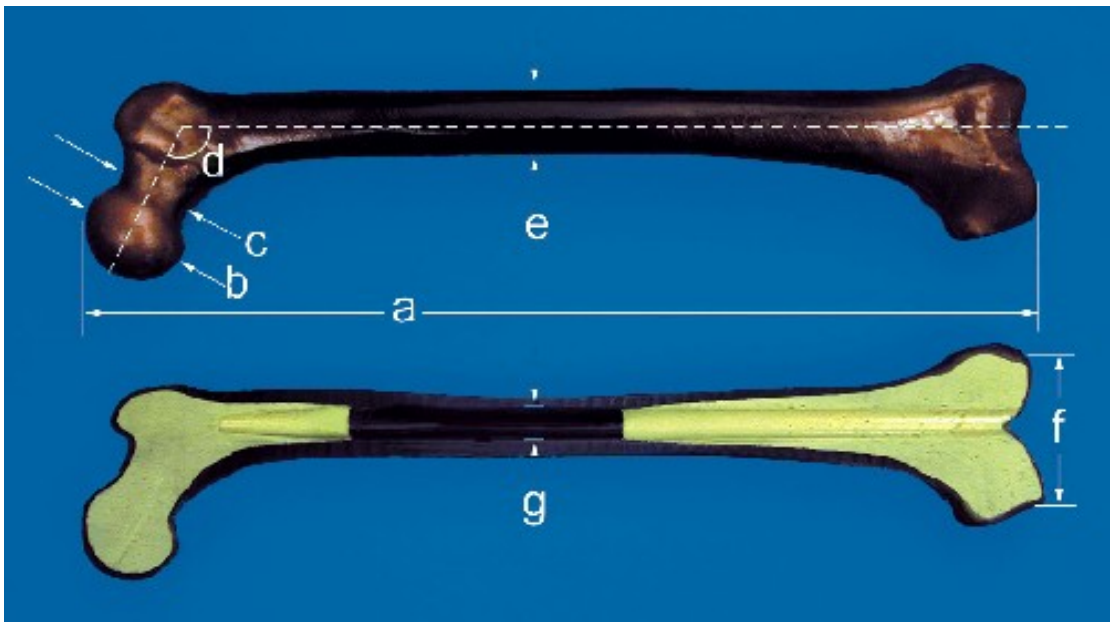

Figure 6-5 Sawbone femur. Third generation composite femur with dimensions a) 455 mm b) 45 mm c) 31 mm d) 135 degrees e) 27 mm f) 74 mm g) 13 mm canal. (www.sawbones.com).

Each model femur was modified to closely resemble those encountered during revision hip replacement surgery with removal of the foam core and increasing the diameter of the canal to 22 mm to represent the loss of all cancellous bone and thinning of the cortex. The distal canal of each femur was occluded 25 mm beneath the anticipated position of the tip of the prosthesis using bone cement.

Figure 6-6 Femoral sawbone post modification. Adapted to best represent revision femora with widening of the internal medullary canal (circle) and thinning of the outer cortices (arrow).

Uniaxial strain gauges (Type FLA-5-11, Techni Measure Ltd, Studley, UK) were attached to each femur using cyanoacrylate adhesive at the medial calcar and in the mid shaft (measurements were taken from lesser trochanter for replicate positioning of the gauges, and the same bones were used for each group of tests to allow direct comparison). Care was taken to ensure the position and alignments of the gauges were consistent between femurs, using the lesser trochanter as a reference position. The gauges were aligned to measure strains perpendicular to the medullary axis of the femur in the circumferential direction ("hoop strain"). The strain gauges and their electrical connections were coated with a layer of low modulus silicone rubber to protect them from fluids exuded by the bone graft during graft compaction.

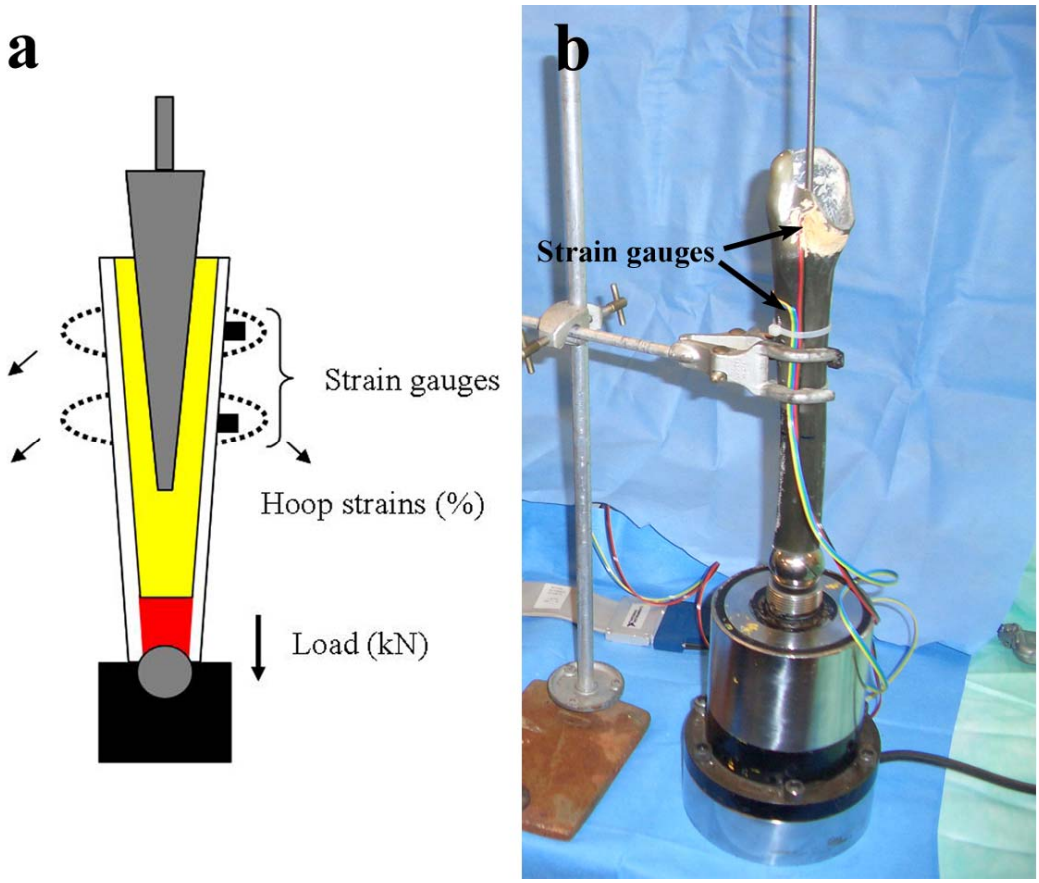

Figure 6-7 Experimental set up. (a) Diagrammatic representation of impaction process with bone graft and phantom and (b) sawbones with strain gauges attached.

Each proximal femur was potted in an aluminium cup using Technovit resin (TAAB Laboratory Equipment, Aldermaston, UK). A potting jig was used to ensure the cup was concentric with the intramedullary canal of the composite model femur. The cup was then fitted into a precision-machined mating hole in the base block of the mechanical testing jig and retained using grub screws. The cup and jig positioned the femur such that the centre line of the medullary canal at the distal cut was oriented at 10° to the vertical in both the frontal and sagittal planes passing through the centre of the femoral head. The accuracy of alignment with this mounting system is estimated to be better than 0.5°. This presented the femur in a similar position and orientation to that described for fatigue testing of hip prostheses (ISO 7206-4:2002 Implants for surgery -- Partial and total hip joint prostheses -- Part 4: Determination of endurance properties of stemmed femoral components), which is designed to represent the hip joint loading at heel strike during a typical gait cycle.

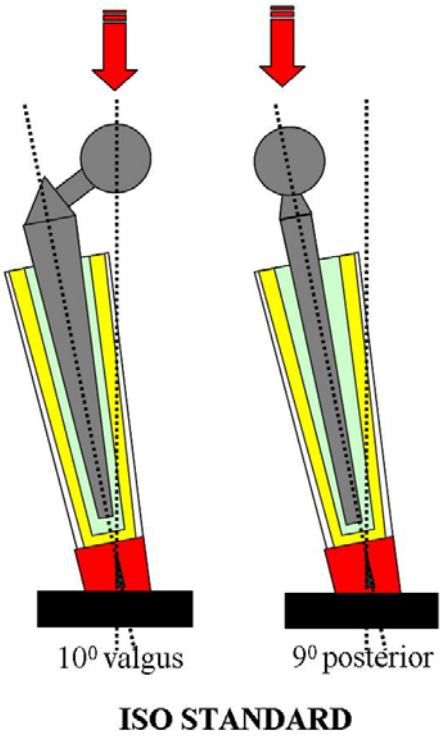

Figure 6-8 Hip stability testing set up. Diagrammatic representation of position required to test the stability of hip prostheses according to the ISO standard (ISO 7206-4:2002 Implants for surgery -- Partial and total hip joint prostheses -- Part 4: Determination of endurance properties of stemmed femoral components).

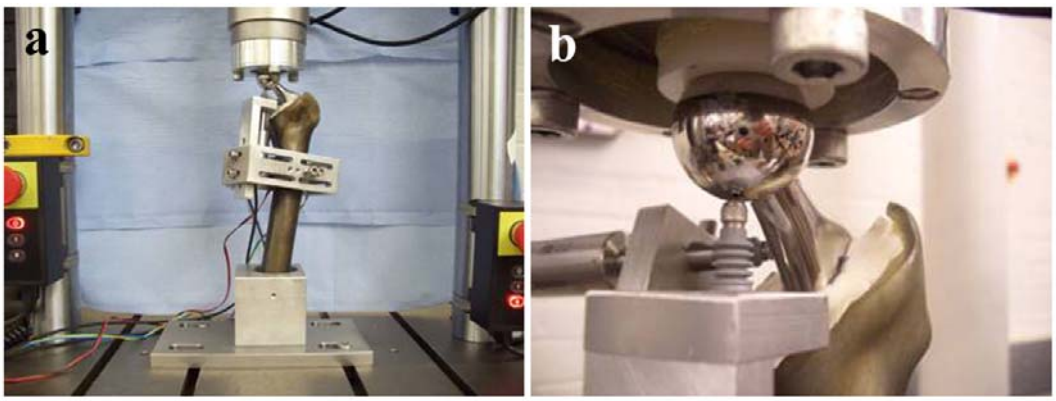

Figure 6-9 Femurs mounted for stability testing. (a) Femurs mounted within potting jig and secured within the Instron device for testing. (b) Displacement transducers (LvDT's) placed on prosthetic head and neck to measure both axial and rotational displacement respectively.

6.4.3 Operative Procedure & Per-operative Measurements

Impaction bone grafting was carried out using a standard protocol for the control and vibration assisted groups, using "Exeter" instrumentation (Stryker UK Ltd, Newbury, UK). Approximately 15 ml of graft was introduced to the distal intramedullary canal and the graft compacted using the distal tamps. This step was repeated a further two times. Further portions of graft were then added to the femur, at each stage the graft being compacted before the next portion of graft was added. In the control group, a standard technique of applying 20 blows per portion of graft was maintained. In the vibration group, the graft was compacted by application of the Vibration hammmer to the tamp / phantom for approximately 10 seconds. The end point of impaction in the control was defined by there being no further movement of the tamp after 10 consecutive blows with the slap hammer and in the vibration group no further movement of the tamp despite force application to the hammer. Preliminary experiments confirmed the end point in the vibration group to correlate with the end point in the control group (ie after vibration assisted compaction, the addition of 10 further blows using the slap hammer, resulted in no further movement of the tamp). A single mix of bone cement (Smartset CMW, DePuy CMW Ltd., Blackpool, UK), prepared in a vacuum mixing system (Cemvac, DePuy CMW Ltd, Blachpool, UK) was inserted retrograde using a revision nozzle and cement gun and pressurised with a proximal cement pressuriser. This was followed by the insertion of a 44 No.2 Exeter femoral prosthesis.

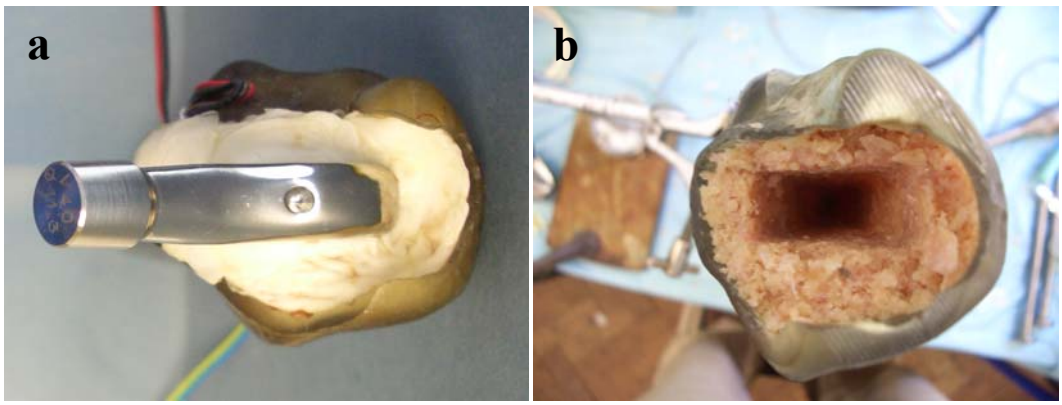

Figure 6-10 Images post impaction and prosthetic cementing. (b) Impacted graft within the modified femoral sawbone (a) Image after Exeter stem has been inserted and cemented into place.

Loads transmitted through the femur during impaction were measured using a load cell taken from a materials testing machine (Instron 1193, 5 kN capacity, Instron Ltd, High Wycombe, UK), upon which the femur was rested.

Load and strain data were recorded at each stage of compaction using a computer equipped with a data acquisition card and signal conditioning unit (DAQCard-AI-16XE-50 and SC-2345, National Instruments Ltd, UK). Data was sampled at a frequency of 10 kHz to ensure capture of the high frequency components of the load and strain signals produced by the compaction.

6.4.4 Micro CT imaging

Micro-CT scans of the grafted femora were obtained using a bench top Microtomography system (X-TEK Systems Ltd, Tring, Hertfordshire, UK) with a photomultiplier detector. X-rays were generated using an electron gun accelerating voltage of 145kV and a beam current of 45μA and a tungsten target. Due to the model size, the femur was scanned in proximal, middle and distal sections. For the proximal scan, the femur was inverted and to permit this, was mounted in a polyethylene tube with base and lid components that connected to the adjustable sample platform of the scanner. After mounting on the sample platform, the femur was centred in the x-ray beam, the electron beam focused, and the detector calibrated under no-x-ray-beam and uninterrupted-x-ray-beam conditions. The samples were then scanned at 1600 angular positions integrating 16 frames at each. After the scanning process the raw data was collected and reconstructed using Next Generation Imaging (NGI) version 1.4.59 software (X-TEK Systems Ltd) with an average voxel size of 120μm.

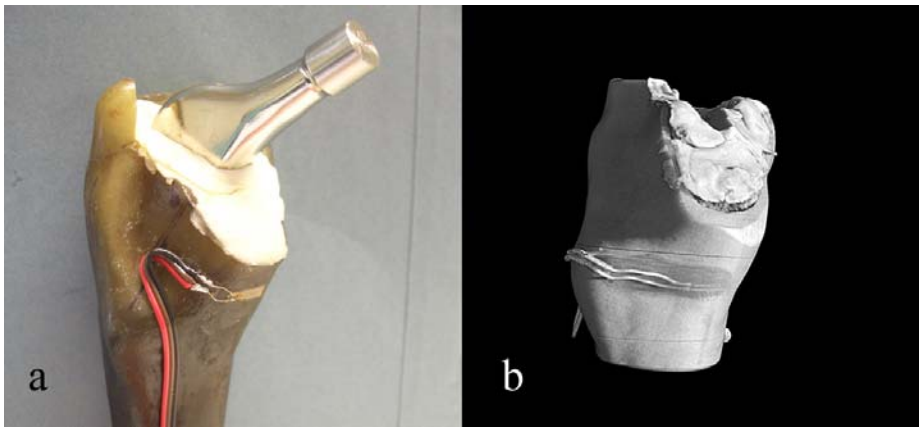

Figure 6-11 Femoral model for impaction bone grafting. (a) Composite femur with Exeter stem cemented in situ. Proximal strain gauge attached to medial calcar. (b) 3D CT reconstruction of proximal femur.

6.4.5 Micro CT analysis

The reconstructed images were visualized using Volume Graphics (VG) Studio Max 1.2.1 software package (Volume Graphics, GmbH, and Heidelberg, Germany) and 3D views (Figure 6-11b) were created along with axial, sagittal and coronal slices. Segmentation tools allowed the extraction of cement, bone graft and femoral sawbone components individually (Figure 6-13). Along with the 3D view of the individual component a histogram plotting the number of voxels against grey scale value was created. To determine the grey scale range for the individual components, the sawbone, air, water, bone graft and cement were all scanned separately, using identical image settings. Regions from the distal, middle and proximal thirds of the femur were analysed (Figure 6-12). Sub-volumes, 2cm in height and 2cm apart, commencing from the tip of the prosthesis were selected and represented distal, middle and proximal regions of interest (ROI). Referencing from the stem tip ensured reproducible volumes were selected, and excluded any variation introduced from depth of stem insertion.

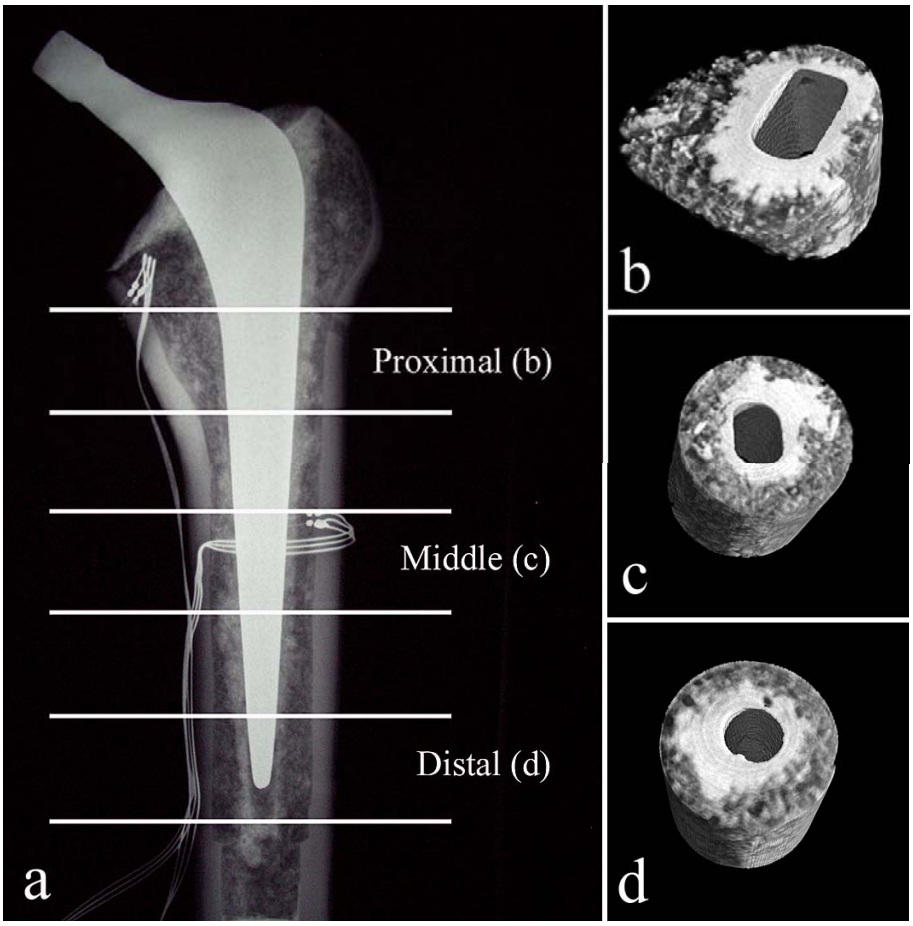

Figure 6-12 Regions of analysis. (a) Scout view of femoral model demonstrating the selected regions analysed. Representative cross sectional 3D reconstructions at (b) proximal, (c) middle and (d) distal regions of interest.

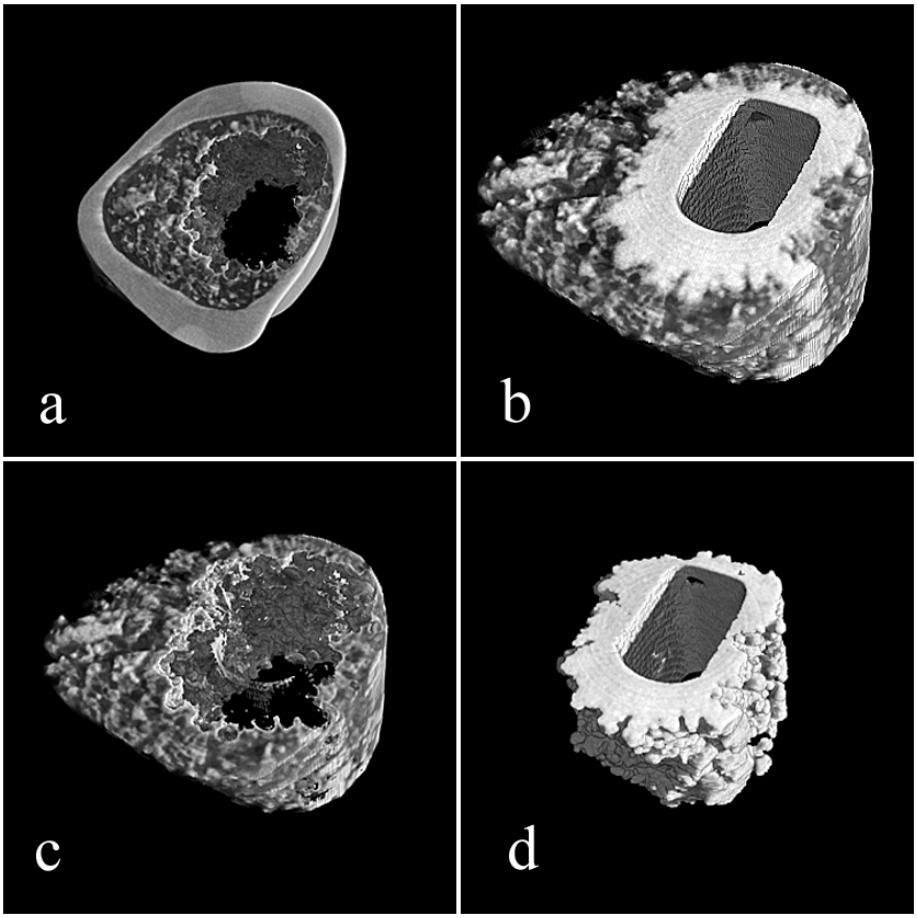

Figure 6-13 Segmented 3D reconstructions of impacted bone graft. (a) sawbone femur and bone graft, (b) bone graft and cement mantle, (c) bone graft only and (d) cement mantle only.

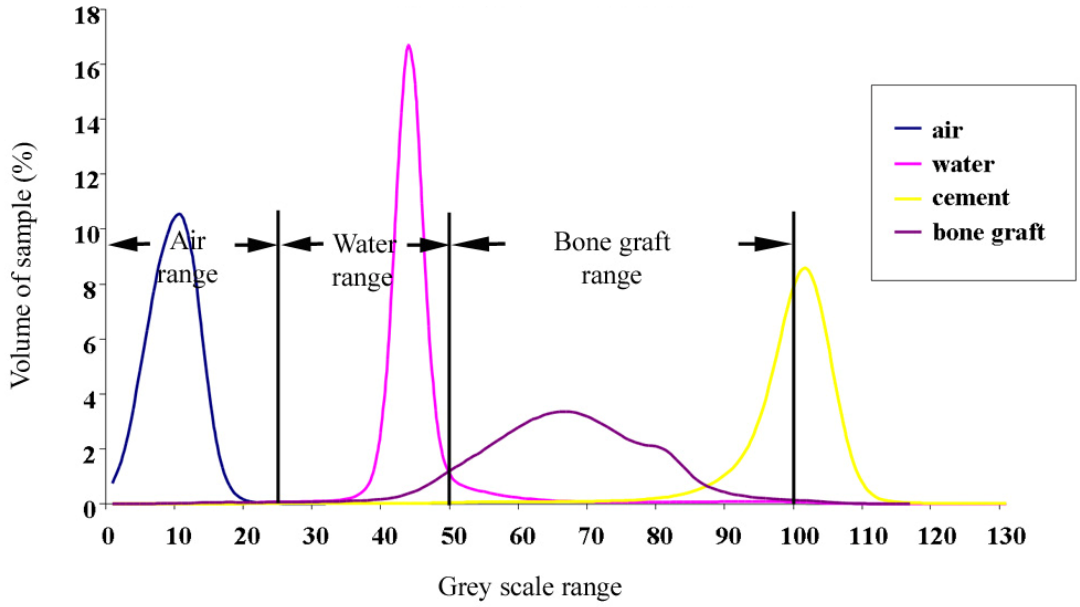

Figure 6-14 CT calibration histogram. Grey scale ranges represented by the individual analysed components of the femoral impaction bone grafting model (air, water, bone graft, cement).

Based on the determined grey scale ranges for separate components (Figure 6-14) the total number of voxels representing cement and bone graft for distal middle and proximal regions for both the control and vibration groups were quantified. The cement volume was expressed both as a percentage of the total ROI and in mm^3 (the resolution of the scan determined the dimension of the voxel from which the volume in mm^3 could be calculated). The segmented bone graft volume also represented proportions of air and water and therefore all three components were quantified separately and measured as a percentage of the total segmented volume. This also had the additional advantage of eradicating any differences in the segmented volumes under analysis.

6.4.6 Stability Measurements

Approximately 48 hours after implantation, the stability of the prosthesis was tested using an Instron 8878 servo-hydraulic materials testing machine (Instron

Ltd, High Wycombe, UK). In addition to the strain gauges which were used in the per-operative measurements, two displacement transducers (Solartron DFg 2.5 LVDT, RS Components Ltd, Corby, UK) were mounted on the femur using aluminium brackets such that axial and rotational relative movements between the prosthesis and bone could be measured. The axial displacement transducer was aligned with the long axis of the femur in the anterior-posterior and medial lateral planes, and the rotational transducer perpendicular to the axial transducer. The axial transducer made contact with the prosthesis on the underside of the femoral head and the rotational transducer approximately 10mm medial to the intersection of the mid shaft and neck axes of the prosthesis (Figure 6-9). We calculated out of plane motion during subsidence to be negligible as we were primarily studying axial and rotational subsidence with loading. After fixing the potted femurs rigidly to the base plate of the testing machine, loads were applied to the femoral head via a bearing which minimised off-axis loading of the femur and testing machine actuator.

The femur was loaded according to a protocol developed by Morlock *et al* (Westphal et al., 2006). To replicate physiological loading, cyclic loads in a sinusoidal pattern were applied to the femoral head. Mean loads, load-amplitudes and number of cycles for each sequence are shown in Figure 6-15.

Sequence	Number of cycles	Minimum load (N)	Maximum load (N)	Mean load (N)	Load Amplitude (N)
1	20	50	200	125	75
2	980	50	800	425	375
3	1000	50	1200	625	575
4	1000	50	1600	825	775
5	47000	50	2100	1075	1025

Figure 6-15 Table of load profiles. Load profiles used for experimental testing of prosthesis subsidence.

6.5 Results

6.5.1 Per-operative Observations

The impaction procedure in the control and vibration groups was performed by a single surgeon. Every attempt was made to standardise the procedures in each group. In all procedures in both groups, three sets of distal impactions were performed with matching portions by weight of graft before moving onto the proximal impaction. In the control group one sawbone developed a proximal third short oblique fracture during the impaction process (Figure 6-16). There were no fractures in the vibration group.

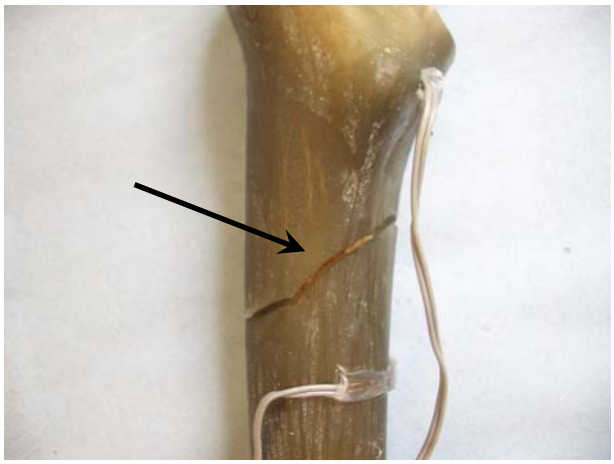

Figure 6-16 Image of fractured sawbone.

The mean amount of allograft used in the control group was 73.1g (SD 1.74) and in the vibration group 79.5g (SD 4.04) The amount of graft used in the vibration group was significantly higher than in the control group ($p<0.01$).

6.5.2 Per-operative measurements - Impaction Loads and Hoop Strains

The peak load and peak hoop strain were determined from the load and strain recordings for each femur from each set of impactions. The means and standard

deviations of these peak values were then calculated and are presented in Figures 6-17, 6-18 and 6-19.

The mean peak load transmitted through the phantom / tamp, bone graft and composite femur to the load cell during proximal compaction was 3.28kN (SD 0.97) in the control group and 1.71kN (SD 0.10) in the vibration group. This difference was statistically significant (p=0.005). During distal compaction there was no statistically significant difference in the mean peak loads (1.59kN, SD 0.47 - control group; 1.47kN, SD 0.15 - vibration group).

With each consecutive set of proximal impactions the mean peak load was significantly higher in the control group than in the vibration group. There was no observed statistically significant difference between groups during the distal impactions (Figure 6-17).

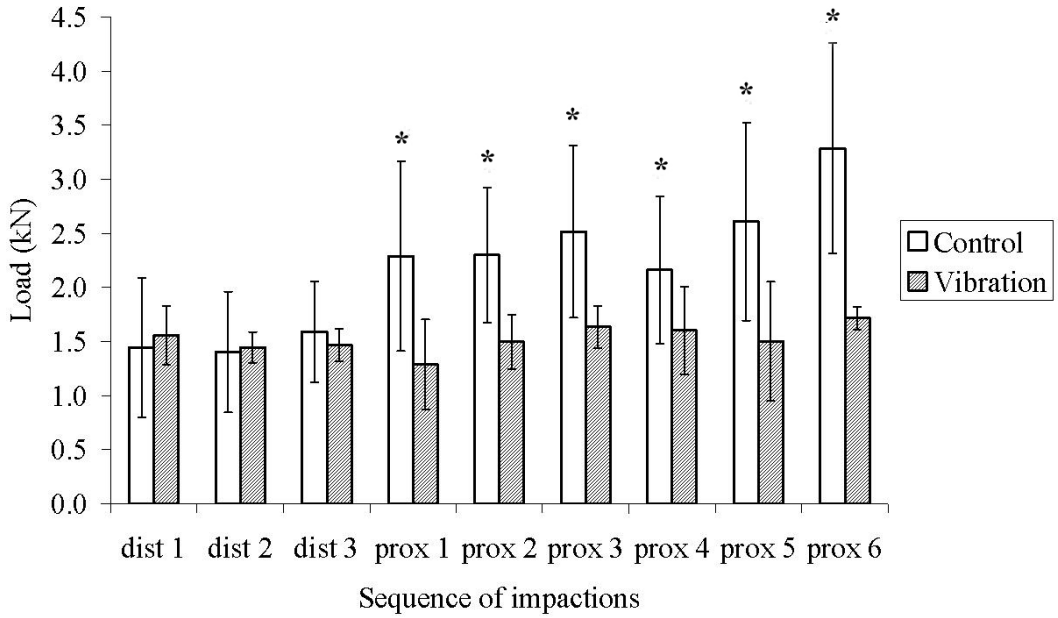

Figure 6-17 Mean peak loads (kN). Data represents mean peak loads (+/- SD, n=5) during each sequence of distal and proximal impactions (**p<0.01, *p<0.05).

The mean peak proximal hoop strain was 13.2% (SD 4.8) in the control group and 4.2% (SD 1.3) in the vibration group. This difference was statistically significant (p=0.009). The mean peak mid shaft hoop strain was 5.6% (SD 1.0) in the control group and 2.7% (SD 0.8) in the vibration group. Again this difference was statistically significant (p=0.006). These correlated closely with the mean peak load in each sample (control group: R^2=0.80, p=0.007; experimental group: R^2=0.70, p= 0.001).

With each consecutive set of impactions the mean peak proximal and mid shaft hoop strain increased in the control group whereas in the vibration group a steady state was achieved (Figure 6-18 and 6-19).

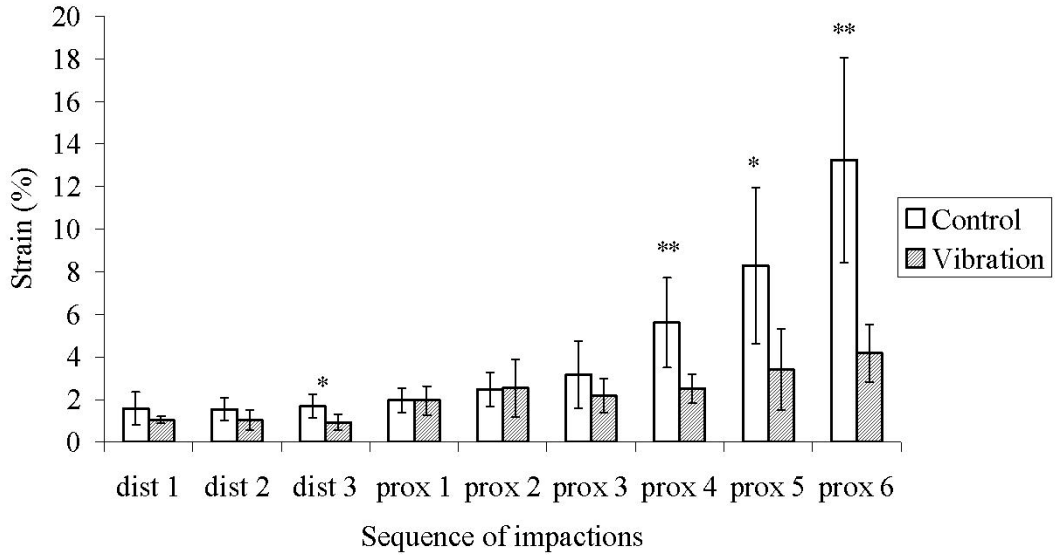

Figure 6-18 Mean peak proximal hoop strains (kPa). Data represents mean peak proximal hoop strains (+/- SD, n=5) during each sequence of distal and proximal impactions (**p<0.01, *p<0.05).

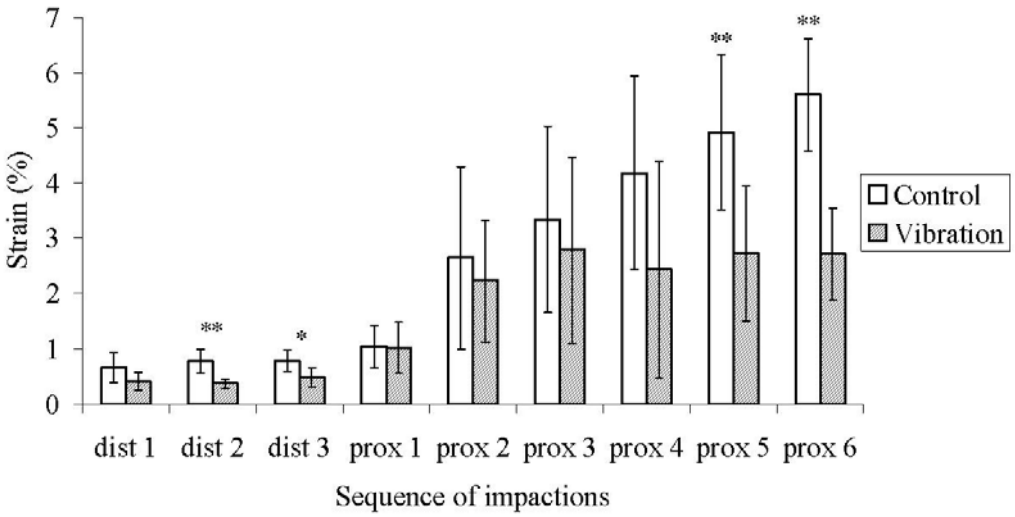

Figure 6-19 Mean peak mid hoop strains (kPa). Data represents mean peak mid hoop strains (+/- SD, n=5) during each sequence of distal and proximal impactions (**p<0.01, *p<0.05).

The range of values recorded for load and strain measurements were reduced in the vibration group compared to the control group, indicated by lower standard deviations.

6.5.3 Micro CT results: Regional analysis

6.5.3.1 Bone graft, air and water proportions; Cement volume (distal ROI).

Cement Volume: The volume of bone cement represented in the distal ROI was 1.21cm^3 (SD 0.26) or 32.1% (SD 6.8) in the control group and 1.29cm^3 (SD 0.38) or 34.0% (SD 9.1) in the vibration group (Figure 6-20). This difference was not statistically different (p=0.72).

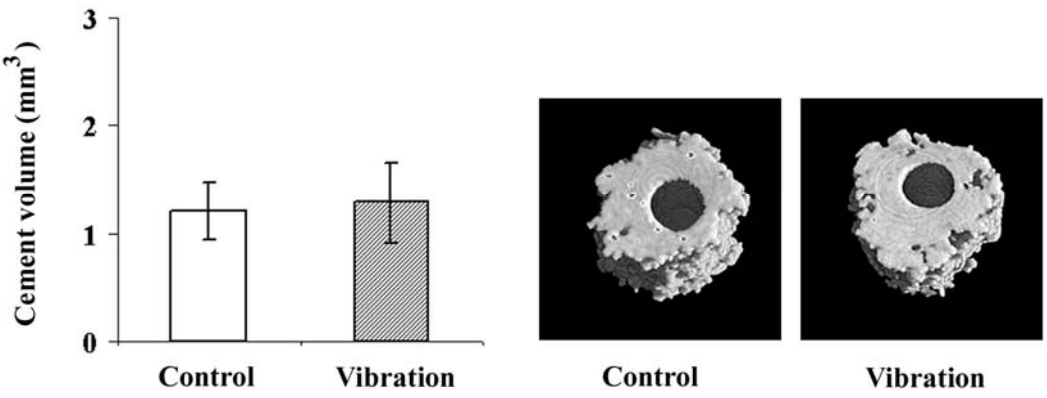

Figure 6-20 Mean Cement Volume (distal ROI). Graphical representation of the mean cement volume (mean cm^3 +/-SD) in the distal region of interest (n=5, *p<0.05, **p<0.01), along with 3D μ-CT images of representative cement mantles from both groups.

Bone graft proportions: The distal ROI was composed of a mean 96.2% (SD 1.5%) bone graft, 3.1% (SD 1.2%) water and 0.4% (SD 0.3%) air in the control group compared to 94.9% (SD 3.3%) bone graft, 3.9% (SD 2.2%) water and 1.0% (SD 1.2%) air in the vibration group (Figure 6-21). For all components the difference between the two groups was not statistically significant (Bone graft: p=0.43; water: p=0.49; air: p=0.35).

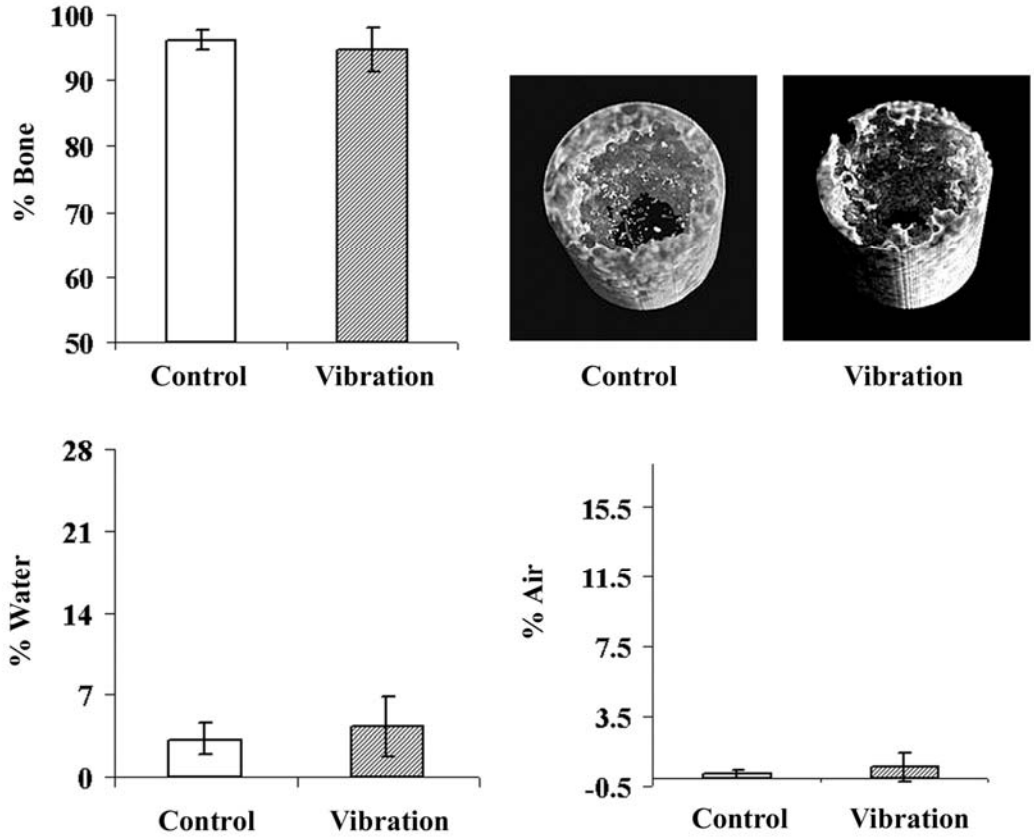

Figure 6-21 Bone graft proportions (distal ROI). Graphical representation of the mean proportions of bone graft (along with representative μ-CT reconstructions of impacted bone graft mantle), water and air (mean % +/-SD) in the distal region of interest (n=5, *p<0.05, **p<0.01).

6.5.3.2 Bone graft, air and water proportions; Cement volume (middle ROI)

Cement Volume: The volume of bone cement represented in the middle ROI was 2.21cm^3 (SD 0.25) or 62.2% (SD 7.4) in the control group and 1.64cm^3 (SD 0.15) or 45.7% (SD 4.4) in the vibration group (Figure 6-22). This difference was statistically different (p<0.01).

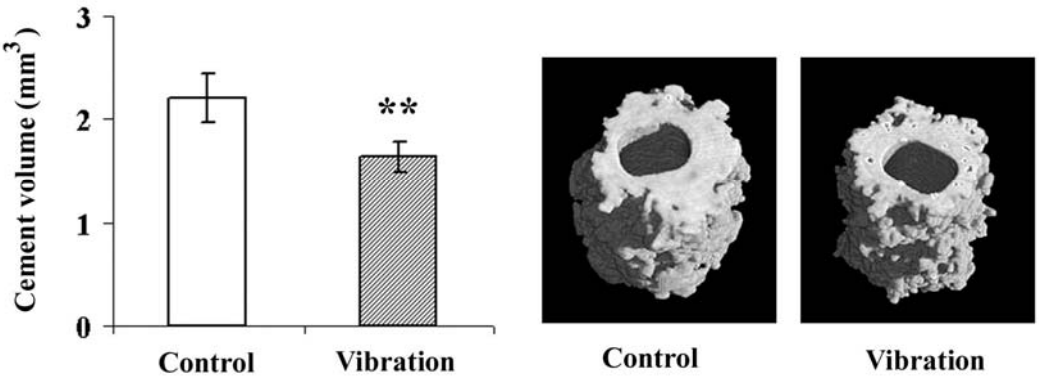

Figure 6-22 Mean cement volume (middle ROI). Graphical representation of the mean cement volume (mean cm3 +/-SD) in the middle region of interest (n=5, *p<0.05, **p<0.01), along with 3D μ-CT images of representative cement mantles from both groups.

Bone graft proportions: The middle ROI was composed of a mean 81.9% (SD 6.0%) bone graft, 12.5% (SD 3.1%) water and 5.5% (SD 3.1%) air in the control group compared to 91.8% (SD 2.3%) bone graft, 6.7% (SD 1.5%) water and 1.2% (SD 1.0%) air in the vibration group (Figure 6-23). The increase in the proportion of bone graft along with a drop in the proportions of water and air in the vibration group compared to the control group was significant in all cases (bone graft: $p<0.05$; water $p<0.01$; air $p<0.05$).

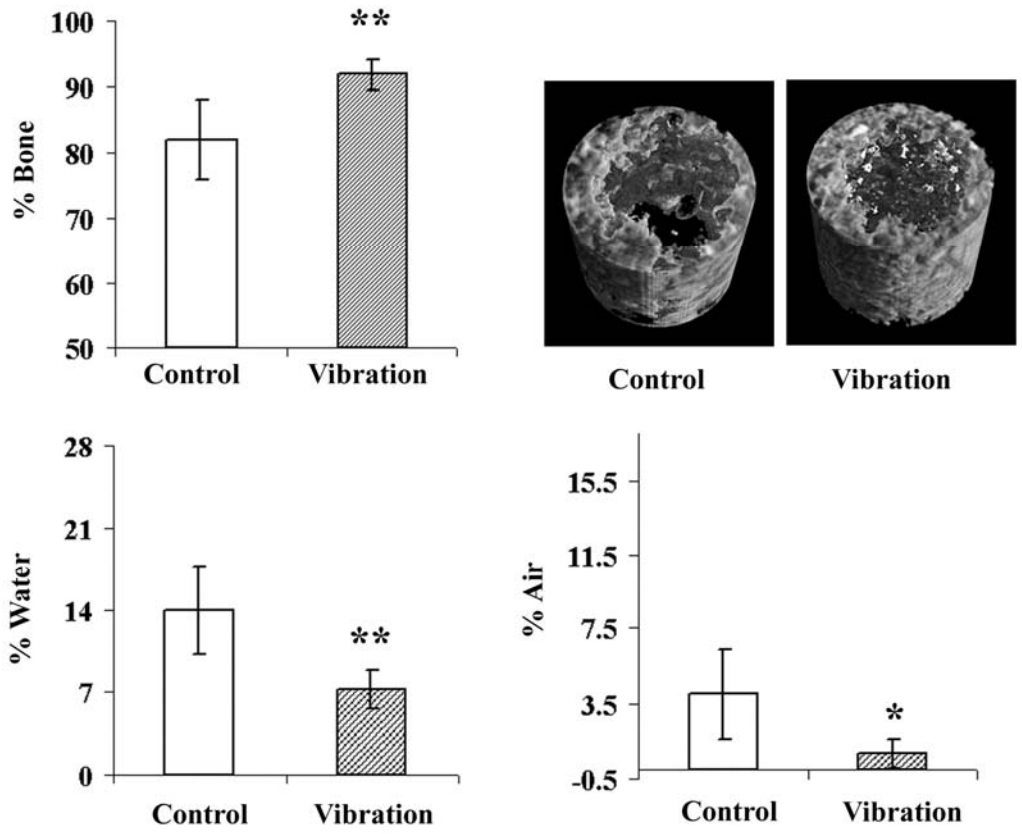

Figure 6-23 Bone graft proportions (middle ROI). Graphical representation of the mean proportions of bone graft (along with representative μ-CT reconstructions of impacted bone graft mantle), water and air (mean % +/-SD) in the middle region of interest (n=5, *p<0.05, **p<0.01).

6.5.3.3 Bone graft, air & water proportions; Cement volume (proximal ROI)

Cement Volume: The volume of bone cement represented in the proximal ROI was 2.34cm^3 (SD 0.33) or 40.8% (SD 5.3) in the control group compared to 2.53cm^3 (SD 0.25) or 43.2% (SD 3.6) in the vibration group (Figure 6-24). This difference was not statistically different (p=0.29).

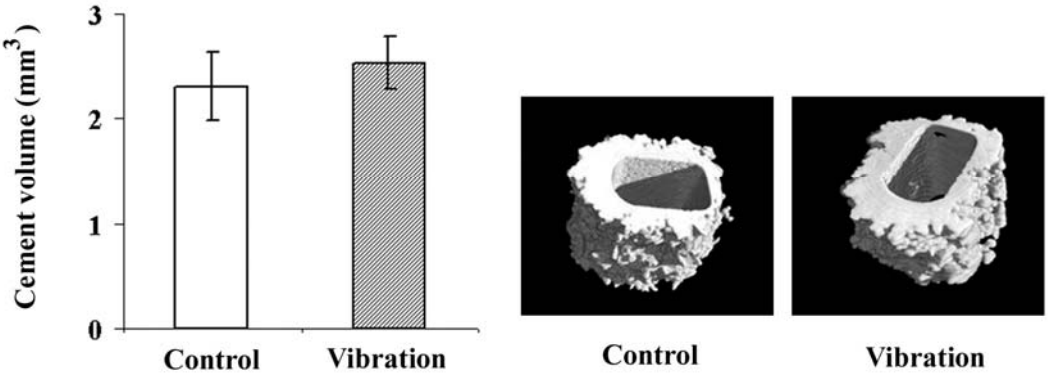

Figure 6-24 Mean cement volume (proximal ROI). Graphical representation of the mean cement volume (mean cm3 +/-SD) in the proximal region of interest (n=5, *p<0.05, **p<0.01), along with 3D µ-CT images of representative cement mantles from both groups.

Bone graft proportions: The proximal ROI was composed of a mean 63.8% (SD 3.1%) bone graft, 22.5% (SD 1.8%) water and 13.5% (SD 1.9%) air in the control group compared to 68.8% (SD 3.1%) bone graft, 19.4% (SD 2.1%) water and 10.8% (SD 1.9%) air in the vibration group (Figure 6-25). The increase in the proportion of bone graft along with a drop in the proportions of water and air in the vibration group compared to the control group was significant in all cases (bone graft: $p<0.05$; water $p<0.05$; air $p<0.05$).

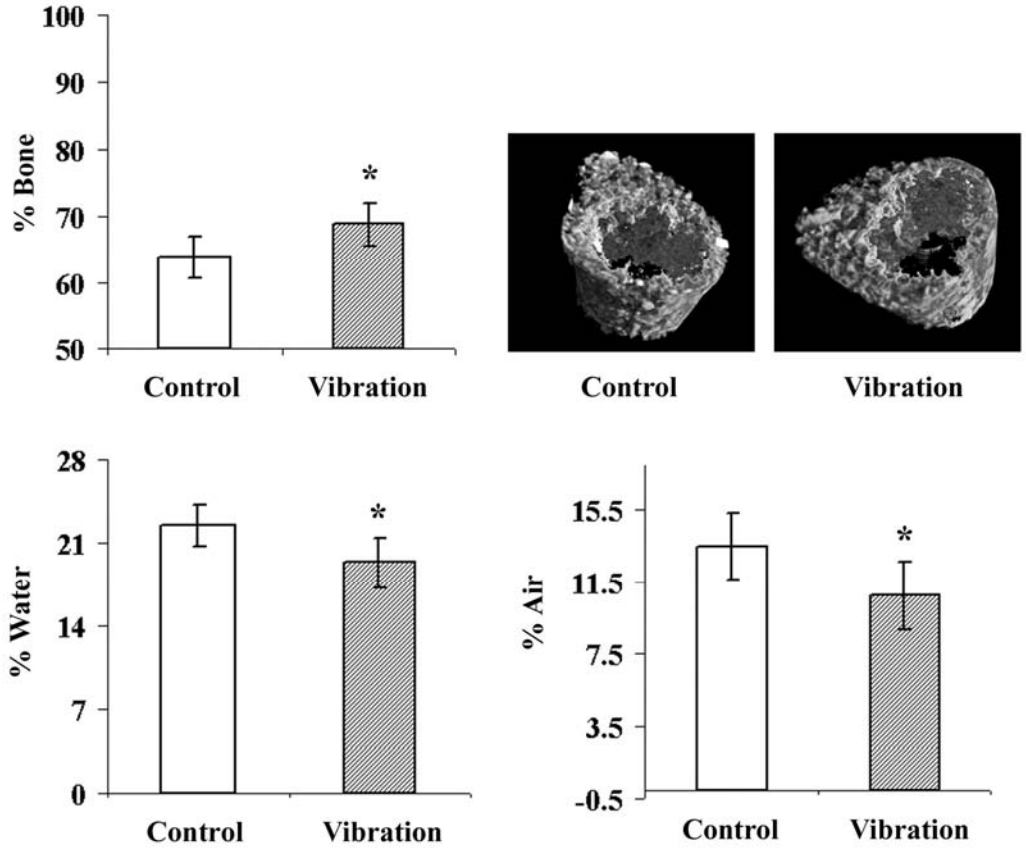

Figure 6-25 Bone graft proportions (proximal ROI). Graphical representation of the mean proportions of bone graft (along with representative μ-CT reconstructions of impacted bone graft mantle), water and air (mean % +/-SD) in the proximal region of interest (n=5, *p<0.05).

6.5.4 Stability Measurements

No specimens failed during cyclical loading. Most subsidence occurred in the initial loading phases. By 50,000 cycles there was ongoing, albeit minor subsidence of the prosthesis relative to the bone. In both groups, visual observations suggested that subsidence was due to the movement between cement and graft or graft and sawbone, rather than between the prosthesis and cement, although this was not directly measured.

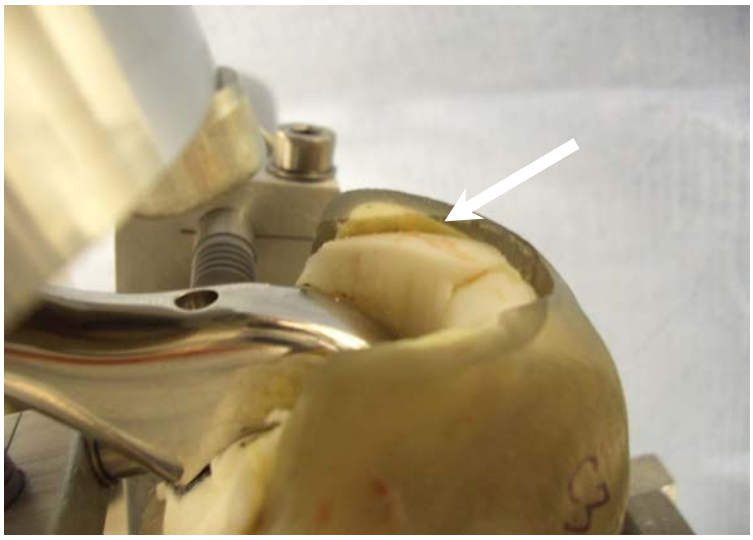

Figure 6-26 Image of subsidence. Subsidence interface appeared to occur between either the bone graft and sawbone cortical shell or between the cement and impacted allograft.

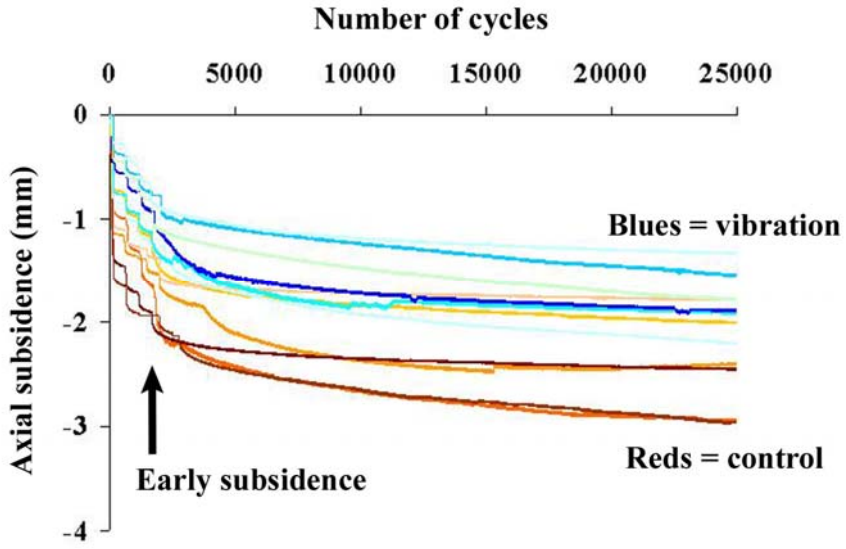

Figure 6-27 Pattern of subsidence. Greatest degree of subsidence occurred early during the cyclical loading before reaching a plateau by the end of the test (n=5).

The mean total axial subsidence after 50,000 cycles was 2.47mm in the control group compared to 1.79mm in the vibration group. This difference was statistically significant (p=0.03)

There was no statistically significant difference in rotational subsidence between groups (0.66mm, SD 0.57 – control group; 0.57mm, SD 0.47 – vibration group).

6.6 Discussion

The risk of fracture and massive subsidence of the prosthesis post-operatively are the two most significant obstacles to the wider adoption by the orthopaedic community of femoral impaction bone grafting in revision hip replacement surgery. The fracture rate has been highlighted as a concern in a number of studies (Fetzer et al., 2001; Meding et al., 1997; Pekkarinen et al., 2000) and varies significantly between series (upto 27%) (Ornstein et al., 2001). In the absence of methods to establish when the graft has been adequately compacted there is a significant learning curve between over-impaction causing a fracture of the femur and under impaction leading to prosthetic instability and massive subsidence (Eldridge et al., 1997).

This experimental study has demonstrated that vibration assisted impaction bone grafting leads to reduced peak loads and strains in the femur during graft compaction presumably indicating a lower risk of femoral fracture for the vibration assisted technique. In addition, the vibration-compacted graft bed provides enhanced implant stability with less prosthetic subsidence.

Studies on soil mechanics have established that vibration applied to an aggregate will result in more efficient particle alignment and reduce the energy required to impact the aggregate (Smith, 1990). Using vibration assisted graft compaction there was a significant reduction in both the peak impaction loads experienced by the femur and the peak hoop strains transmitted to the femoral cortex. The range of values observed for both peak loads and strains were also much smaller in the vibration group. Changing the load the surgeon applied to the vibration device resulted in a negligible increase in peak load and peak hoop strain. From this study, it appeared that the peak loads were limited by the vibration device itself rather than the surgeon, potentially a useful characteristic in a surgical tool. In contrast the loads and

strains transmitted in the standard technique were dependent on how hard the tamp was hit with the slap hammer and therefore were prone to increased variability (as shown by the higher standard deviation values in the control group).

Previous studies have standardised the amount of energy transmitted to the bone graft using a weight dropping from a known height. In this study the impaction force was not standardized in this way because the variability of the standard technique, as a result of human factors, was thought to be an important characteristic of the procedure. This variability was observed with a surgeon, highly experienced in the field of IBG, performing all the impactions. This was in contrast to the vibration technique which resulted in less variable load and strain values in the hands of the same experienced surgeon, therefore offering greater control and reproducibility over the existing technique.

One of the fundamental difficulties with IBG is ascertaining intraoperatively when the graft is adequately impacted. Only one study to date has suggested a method to assess rotational stability of the femoral phantom using a modified torque wrench (Hostner et al., 2001). With vibration assisted graft compaction a plateau is reached whereby further use of the vibration device does not result in higher loads and strains being generated which may provide a "safety net" against inducing strains at which a fracture is more likely to occur. In addition it was also noticed that completion of graft compaction (indicated by cessation of further subsidence of the phantom / tamp within the bone graft mantle) coincided with clear auditory and tactile changes in the vibration instrumentation. The ability to determine the point of adequate compaction intraoperatively would be a significant advantage to the surgeon and should potentially avoid over impaction and its potential risk of fracture.

This study has also demonstrated that vibration and drainage can improve the compaction of aggregates such as bone graft, through better alignment of the particles with denser packing and greater interparticulate surface area contact. In doing so the volume in between the particles, consisting of air and fluid is reduced. In the field of civil engineering this has been shown to occur with the application of vibration (Smith, 1990; Lambe, 1979). Vibration gives the particulate material a better chance to come into a denser packing provided that the void space reduction is

allowed by adequate drainage of the fluids in the void space. In the presence of excess fluid in a contained space, compaction effort is transmitted not only to the bone graft but also to the fluid resulting in poorer impaction of the graft particles (Dunlop et al., 2003). Drainage is used widely for in-situ densification of loosely deposited sands to alleviate the risk of soil liquefaction under earthquake loading. Improved closer packing increases the inter-particulate contacts and the shear strength of the particulate material (Brennan et al., 2005; Coelho et al., 2007).

In this study the proportion of bone graft in the vibration group was increased in both the proximal and middle regions of the femur, with a concomitant decrease in the proportions of air and water. These findings are consistent with improved denser packing and compaction of the graft. In the distal region there was no difference in proportions of bone graft, air or water between the two groups. This has been supported by a previous femoral impaction bone grafting study on cadaveric femora which also demonstrated increased graft compaction in the region where the distal impactors were used (Frei et al., 2004). There are several possibilities for this. The distal impactors have a much smaller surface area in contact with the bone graft and therefore the vibrating area will have less contact and therefore less effect on realigning the bone graft particles. An axial compressive force is transmitted during distal impaction rather than a radial compressive force (that occur with the tapered proximal impactors). Consequently, the bone graft distally is often well compacted using the standard technique, making it more difficult to detect a significant improvement. Finally, the length of column of distal graft impacted is much less than in the proximal impactions, resulting in the dissipation of fluid around the sides and top of the distal impactors, thus nullifying the potential benefits from the addition of drainage holes to distal impactors.

It is important to note the improvement in bone graft compaction not only has a mechanical but also a potential biological advantage. Greater bone graft compaction should result in less cement penetration into the interparticulate spaces leaving a greater bone graft mantle for neovascularisation and bone remodelling to take place. Studies have demonstrated a positive correlation between increased cement penetration and delayed revascularisation of the endosteal surface, essential for graft incorporation and remodelling (de Waal et al., 1988).

The cement volume in the vibration group, in the middle region of the femur, was reduced, which correlated with the improved graft compaction also observed in this region. In the distal region where there was no difference in graft compaction the cement volume also remained unchanged between the two groups. However in the proximal region the cement volume remained the same despite an increase in % bone graft, suggesting inferior compaction in comparison to the middle region. Possible explanations include the fact that the proximal bone graft not only sustains the fewest impactions / exposure to vibration but also is the most difficult to contain, an essential requirement for good graft impaction.

With better graft impaction and therefore support for the prosthesis, the second associated complication with IBG, namely post operative subsidence of the prosthesis, would hopefully be addressed. The frequency of massive subsidence (10mm) has been reported as high as 11% (Eldridge et al., 1997). This current study has demonstrated that less subsidence occurs with vibration assisted compaction. This can be explained again by basic soil mechanics principles. According to the Mohr Coulomb theory of the strength of granular materials, the shear strength of a granular aggregate like bone graft depends on the internal friction (Φ), expressed as the angle at which the aggregate will slide, and the interlocking of the particles (c), expressed as a stress ($\tau = c + \sigma \tan\Phi$). It is postulated that vibration improves the packing of the aggregate particles increasing the particle interlocking ($\uparrow c$) and according to the Mohr Coulomb failure Law, shear strength of the aggregate ($\uparrow \tau$).

$$\uparrow \tau = \sigma \tan\varphi + \uparrow c$$

This study has demonstrated that the use of vibration and drainage (in the form of a perforated tamp) can lead to an improvement in graft compaction, stem stability and lower peak hoop strains and loads. Although it has been established that vibration alone will improve aggregate strength (as long as there is free drainage of fluid), the effect of the perforated tamps (i.e. drainage alone) in the absence of vibration are unknown. We can hypothesize that the perforations alone would reduce the hoop strains and loads, but on their own, would not improve particulate

realignment and interlocking and therefore not improve graft compaction and strength to the extent that was found. Future studies are planned to test this hypothesis along with investigating parameters characterising the vibration hammer and perforated tamps to establish optimum impaction conditions, including the effects of vibration frequency and amplitude, air pressure and the number, size and position of the holes in the tamps.

6.7 Summary

This experimental study has demonstrated that vibration-assisted impaction bone grafting leads to reduced peak loads and hoop strains in the femur during graft compaction. This may reduce the risk of femoral fracture. The resulting graft is better able to resist subsidence of the prosthesis in the laboratory situation.

The peak loads and strains recorded during vibration-assisted compaction reached a steady level during the compaction process providing a clear end point to graft compaction. This end point was indicated by audible and tactile changes in the behaviour of the instrumentation during the procedure providing a clear indication to the surgeon when the procedure was complete. This is in contrast to the current clinically adopted control technique. Ongoing use of the vibration hammer during graft compaction does not appear to increase the load or hoop strains transmitted to the femur and therefore reduces the potential of over-impaction and the associated risk of fracture.

A safer, more flexible method to compact bone graft should lead to the more widespread use of IBG as a technique to deal with extensive bone loss in revision hip surgery. Further studies, using the perforated tamps individually rather than in combination with vibration, would clearly define the effect of each individual component on strain, load and stability.

6.8 Conclusion

The results in the context of the null hypothesis were examined:

1. "The use of vibration coupled with a drainage system to impact bone graft does not reduce the peak forces and hoop strains created during impaction"

This hypothesis is ***false***

2. "The use of vibration coupled with a drainage system to impact bone graft does not improve graft compaction"

This hypothesis is ***false***

3. "The use of vibration coupled with a drainage system to impact bone graft does not result in less subsidence of the prosthesis under cyclical loading"

This hypothesis is ***false***

PATENT

The design of the vibration impaction bone grafting system is now represented with a patent.

- **Patent No. 0613274.0 (July 06) Centre for Enterprise & Innovation, University of Southampton.**
- **Renewed July 07**

6.9 Appendix

Peak Load, Proximal strain and mid strain values in control and experimental groups (commencing with last sequence of proximal impactions)

	Peak load	Min prox strain	Min Mid strain			Peak load	Min prox strain	Min Mid strain
Cont 1	2.06	52.05	54.95		**Vib 1**	1.59	39.00	26.00
Cont 2	4.29	163.84	50.08		**Vib 2**	1.76	41.90	34.80
Cont 3	3.62	145.68	48.85		**Vib 3**	1.83	19.60	39.40
Cont 4	3.13	102.29	47.15		**Vib 4**	1.82	47.00	18.20
Cont 5	2.80	145.00	61.00		**Vib 5**	1.60	41.40	19.80
Cont 6	4.70	186.00	74.00		**Vib 6**	1.70	61.20	24.40
Mean strain (x100)		132.48	56.01				41.68	27.10
Mean (N,%,%)	3.43	13.25	5.60			1.72	4.17	2.71
SD	0.97	4.81	1.01			0.11	1.34	0.84

	Peak load	Min prox strain	Min Mid strain			Peak load	Min prox strain	Min Mid strain
Cont 1	2.01	68.83	58.16		**Vib 1**	0.43	12.00	10.00
Cont 2	4.25	57.90	48.60		**Vib 2**	1.99	25.00	34.40
Cont 3	2.07	89.02	37.02		**Vib 3**	1.78	22.00	40.80
Cont 4	2.89	39.81	30.21		**Vib 4**	1.71	60.10	14.40
Cont 5	2.00	96.00	52.00		**Vib 5**	1.60	31.60	34.00
Cont 6	3.30	145.00	69.00		**Vib 6**	1.50	54.50	29.70
Mean strain (x100)		82.76	49.17				34.20	27.22
Mean (N,%,%)	2.75	8.28	4.92			1.50	3.42	2.72
SD	0.91	3.67	1.41			0.55	1.91	1.22

	Peak load	Min prox strain	Min Mid strain			Peak load	Min prox strain	Min Mid strain
Cont 1	2.10	52.56	41.40		**Vib 1**	1.60	29.00	23.50
Cont 2	1.38	31.40	11.50		**Vib 2**	2.09	34.40	41.10
Cont 3	2.21	50.46	45.70		**Vib 3**	1.79	25.00	34.40
Cont 4	2.33	39.85	40.05		**Vib 4**	1.82	25.70	10.70
Cont 5	2.40	85.60	46.10		**Vib 5**	1.40	22.60	40.50
Cont 6	3.00	77.00	66.00		**Vib 6**	0.92	13.90	17.10
Mean strain (x100)		56.15	41.79				25.10	24.32
Mean (N,%,%)	2.24	5.61	4.18			0.16	2.51	2.43
SD	0.52	2.11	1.76			0.04	0.68	1.96

	Peak load	Min prox strain	Min Mid strain			Peak load	Min prox strain	Min Mid strain
Cont 1	2.93	30.13	42.74		**Vib 1**	1.52	22.50	16.30
Cont 2	1.82	14.15	7.25		**Vib 2**	1.53	36.30	46.20
Cont 3	2.02	18.26	27.05		**Vib 3**	1.97	15.40	48.60
Cont 4	1.92	33.45	30.85		**Vib 4**	1.75	23.00	16.65
Cont 5	2.50	59.20	58.20		**Vib 5**	1.45	15.00	31.00
Cont 6	3.90	35.00	34.50		**Vib 6**	1.60	18.50	8.30
Strain (x100)		31.70	33.43			1.64	21.78	27.84
Mean (N,%,%)	2.52	3.17	3.34			0.16	2.18	2.78
SD	0.80	1.59	1.69			0.02	0.79	1.68

	Peak load	Min prox strain	Min Mid strain			Peak load	Min prox strain	Min Mid strain
Cont 1	2.82	25.43	45.83		**Vib 1**	1.55	30.00	8.00
Cont 2	1.33	15.00	15.00		**Vib 2**	1.80	30.10	23.80
Cont 3	1.98	21.98	6.98		**Vib 3**	1.72	12.20	39.00
Cont 4	2.26	31.93	21.52		**Vib 4**	1.42	11.70	29.30
Cont 5	2.30	35.50	47.30		**Vib 5**	1.40	47.70	20.00
Cont 6	3.10	18.00	22.00		**Vib 6**	1.10	20.30	13.70
Strain (x100)		24.64	26.44			1.50	25.33	22.30
Mean (N,%,%)	2.30	2.46	2.64				2.53	2.23
SD	0.63	0.79	1.65				1.36	1.11

	Peak load	Min prox strain	Min Mid strain			Peak load	Min prox strain	Min Mid strain
Cont 1	2.13	15.39	10.30		**Vib 1**	1.18	20.60	5.50
Cont 2	1.52	29.00	16.12		**Vib 2**	1.56	19.00	15.20
Cont 3	1.52	23.17	6.98		**Vib 3**	1.40	22.50	14.90
Cont 4	2.17	21.43	7.90		**Vib 4**	1.13	12.20	4.00
Cont 5	3.90	13.90	13.90		**Vib 5**	1.30	15.00	11.00
Cont 6	2.50	15.20	7.20		**Vib 6**	0.72	16.50	10.30
Strain (x100)		19.68	10.40			1.22	17.63	10.15
Mean (N,%,%)	2.29	1.97	1.04				1.76	1.02
SD	0.88	0.59	0.38				0.38	0.47

Peak Load, Proximal strain and mid strain values in control and experimental groups (commencing with <u>last</u> sequence of distal impactions)

	Peak load	Min prox strain	Min Mid strain			Peak load	Min prox strain	Min Mid strain
Cont 1	1.34	20.60	9.60		**Vib 1**	1.50	15.00	5.00
Cont 2	0.92	12.50	8.20		**Vib 2**	1.62	11.00	7.40
Cont 3	1.93	21.25	6.63		**Vib 3**	1.53	8.30	3.10
Cont 4	2.26	23.55	9.27		**Vib 5**	1.48	7.00	5.20
Cont 5	1.50	10.40	4.50		**Vib 6**	1.22	5.60	3.50
Cont 6	1.60	13.00	8.60					
Strain (x100)		16.88	7.80			1.47	9.38	4.84
Mean (N,%,%)	1.59	1.69	0.78			1.47	0.94	0.48
SD	0.47	0.55	0.19			0.15	0.37	0.17

	Peak load	Min prox strain	Min Mid strain			Peak load	Min prox strain	Min Mid strain
Cont 1	1.07	9.70	9.70		**Vib 1**	1.49	12.40	4.20
Cont 2	0.62	10.00	11.00		**Vib 2**	1.47	17.00	5.00
Cont 3	1.50	19.37	6.36		**Vib 3**	1.57	10.20	3.00
Cont 4	1.53	23.49	5.59		**Vib 5**	1.50	6.60	3.00
Cont 5	1.40	15.30	6.00		**Vib 6**	1.20	5.60	3.50
Cont 6	2.30	14.50	8.00					
Strain (x100)		15.39	7.78			1.45	10.36	3.74
Mean (N,%,%)	1.40	1.54	0.78			1.45	1.04	0.37
SD	0.56	0.54	0.22			0.14	0.46	0.09

	Peak load	Min prox strain	Min Mid strain			Peak load	Min prox strain	Min Mid strain
Cont 1	0.86	12.00	9.40		**Vib 1**	1.89	12.90	2.80
Cont 2	0.65	7.70	10.10		**Vib 2**	1.35	8.50	3.00
Cont 3	1.59	19.50	5.62		**Vib 3**	1.81	11.00	5.20
Cont 4	1.27	29.54	6.59		**Vib 5**	1.44	10.20	6.34
Cont 5	2.30	13.40	4.80		**Vib 6**	1.30	10.00	3.10
Cont 6	2.00	13.20	3.00					
Strain (x100)		15.89	6.59			1.56	10.52	4.09
Mean (N,%,%)	1.45	1.59	0.66			1.56	1.05	0.41
SD	0.64	0.77	0.27			0.27	0.16	0.16

Proportions of Cement, Bone, Water and Air in distal, middle and proximal regions of interest in both control and experimental groups.

		Cement	Bone Graft	Air	Water			Cement	Bone Graft	Air	Water
Distal ROI	**Cont 1**	914422	95.19	0.18	4.35		**Vib 1**	837097	96.93	0.18	2.58
	Cont 2	1017079	96.87	0.11	2.66		**Vib 2**	1249533	94.84	0.32	4.47
	Cont 3	1411986	98.13	0.02	1.57		**Vib 3**	1166193	96.09	0.34	3.26
	Cont 4	1159081	94.34	0.59	4.72		**Vib 4**	1882622	89.17	2.18	8.46
	Cont 5	1536542	96.67	0.32	2.84		**Vib 5**	1293010	97.22	0.17	2.36
Mean (voxels)		1207822						1285691			
Mean (cm3,%)		**1.21**	**96.24**	**0.24**	**3.23**			**1.29**	**94.85**	**0.64**	**4.22**
SD		**0.26**	**1.49**	**0.22**	**1.30**			**0.38**	**3.31**	**0.87**	**2.50**
Middle ROI	**Cont 1**	2049480	77.48	4.88	17.57		**Vib 1**	1706607	90.75	0.52	8.45
	Cont 2	2621667	75.92	6.83	16.89		**Vib 2**	1542723	92.27	0.37	7.19
	Cont 3	2206145	83.52	3.06	13.35		**Vib 3**	1868286	92.24	0.92	6.65
	Cont 4	2173019	81.50	4.73	13.70		**Vib 4**	1476213	88.82	2.16	8.70
	Cont 5	1992022	91.25	0.53	8.04		**Vib 5**	1606999	94.98	0.26	4.60
Mean (voxels)		2208467						1640166			
Mean (cm3,%)		**2.21**	**81.93**	**4.01**	**13.91**			**1.64**	**91.81**	**0.85**	**7.12**
SD		**0.25**	**6.03**	**2.36**	**3.78**			**0.15**	**2.26**	**0.78**	**1.65**
Proximal ROI	**Cont 1**	1987589	64	14.3854	21		**Vib 1**	2144278	64.60	12.29	22.49
	Cont 2	2161779	62	13.2601	25		**Vib 2**	2647709	70.02	9.54	20.28
	Cont 3	2009731	66	11.7576	22		**Vib 3**	2508902	68.92	11.61	18.06
	Cont 4	2699281	60	16.1878	24		**Vib 4**	2831574	67.38	12.42	19.01
	Cont 5	2685675	68	11.8028	20		**Vib 5**	2525819	72.96	8.09	17.10
Mean (voxels)		2308811						2531656			
Mean (cm3,%)		**2.31**	**63.77**	**13.48**	**22.50**			**2.53**	**68.78**	**10.79**	**19.39**
SD		**0.36**	**3.11**	**1.87**	**1.80**			**0.25**	**3.10**	**1.90**	**2.09**

CHAPTER 7.

Future Direction

This thesis has utilised a number of modalities to improve the mechanical and biological properties of allograft for use in the field of impaction bone grafting. Furthermore these studies have highlighted a potential synthetic graft as an alternative to allograft for potential use in this field. These modalities have included mesenchymal stem cell biology, mechanical engineering and clinical orthopaedics. With expertise also available in fields including, finite element analysis and modelling, cell-manipulation surface engineering and materials chemistry a number of future proposals have been developed on the background of the pilot studies within this thesis. These questions and study proposals include:

Biological Augmentation

Current studies have utilised unfractionated human bone marrow samples but have neither explored the effect of pure bone marrow alone or the potential of cell sorting techniques to further augment the biological and mechanical capabilities of the seeded cell population.

Bone marrow aspirate (BMA): Cell sorting techniques have been used in tissue engineering to select and isolate cell populations with the proposed benefit of augmenting the yield and cellular potential. However there are few studies, including those in this thesis that has determined whether cell selection in any form has any benefit (either biological or mechanical) over bone marrow aspirate alone. Clarke et al (Clarke et al., 2007), in an in vivo ulna defect rabbit model using a TCP scaffold, demonstrated more bone formation with the addition of BMA alone than culture expanded HBMSC's. Clinically BMA has been used in combination with allograft in impaction bone grafting (Deakin, Bannister, 2007) with reported improved graft incorporation. However this study was performed without a comparison to either allograft alone or culture expanded cells. Culture expansion is not without issues,

including expense (GMP facility), variable patient cellular response to in vitro expansion conditions and the concern over contamination. Therefore in impaction bone grafting it would be prudent to compare the potential degree of biological and mechanical augmenation with the addition of cellular expanded over bone marrow aspirate alone to justify its necessity.

Cell selection: The most simple is the extraction of the mononuclear cell fraction only, (using centrifugation or density gradient medium). More complex sorting techniques and the current main methods that exist for the sorting of mesenchymal stem cells, based on their surface markers include flow cytometry and magnetic-activated cell separation (MACS). Both employ labelled antibodies (Abs) to the cell surface marker antigens (Ag). Flow cytometry uses fluorescence labelled antibodies which bind to the Ab-Ag complex on the MSC surface and can separate cells in a culture according to fluorescing Abs when the cells are passed through a FACS (fluorescence-activated cell sorter) device. Examples of the fluorescent labelled Abs include FITC-conjugated (Fluorescin Isocyanate) anti-mouse IgM (Immunoglobulin M) or IgG_1. For the MACS method the Abs to the cell surface Ags are allowed to bind, then the Abs in turn are bound to anti-mouse IgM or IgG_1 molecules which are fused to magnetic microbeads. Under the presence of a magnetic field these cells are separated from the other cells present in the medium and can be subcultured separately.

A future proposal therefore is to determine if these cell sorted populations seeded onto impacted scaffold (either synthetic or natural) result in an improved yield of cells with osteogenic potential in vitro (2D culture, 3D seeded onto scaffold) and in vivo (3D seeded onto scaffold) and further augment the biological and mechanical properties of the living composites when compared to unsorted populations, BMA alone or scaffolds alone.

Effects of mechanical loading on graft / HBMSC constructs

Current studies have utilised unloaded in vivo animal models. In the clinical setting the femoral and acetabula prosthetic components and the adjacent impacted bone graft undergo daily variable physiological loads. In the acetabulum the bone graft is

subjected mainly to compression and the femoral graft more to shear forces. From these studies the effect of daily loading on the impacted living composite of scaffold / HBMSC has yet to be established. Methodology and surgical protocol for a large animal (ovine) model to explore these effects is currently in development. From these studies the biological boost with the addition of HBMSC to morsellised scaffold did not appear to upset the normal balanced coupling process of bone remodelling. Loading the biological grafts will provide an additional stimulus, which effect on the balance between bone formation and resorption has not been established. The temporal changes that occur within the scaffold / HBMSC composites upon loading will be important in providing evidence for the surgeon to determine post operative management with regard to the weight bearing status of the patient. A future proposal therefore is to establish using a large animal ovine model, the biological effects of mechanical loading on allograft / HBMSC or $P_{DL}LA$ / HBMSC constructs with respect to the balance of graft resorption Vs. new bone formation over time.

Scaffold combinations

Advances in scaffold technology are constantly creating novel scaffold designs. Although not a novel material $P_{DL}LA$ is a highly versatile scaffold for use in tissue engineering. The versatile manufacturing process renders it possible to encapsulate growth factors and modify overall microarchitecture. Possible graft composite alternatives include

- $P_{DL}LA$ / allograft mix (50:50; 90:10)
- $P_{DL}LA$ / HA composite
- $P_{DL}LA$ containing encapsulated vEGF / BMP-2 scaffolds.Scaffold technology.

Current studies have used 100% allograft or 100% $P_{DL}LA$ combined with culture expanded HBMSC. A future proposal is to explore the biological and mechanical effects of these various $P_{DL}LA$ scaffolds either alone or in combination with varying proportions of morsellised allograft.

Vibration IBG

Current pilot study demonstrated an improvement in bone graft compaction and reduction in the fracture risk with the use of vibration and drainage for bone graft impaction. However this has yet to be performed on an acetabula model and many of the optimum vibration and drainage parameters are yet to be determined. Therefore further studies are planned to establish if (a) the same advantages demonstrated on the femoral model is also observed when using vibration and drainage on an equivalent acetabula model; (b) what are the optimum number, size and position of the drainage holes; (c) what is the optimum amplitude and frequency of the vibration hammer.

Ultimately optimisation in each of these areas will aid in the development of the desired scaffold, cell population, and surgical technique for use in IBG in the clinical setting.

CHAPTER 8

References

1. **Anderson MJ, Keyak JH, Skinner HB**. Compressive mechanical properties of human cancellous bone after gamma irradiation. *J.Bone Joint Surg.Am.* 1992; 74:747-752

2. **Antonov EN, Bagratashvili VN, Whitaker MJ, Barry JJ, Shakesheff KM, Konovalov AN, Popov VK, Howdle SM**. Three-Dimensional Bioactive and Biodegradable Scaffolds Fabricated by Surface-Selective Laser Sintering. *Adv.Mater.Deerfield.* 2004; 17:327-330

3. **Arinzeh TL, Peter SJ, Archambault MP, van den BC, Gordon S, Kraus K, Smith A, Kadiyala S**. Allogeneic mesenchymal stem cells regenerate bone in a critical-sized canine segmental defect. *J.Bone Joint Surg.Am.* 2003; 85-A:1927-1935

4. **Arts JJ, Gardeniers JW, Welten ML, Verdonschot N, Schreurs BW, Buma P**. No negative effects of bone impaction grafting with bone and ceramic mixtures. *Clin.Orthop.Relat Res.* 2005; 438:239-247

5. **Barry JJ, Silva MM, Popov VK, Shakesheff KM, Howdle SM**. Supercritical carbon dioxide: putting the fizz into biomaterials. *Philos.Transact.A Math.Phys.Eng Sci.* 2006; 364:249-261

6. **Bianco P, Robey PG**. Stem cells in tissue engineering. *Nature* 2001; 414:118-121

7. **Birrell F, Johnell O, Silman A**. Projecting the need for hip replacement over the next three decades: influence of changing demography and threshold for surgery. *Ann.Rheum.Dis.* 1999; 58:569-572

8. **Blom AW, Cunningham JL, Hughes G, Lawes TJ, Smith N, Blunn G, Learmonth ID, Goodship AE**. The compatibility of ceramic bone graft substitutes as allograft extenders for use in impaction grafting of the femur. *J.Bone Joint Surg.Br.* 2005; 87:421-425

9. **Board TN, Rooney P, Kearney JN, Kay PR**. Impaction allografting in revision total hip replacement. *J.Bone Joint Surg.Br.* 2006; 88:852-857

10. **Bolland BJ, Partridge K, Tilley S, New AM, Dunlop DG, Oreffo RO**. Biological and mechanical enhancement of impacted allograft seeded with human bone marrow stromal cells: potential clinical role in impaction bone grafting. *Regen.Med.* 2006; 1:457-467

11. **Bolland BJ, Tilley S, New AM, Dunlop DG, Oreffo RO**. Adult mesenchymal stem cells and impaction grafting: a new clinical paradigm shift. *Expert.Rev.Med.Devices* 2007; 4:393-404

12. **Bonfiglio M, Jeter WS**. Immunological responses to bone. *Clin.Orthop.Relat Res.* 1972; 87:19-27

13. **Bozic KJ, Durbhakula S, Berry DJ, Naessens JM, Rappaport K, Cisternas M, Saleh KJ, Rubash HE**. Differences in patient and procedure characteristics and hospital resource use in primary and revision total joint arthroplasty: a multicenter study. *J.Arthroplasty* 2005; 20:17-25

14. **Brennan AJ, Madabhushi SPG**. Liquefaction and drainage in stratified soil. *Journal of Geotechnical and GeoEnv.Engineering* 2005; 131:876

15. **Brewster NT, Gillespie WJ, Howie CR, Madabhushi SP, Usmani AS, Fairbairn DR**. Mechanical considerations in impaction bone grafting. *J.Bone Joint Surg.Br.* 1999; 81:118-124

16. **Brey EM, King TW, Johnston C, McIntire LV, Reece GP, Patrick CW, Jr.** A technique for quantitative three-dimensional analysis of microvascular structure. *Microvasc.Res.* 2002; 63:279-294

17. **Brey EM, Patrick CW, Jr.** Tissue engineering applied to reconstructive surgery. *IEEE Eng Med Biol.Mag.* 2000; 19:122-125

18. **Brodt MD, Swan CC, Brown TD**. Mechanical behavior of human morselized cancellous bone in triaxial compression testing. *J.Orthop.Res.* 1998; 16:43-49

19. **Bruder SP, Kraus KH, Goldberg VM, Kadiyala S**. The effect of implants loaded with autologous mesenchymal stem cells on the healing of canine segmental bone defects. *J.Bone Joint Surg.Am.* 1998; 80:985-996

20. **Buck BE, Malinin TI, Brown MD**. Bone transplantation and human immunodeficiency virus. An estimate of risk of acquired immunodeficiency syndrome (AIDS). *Clin.Orthop.Relat Res.* 1989;129-136

21. **Burwell RG**. Studies in the transplantation of bone. VII. The fresh composite homograft-autograft of cancellous bone; An analysis of factors leading to osteogenesis in marrow transplants and in marrow containing bone grafts. *The Journal of Bone and Joint Surgery (Proceedings)* 1964;110-140

22. **Burwell RG**. The function of bone marrow in the incorporation of bone graft. *Clin.Orthop.Relat Res.* 1985;125-141

23. **Chappard C, Peyrin F, Bonnassie A, Lemineur G, Brunet-Imbault B, Lespessailles E, Benhamou CL**. Subchondral bone micro-architectural alterations in osteoarthritis: a synchrotron micro-computed tomography study. *Osteoarthritis.Cartilage.* 2006; 14:215-223

24. **Clarke SA, Hoskins NL, Jordan GR, Marsh DR**. Healing of an ulnar defect using a proprietary TCP bone graft substitute, JAX, in association with autologous osteogenic cells and growth factors. *Bone* 2007; 40:939-947

25. **Coelho PA, Haigh SK, Madabhushi SPG, O'Brien AS**. Post-earthquake behaviour of footings when using densification as a liquefaction resistance measure. *Ground Improvement Journal (Invited paper)* 2007; 11:

26. **Cornu O, Banse X, Docquier PL, Luyckx S, Delloye C**. Effect of freeze-drying and gamma irradiation on the mechanical properties of human cancellous bone. *J.Orthop.Res.* 2000; 18:426-431

27. **Cornu O, Bavadekar A, Godts B, Van TJ, Delloye C, Banse X**. Impaction bone grafting with freeze-dried irradiated bone. Part II. Changes in stiffness and compactness of morselized grafts: experiments in cadavers. *Acta Orthop.Scand.* 2003; 74:553-558

28. Cra**ig RF**. *Soil mechanics. London: Chapman and Hall*. 1993

29. **Crowe JF, Sculco TP, Kahn B**. Revision total hip arthroplasty: hospital cost and reimbursement analysis. *Clin.Orthop.Relat Res.* 2003;175-182

30. **Dai KR, Xu XL, Tang TT, Zhu ZA, Yu CF, Lou JR, Zhang XL**. Repairing of goat tibial bone defects with BMP-2 gene-modified tissue-engineered bone. *Calcif.Tissue Int.* 2005; 77:55-61

31. **Davies OR, Lewis AL, Whitaker MJ, Tai H, Shakesheff KM, Howdle SM**. Applications of supercritical CO(2) in the fabrication of polymer systems for drug delivery and tissue engineering. *Adv.Drug Deliv.Rev.* 2008; 60:373-387

32. **Deakin DE, Bannister GC**. Graft incorporation after acetabular and femoral impaction grafting with washed irradiated allograft and autologous marrow. *J Arthroplasty* 2007; 22:89-94

33. **de Waal MJ, Slooff TJ, Huiskes R, de Laat EA, Barentsz JO**. Vascular changes following hip arthroplasty. The femur in goats studied with and without cementation. *Acta Orthop.Scand.* 1988; 59:643-649

34. **den Boer FC, Wippermann BW, Blokhuis TJ, Patka P, Bakker FC, Haarman HJ**. Healing of segmental bone defects with granular porous hydroxyapatite augmented with recombinant human osteogenic protein-1 or autologous bone marrow. *J.Orthop.Res.* 2003; 21:521-528

35. **Deschaseaux F, Gindraux F, Saadi R, Obert L, Chalmers D, Herve P**. Direct selection of human bone marrow mesenchymal stem cells using an anti-CD49a antibody reveals their CD45med,low phenotype. *Br.J.Haematol.* 2003; 122:506-517

36. **Dixon T, Shaw M, Ebrahim S, Dieppe P**. Trends in hip and knee joint replacement: socioeconomic inequalities and projections of need. *Ann.Rheum.Dis.* 2004; 63:825-830

37. **Djonov V, Andres AC, Ziemiecki A**. Vascular remodelling during the normal and malignant life cycle of the mammary gland. *Microsc.Res.Tech.* 2001; 52:182-189

38. **Dunlop DG, Brewster NT, Madabhushi SP, Usmani AS, Pankaj P, Howie CR**. Techniques to improve the shear strength of impacted bone graft: the effect of particle size and washing of the graft. *J.Bone Joint Surg.Am.* 2003; 85-A:639-646

39. **Duvall CL, Taylor WR, Weiss D, Guldberg RE**. Quantitative microcomputed tomography analysis of collateral vessel development after ischemic injury. *Am.J Physiol Heart Circ.Physiol* 2004; 287:H302-H310

40. **Eldridge JD, Smith EJ, Hubble MJ, Whitehouse SL, Learmonth ID**. Massive early subsidence following femoral impaction grafting. *J.Arthroplasty* 1997; 12:535-540

41. **Feinberg SE, Aghaloo TL, Cunningham LL, Jr.** Role of tissue engineering in oral and maxillofacial reconstruction: findings of the 2005 AAOMS Research Summit. *J.Oral Maxillofac.Surg.* 2005; 63:1418-1425

42. **Fetzer GB, Callaghan JJ, Templeton JE, Goetz DD, Sullivan PM, Johnston RC**. Impaction allografting with cement for extensive femoral bone loss in revision hip surgery: a 4- to 8-year follow-up study. *J.Arthroplasty* 2001; 16:195-202

43. **Ficat RP**. Idiopathic bone necrosis of the femoral head. Early diagnosis and treatment. *J.Bone Joint Surg.Br.* 1985; 67:3-9

44. **Frei H, Mitchell P, Masri BA, Duncan CP, Oxland TR**. Allograft impaction and cement penetration after revision hip replacement. A histomorphometric analysis in the cadaver femur. *J.Bone Joint Surg.Br.* 2004; 86:771-776

45. **Friedlaender GE**. Bone grafts. The basic science rationale for clinical applications. *J.Bone Joint Surg.Am.* 1987; 69:786-790

46. **Fujishiro T, Nishikawa T, Niikura T, Takikawa S, Nishiyama T, Mizuno K, Yoshiya S, Kurosaka M**. Impaction bone grafting with hydroxyapatite: increased femoral component stability in experiments using Sawbones. *Acta Orthop.* 2005; 76:550-554

47. **Gangji V, Hauzeur JP**. Treatment of osteonecrosis of the femoral head with implantation of autologous bone-marrow cells. Surgical technique. *J.Bone Joint Surg.Am.* 2005; 87 Suppl 1:106-112

48. **Gangji V, Hauzeur JP, Matos C, De M, V, Toungouz M, Lambermont M**. Treatment of osteonecrosis of the femoral head with implantation of autologous bone-marrow cells. A pilot study. *J.Bone Joint Surg.Am.* 2004; 86-A:1153-1160

49. **Gangji V, Toungouz M, Hauzeur JP**. Stem cell therapy for osteonecrosis of the femoral head. *Expert.Opin.Biol.Ther.* 2005; 5:437-442

50. **Gie GA, Linder L, Ling RS, Simon JP, Slooff TJ, Timperley AJ**. Contained morselized allograft in revision total hip arthroplasty. Surgical technique. *Orthop.Clin.North Am.* 1993; 24:717-725

51. **Goshima J, Goldberg VM, Caplan AI**. The osteogenic potential of culture-expanded rat marrow mesenchymal cells assayed in vivo in calcium phosphate ceramic blocks. *Clin.Orthop.Relat Res.* 1991;298-311

52. **Green D, Howard D, Yang X, Kelly M, Oreffo RO**. Natural marine sponge fiber skeleton: a biomimetic scaffold for human osteoprogenitor cell attachment, growth, and differentiation. *Tissue Eng* 2003; 9:1159-1166

53. **Guldberg RE, Lin AS, Coleman R, Robertson G, Duvall C**. Microcomputed tomography imaging of skeletal development and growth. *Birth Defects Res.C.Embryo.Today* 2004; 72:250-259

54. **Halliday BR, English HW, Timperley AJ, Gie GA, Ling RS**. Femoral impaction grafting with cement in revision total hip replacement. Evolution of the technique and results. *J.Bone Joint Surg.Br.* 2003; 85:809-817

55. **Heiner AD, Brown TD**. Structural properties of a new design of composite replicate femurs and tibias. *J.Biomech.* 2001; 34:773-781

56. **Heinzer S, Krucker T, Stampanoni M, Abela R, Meyer EP, Schuler A, Schneider P, Muller R**. Hierarchical microimaging for multiscale analysis of large vascular networks. *Neuroimage.* 2006; 32:626-636

57. **Hernigou P, Beaujean F**. Treatment of osteonecrosis with autologous bone marrow grafting. *Clin.Orthop.Relat Res.* 2002;14-23

58. **Hernigou P, Poignard A, Beaujean F, Rouard H**. Percutaneous autologous bone-marrow grafting for nonunions. Influence of the number and concentration of progenitor cells. *J.Bone Joint Surg.Am.* 2005; 87:1430-1437

59. **Hostner J, Hultmark P, Karrholm J, Malchau H, Tveit M**. Impaction technique and graft treatment in revisions of the femoral component: laboratory studies and clinical validation. *J.Arthroplasty* 2001; 16:76-82

60. **Huttmann A, Li CL, Duhrsen U**. Bone marrow-derived stem cells and "plasticity". *Ann.Hematol.* 2003; 82:599-604

61. **Jaffe KA, Dunham WK**. Treatment of benign lesions of the femoral head and neck. *Clin.Orthop.Relat Res.* 1990;134-137

62. **Jaffe KA, Launer EP, Scholl BM**. Use of a fibular allograft strut in the treatment of benign lesions of the proximal femur. *Am.J.Orthop.* 2002; 31:575-578

63. **Jaiswal N, Haynesworth SE, Caplan AI, Bruder SP**. Osteogenic differentiation of purified, culture-expanded human mesenchymal stem cells in vitro. *J.Cell Biochem.* 1997; 64:295-312

64. **Janderova L, McNeil M, Murrell AN, Mynatt RL, Smith SR**. Human mesenchymal stem cells as an in vitro model for human adipogenesis. *Obes.Res.* 2003; 11:65-74

65. **Jeppsson C, Astrand J, Tagil M, Aspenberg P**. A combination of bisphosphonate and BMP additives in impacted bone allografts. *Acta Orthop.Scand.* 2003; 74:483-489

66. **Kanczler JM, Barry J, Ginty P, Howdle SM, Shakesheff KM, Oreffo RO**. Supercritical carbon dioxide generated vascular endothelial growth factor encapsulated poly(DL-lactic acid) scaffolds induce angiogenesis in vitro. *Biochem.Biophys.Res.Commun.* 2007; 352:135-141

67. **Karrholm J, Hourigan P, Timperley J, Razaznejad R**. Mixing bone graft with OP-1 does not improve cup or stem fixation in revision surgery of the hip: 5-year follow-up of 10 acetabular and 11 femoral study cases and 40 control cases. *Acta Orthop.* 2006; 77:39-48

68. **Khanal GP, Garg M, Singh GK**. A prospective randomized trial of percutaneous marrow injection in a series of closed fresh tibial fractures. *Int.Orthop.* 2004; 28:167-170

69. **Kindlmann GL, Weinstein DM, Jones GM, Johnson CR, Capecchi MR, Keller C**. Practical vessel imaging by computed tomography in live transgenic mouse models for human tumors. *Mol.Imaging* 2005; 4:417-424

70. **Klawitter JJ, Bagwell JG, Weinstein AM, Sauer BW**. An evaluation of bone growth into porous high density polyethylene. *J.Biomed.Mater.Res.* 1976; 10:311-323

71. **Knight JL, Helming C**. Collarless polished tapered impaction grafting of the femur during revision total hip arthroplasty: pitfalls of the surgical technique and follow-up in 31 cases. *J.Arthroplasty* 2000; 15:159-165

72. **Korda M, Blunn G, Phipps K, Rust P, Di SL, Coathup M, Goodship A, Hua J**. Can mesenchymal stem cells survive under normal impaction force in revision total hip replacements? *Tissue Eng* 2006; 12:625-630

73. **Korovessis P, Koureas G, Zacharatos S, Papazisis Z, Lambiris E**. Correlative radiological, self-assessment and clinical analysis of evolution in instrumented dorsal and lateral fusion for degenerative lumbar spine disease. Autograft versus coralline hydroxyapatite. *Eur.Spine J.* 2005; 14:630-638

74. **Kurtz S, Ong K, Lau E, Mowat F, Halpern M**. Projections of primary and revision hip and knee arthroplasty in the United States from 2005 to 2030. *J.Bone Joint Surg.Am.* 2007; 89:780-785

75. **Lambe**. *Soil Mechanics - SI Version. London, John Wiley & Sons.* 1979

76. **Langer R, Vacanti JP**. Tissue engineering. *Science* 1993; 260:920-926

77. **Langheinrich AC, Ritman EL**. Quantitative imaging of microvascular permeability in a rat model of lipopolysaccharide-induced sepsis: evaluation using cryostatic micro-computed tomography. *Invest Radiol.* 2006; 41:645-650

78. **LeGeros RZ, Lin S, Rohanizadeh R, Mijares D, LeGeros JP**. Biphasic calcium phosphate bioceramics: preparation, properties and applications. *J.Mater.Sci.Mater.Med.* 2003; 14:201-209

79. **Leung PC, Chow YY**. Reconstruction of proximal femoral defects with a vascular-pedicled graft. *J.Bone Joint Surg.Br.* 1984; 66:32-37

80. **Ling RS, Timperley AJ, Linder L**. Histology of cancellous impaction grafting in the femur. A case report. *J.Bone Joint Surg.Br.* 1993; 75:693-696

81. **Lodie TA, Blickarz CE, Devarakonda TJ, He C, Dash AB, Clarke J, Gleneck K, Shihabuddin L, Tubo R**. Systematic analysis of reportedly distinct populations of multipotent bone marrow-derived stem cells reveals a lack of distinction. *Tissue Eng* 2002; 8:739-751

82. **Lord CF, Gebhardt MC, Tomford WW, Mankin HJ**. Infection in bone allografts. Incidence, nature, and treatment. *J.Bone Joint Surg.Am.* 1988; 70:369-376

83. **Lu C, Marcucio R, Miclau T**. Assessing angiogenesis during fracture healing. *Iowa Orthop.J.* 2006; 26:17-26

84. **Malyar NM, Gossl M, Beighley PE, Ritman EL**. Relationship between arterial diameter and perfused tissue volume in myocardial microcirculation: a micro-CT-based analysis. *Am.J Physiol Heart Circ.Physiol* 2004; 286:H2386-H2392

85. **McGee MA, Findlay DM, Howie DW, Carbone A, Ward P, Stamenkov R, Page TT, Bruce WJ, Wildenauer CI, Toth C**. The use of OP-1 in femoral impaction grafting in a sheep model. *J.Orthop.Res.* 2004; 22:1008-1015

86. **Meding JB, Ritter MA, Keating EM, Faris PM**. Impaction bone-grafting before insertion of a femoral stem with cement in revision total hip arthroplasty. A minimum two-year follow-up study. *J.Bone Joint Surg.Am.* 1997; 79:1834-1841

87. **Mikhail WE, Weidenhielm LR, Wretenberg P, Mikhail N, Bauer TW**. Femoral bone regeneration subsequent to impaction grafting during hip revision: histologic analysis of a human biopsy specimen. *J.Arthroplasty* 1999; 14:849-853

88. **Mirels H**. Metastatic disease in long bones. A proposed scoring system for diagnosing impending pathologic fractures. *Clin.Orthop.Relat Res.* 1989;256-264

89. **Moore DC, Leblanc CW, Muller R, Crisco JJ, III, Ehrlich MG**. Physiologic weight-bearing increases new vessel formation during distraction osteogenesis: a micro-tomographic imaging study. *J.Orthop.Res.* 2003; 21:489-496

90. **Muschler GF, Boehm C, Easley K**. Aspiration to obtain osteoblast progenitor cells from human bone marrow: the influence of aspiration volume. *J.Bone Joint Surg.Am.* 1997; 79:1699-1709

91. **Mushipe MT, Chen X, Jennings D, Li G**. Cells seeded on MBG scaffold survive impaction grafting technique: Potential application of cell-seeded biomaterials for revision arthroplasty. *J.Orthop.Res.* 2006; 24:501-507

92. **Nelissen RG, Bauer TW, Weidenhielm LR, LeGolvan DP, Mikhail WE**. Revision hip arthroplasty with the use of cement and impaction grafting. Histological analysis of four cases. *J.Bone Joint Surg.Am.* 1995; 77:412-422

93. **Nelissen RG, Valstar ER, Poll RG, Garling EH, Brand R**. Factors associated with excessive migration in bone impaction hip revision surgery: a radiostereometric analysis study. *J.Arthroplasty* 2002; 17:826-833

94. **Nuttall ME, Gimble JM**. Controlling the balance between osteoblastogenesis and adipogenesis and the consequent therapeutic implications. *Curr.Opin.Pharmacol.* 2004; 4:290-294

95. **Oonishi H, Hench LL, Wilson J, Sugihara F, Tsuji E, Kushitani S, Iwaki H**. Comparative bone growth behavior in granules of bioceramic materials of various sizes. *J.Biomed.Mater.Res.* 1999; 44:31-43

96. **Ornstein E, Atroshi I, Franzen H, Johnsson R, Sandquist P, Sundberg M**. Results of hip revision using the Exeter stem, impacted allograft bone, and cement. *Clin.Orthop.Relat Res.* 2001;126-133

97. **Ornstein E, Atroshi I, Franzen H, Johnsson R, Sandquist P, Sundberg M**. Early complications after one hundred and forty-four consecutive hip

revisions with impacted morselized allograft bone and cement. *J.Bone Joint Surg.Am.* 2002; 84-A:1323-1328

98. **Owen M, Friedenstein AJ**. Stromal stem cells: marrow-derived osteogenic precursors. *Ciba Found.Symp.* 1988; 136:42-60

99. **Park SR, Oreffo RO, Triffitt JT**. Interconversion potential of cloned human marrow adipocytes in vitro. *Bone* 1999; 24:549-554

100. **Pekkarinen J, Alho A, Lepisto J, Ylikoski M, Ylinen P, Paavilainen T**. Impaction bone grafting in revision hip surgery. A high incidence of complications. *J.Bone Joint Surg.Br.* 2000; 82:103-107

101. **Pelker RR, Friedlaender GE, Markham TC, Panjabi MM, Moen CJ**. Effects of freezing and freeze-drying on the biomechanical properties of rat bone. *J.Orthop.Res.* 1984; 1:405-411

102. **Peng H, Usas A, Olshanski A, Ho AM, Gearhart B, Cooper GM, Huard J**. VEGF improves, whereas sFlt1 inhibits, BMP2-induced bone formation and bone healing through modulation of angiogenesis. *J Bone Miner.Res.* 2005; 20:2017-2027

103. **Pittenger M, Vanguri P, Simonetti D, Young R**. Adult mesenchymal stem cells: potential for muscle and tendon regeneration and use in gene therapy. *J.Musculoskelet.Neuronal.Interact.* 2002; 2:309-320

104. **Pittenger MF, Mackay AM, Beck SC, Jaiswal RK, Douglas R, Mosca JD, Moorman MA, Simonetti DW, Craig S, Marshak DR**. Multilineage potential of adult human mesenchymal stem cells. *Science* 1999; 284:143-147

105. **Plouraboue F, Cloetens P, Fonta C, Steyer A, Lauwers F, Marc-Vergnes JP**. X-ray high-resolution vascular network imaging. *J.Microsc.* 2004; 215:139-148

106. **Roposch A, Saraph V, Linhart WE**. Treatment of femoral neck and trochanteric simple bone cysts. *Arch.Orthop.Trauma Surg.* 2004; 124:437-442

107. **Rowley SD, Prather K, Bui KT, Appel M, Felt T, Bensinger WI**. Collection of peripheral blood progenitor cells with an automated leukapheresis system. *Transfusion* 1999; 39:1200-1206

108. **Schreurs BW, Arts JJ, Verdonschot N, Buma P, Slooff TJ, Gardeniers JW**. Femoral component revision with use of impaction bone-grafting and a cemented polished stem. *J.Bone Joint Surg.Am.* 2005; 87:2499-2507

109. **Segal HE, Bellamy TN**. The Joint Health Benefits Delivery Program: improving access and reducing costs--successes and pitfalls. *Mil.Med.* 1988; 153:430-431

110. **Seshi B, Kumar S, King D**. Multilineage gene expression in human bone marrow stromal cells as evidenced by single-cell microarray analysis. *Blood Cells Mol.Dis.* 2003; 31:268-285

111. **Sharpe P**. Impaction grafting or cement alone for femoral revision hip replacement. *Conference proceedings,* 1998; ANZORS; Sydney, Australia:

112. **Shih HN, Cheng CY, Chen YJ, Huang TJ, Hsu RW**. Treatment of the femoral neck amd trochanteric benign lesions. *Clin.Orthop.Relat Res.* 1996;220-226

113. **Simmons PJ, Torok-Storb B**. Identification of stromal cell precursors in human bone marrow by a novel monoclonal antibody, STRO-1. *Blood* 1991; 78:55-62

114. **Simonds RJ, Holmberg SD, Hurwitz RL, Coleman TR, Bottenfield S, Conley LJ, Kohlenberg SH, Castro KG, Dahan BA, Schable CA, .** Transmission of human immunodeficiency virus type 1 from a seronegative organ and tissue donor. *N.Engl.J.Med.* 1992; 326:726-732

115. **Slooff TJ, Huiskes R, van HJ, Lemmens AJ**. Bone grafting in total hip replacement for acetabular protrusion. *Acta Orthop.Scand.* 1984; 55:593-596

116. **Smith GN**. *Elements of Soil Mechanics. 6th ed. Oxford, Blackwell Science*. 1990

117. **Stewart K, Monk P, Walsh S, Jefferiss CM, Letchford J, Beresford JN**. STRO-1, HOP-26 (CD63), CD49a and SB-10 (CD166) as markers of primitive human marrow stromal cells and their more differentiated progeny: a comparative investigation in vitro. *Cell Tissue Res.* 2003; 313:281-290

118. **Stock UA, Vacanti JP**. Tissue engineering: current state and prospects. *Annu.Rev.Med.* 2001; 52:443-451

119. **Tagil M, Aspenberg P**. Impaction of cancellous bone grafts impairs osteoconduction in titanium chambers. *Clin.Orthop.Relat Res.* 1998;231-238

120. **Tagil M, Jeppsson C, Aspenberg P**. Bone graft incorporation. Effects of osteogenic protein-1 and impaction. *Clin.Orthop.Relat Res.* 2000;240-245

121. **Thurecht KJ, Gregory AM, Villarroya S, Zhou J, Heise A, Howdle SM**. Simultaneous enzymatic ring opening polymerisation and RAFT-mediated polymerisation in supercritical CO2. *Chem.Commun.(Camb.)* 2006;4383-4385

122. **Toms AD, Barker RL, Jones RS, Kuiper JH**. Impaction bone-grafting in revision joint replacement surgery. *J.Bone Joint Surg.Am.* 2004; 86-A:2050-2060

123. **Toyota E, Fujimoto K, Ogasawara Y, Kajita T, Shigeto F, Matsumoto T, Goto M, Kajiya F**. Dynamic changes in three-dimensional architecture and vascular volume of transmural coronary microvasculature between diastolic- and systolic-arrested rat hearts. *Circulation* 2002; 105:621-626

124. **Triffitt JT**. Stem cells and the philosopher's stone. *J.Cell Biochem.Suppl* 2002; 38:13-19

125. **Uhrich KE, Cannizzaro SM, Langer RS, Shakesheff KM**. Polymeric systems for controlled drug release. *Chem.Rev.* 1999; 99:3181-3198

126. **Ullmark G, Obrant KJ**. Histology of impacted bone-graft incorporation. *J.Arthroplasty* 2002; 17:150-157

127. **Vaccaro AR, Chiba K, Heller JG, Patel TC, Thalgott JS, Truumees E, Fischgrund JS, Craig MR, Berta SC, Wang JC**. Bone grafting alternatives in spinal surgery. *Spine J.* 2002; 2:206-215

128. **van der DS, Weernink T, Buma P, Aspenberg P, Slooff TJ, Schreurs BW**. Rinsing morselized allografts improves bone and tissue ingrowth. *Clin.Orthop.Relat Res.* 2003;302-310

129. **van Haaren EH, Heyligers IC, Alexander FG, Wuisman PI**. High rate of failure of impaction grafting in large acetabular defects. *J.Bone Joint Surg.Br.* 2007; 89:296-300

130. **van Haaren EH, Smit TH, Phipps K, Wuisman PI, Blunn G, Heyligers IC**. Tricalcium-phosphate and hydroxyapatite bone-graft extender for use in impaction grafting revision surgery. An in vitro study on human femora. *J.Bone Joint Surg.Br.* 2005; 87:267-271

131. **Wang Y, Wan C, Deng L, Liu X, Cao X, Gilbert SR, Bouxsein ML, Faugere MC, Guldberg RE, Gerstenfeld LC, Haase VH, Johnson RS, Schipani E, Clemens TL**. The hypoxia-inducible factor alpha pathway couples angiogenesis to osteogenesis during skeletal development. *J Clin.Invest* 2007; 117:1616-1626

132. **Westphal FM, Bishop N, Honl M, Hille E, Puschel K, Morlock MM**. Migration and cyclic motion of a new short-stemmed hip prosthesis - a biomechanical in vitro study. *Clin.Biomech.(Bristol., Avon.)* 2006;

133. **Yang X, Tare RS, Partridge KA, Roach HI, Clarke NM, Howdle SM, Shakesheff KM, Oreffo RO**. Induction of human osteoprogenitor chemotaxis, proliferation, differentiation, and bone formation by osteoblast stimulating factor-1/pleiotrophin: osteoconductive biomimetic scaffolds for tissue engineering. *J Bone Miner.Res.* 2003; 18:47-57

134. **Zhang X, Xie C, Lin AS, Ito H, Awad H, Lieberman JR, Rubery PT, Schwarz EM, O'Keefe RJ, Guldberg RE**. Periosteal progenitor cell fate in segmental cortical bone graft transplantations: implications for functional tissue engineering. *J.Bone Miner.Res.* 2005; 20:2124-2137

CHAPTER 9

Appendix - Publications